國 立 交 通 大 學

生 物 科 技 學 院

生 化 工 程 研 究 所

博士論文

建立循環流動系統壓電式生物感測器用於及時檢測病原菌大腸桿菌 O157:H7 及登革熱病毒

Establishing a Circulating-flow System of Piezoelectric Biosensor for In-time Detection of Pathogen, *Escherichia coli* O157:H7 and Dengue Virus

研 究 生： 陳思豪

指導教授： 林志生 博士

中 華 民 國 九 十 八 年 七 月

建立循環流動系統壓電式生物感測器用於及時檢測病原菌大腸桿菌 O157:H7 及登革熱病毒

Establishing a Circulating-flow System of Piezoelectric Biosensor for In-time Detection of Pathogen *Escherichia coli* O157:H7 and Dengue Virus

研 究 生：陳思豪　　Student：Sz-Hau Chen

指導教授：林志生　　Advisor：Chih-Sheng Lin Ph.D.

國 立 交 通 大 學

生化工程研究所

博 士 論 文

A Thesis

Submitted to Institute of Biochemical Engineering

College of Biological Science and Technology

National Chiao Tung University

In partial Fulfillment of the Requirements

For the Degree of Ph.D.

In

Biological Science and Technology

July 2009

Hsinchu, Taiwan, Republic of China

中 華 民 國 九 十 八 年 七 月

謝　誌

博士四年的生涯終於結束了，而我也即將邁向了另一個人生的開始，在這過程中不知有多少人問過我同樣的問題”為什麼妳你想要唸博士？”而我始終如一的回答是”想不開”。博士的生涯是如此的繁忙與艱辛，整天和研究與書本為伍。在這四年期間實驗室幾乎成為我第二個家，在每天從實驗室走回宿舍的路上，拖著疲憊的步伐看著皎潔的月光或剛初昇的太陽，但我知道我正在一步一步達成想要的目標。而這過程必須感謝許多人給於我的幫助與鼓勵，讓我的博士班生涯多采多姿。

首先我非常感謝指導教授 **林志生** 老師，指導了我許多做學問的態度、邏輯觀念的指引與多方角度的思維，並適時的給予鼓勵與肯定，以及生活與人生的方向的關懷與幫助，讓我在人生的道路上的經歷更加豐富。千言萬語都無法表達我對於您的感謝，能在您的門下是我這一輩子最大的福氣。另外，也非常感謝美國緬因大學 **吳啟華** 教授在這四年來於研究上指導與生活上的關懷，以及擔任口試委員在論文上提供寶貴的意見。亦非常感謝口試委員兼召集人大同大學 **顏聰榮** 教授，以及口試委員文化大學 **蘇平貴** 教授、中興大學 **溫曉薇** 教授及交通大學 **楊昀良** 教授，百忙之中能抽空前來並給予審閱及斧正，使本論文能更加的完整。

在四年實驗室生活中，往事依舊歷歷在目，感謝博班三人組歌壇唱將**建龍**學長與冷面笑將**俊旭**學長在實驗與生活上的幫助，多少個苦悶的夜晚有你們陪伴一起吃宵夜的日子，讓生活更添動力；**棠青**多虧有你的有求必應的個性與幫忙，讓事情作起來格外順利；**筱晶**的一流聲音，讓實驗室的每個夜晚都不會寂寞；**聖壹**與**千雅**的雙簧二人組更是讓實驗室充滿歡樂與朝氣；**曜禎**的體力無限與在實驗上的協助，只能說好在有你阿，接下來 biosensor 組就看你了；**証皓**的辦事效率及認真態度與停不下來的話匣子，讓大家不感寂寞，**明達**的開朗個性與南部人的率直，使實驗室充滿陽光；打字能手的帥氣**榕均**學妹，妳做事的細心及在實驗瑣事上的幫助，讓事情趨於簡單；實驗室四朵花-**庭妤**、**郡誼**、**瀞韓**及**子慧**，除了在實驗管理上的幫忙，更讓實驗室增色不少；**逸柔**、**家瑋**、**怡萱**、**唯婷**、**修兆**、**竣瑋**、**欣儒**、**政庭**及**祥婷**在生活上的相互幫忙，感謝你們的支持與幫助，因為有你們而更覺得豐富。

最後僅以這本論文獻給我最親愛的父母及家人，感謝父母的栽培與關懷，你們的期待與鼓勵是我最大的原動力，沒有你們一路的支持就沒有今日的我，謝謝你們對我的付出，是我心靈的最佳避風港，對你們獻上無盡的謝意。

陳思豪　　謹誌

國立交通大學 生化工程研究所

生醫工程實驗室

中華民國九十八年七月

建立循環流動系統壓電式生物感測器用於及時檢測病原菌大腸桿菌 O157:H7 及登革熱病毒

研究生：陳思豪　　指導教授：林志生 博士

國 立 交 通 大 學

生 物 科 技 學 院

生 化 工 程 研 究 所 博 士 班

中 文 摘 要

在公共衛生的觀點上，病原菌的感染已經成為嚴重的疾病問題。 然而，在我們的日常生活中，有許多病原菌類別存在，包括致病性的病毒、細菌、黴菌、寄生蟲、海生的浮游植物及藍綠藻等。 病原菌的傳播機制不僅只有利用環境的因子如水、空氣或者是土壤，也包含食品的污染，血液的輸送或接觸的感染等。 由於在每個國家中致死性的病原菌往往伴隨著經濟的損失及人民的死亡，因此，如何預防及前期偵測病原菌的感染爆發是一重要的任務。

生物感測器為快速檢測生物分子的一新穎技術，此研究主要為發展在循環流動系統中一核酸壓電式生物感測方法用以及時偵測病原菌及病毒。 首先設計一具有 30 個去氧核苷酸及額外具有 12 個去氧單磷酸胸腺苷（dT）的專一性核酸探針以解決生物感測系統上空間的阻礙。 此具有 12 dT 於探針上如同一 spacer，可顯著的增強雜交的效率（$P < 0.05$）。 結果中指出當探針分別與 30 mer 與 104 mer 的目標物雜交時，spacer 增加雜交效率分別為 1.4 倍及 2 倍。 尤其當探針與較長的核酸目標物雜交時，spacer 減少了固定化的核酸探針與目標物雜交時的空間阻礙並提供雜交行為的支援。 此核酸壓電式生物感測系統也被用於從大腸桿菌 O157:H7 的 PCR 擴增的 DNA 產物的真實樣本上的檢測過程中所使用，其雜交效率的結果 PCR 放大的雙股 DNA 可相當於合成的目標物 T-104AS 之單股 DNA。

更進一步地，此循環流動系統之壓電式生物感測器基於奈米金球的放大與驗證方法被用於一食品中病原菌大腸桿菌 O157:H7 的及時檢測。 延續前部分的研究，一含有 12-dT 及修飾硫醇且互補於目標物序列的第二探針被與奈米金球結合，並且作為像一質量的放大者及序列的檢驗者，用於放大在 DNA 壓電式生物感測器上頻率的改變。 在大腸桿菌 O157:H7 的樣品檢測方面，經由後 PCR 的放大後，可藉由此 DNA 壓電式生物感

測器所測得 1.2×10^2 CFU/ml 的大腸桿菌 O157:H7，並且當大腸桿菌 O157:H7 從 10^2 至 10^6 CFU/ml 時其具有線性相關。 在真實的食物樣品的檢測上，此 DNA 壓電式生物感測器亦可檢測出目標物。

除了病原菌的檢測，病毒的檢測是在壓電式生物感測器上的一個挑戰，考慮到病毒需要許多時間以傳統的方法進行檢測，此部分基於前面利用及時與可連至電腦的檢測成果，並結合奈米金球層疊的方法用於快速檢測病毒。 在此研究中，一對在登革熱病毒外膜蛋白的基因保留區的通用型引子對被設計用來放大其 DNA 片段，並且設計兩專一性探針用以識別在台灣登革熱病毒二型常見亞型。 根據先前的方法，在 DNA 壓電式生物感測器的表面上，第一探針與目標物進行雜交用以辨識登革熱病毒。 然後，第二探針結合奈米金球並且與目標物進行雜交，用以增加訊號值與驗證。 為了增加更多的雜交效率，第一探針被結合至不同大小粒徑的奈米金球並以層疊法引入，且與自由流動的目標物進行雜交。 接著，第二探針與目標物雜交於另一端，此經由層疊法的結構類似樹枝狀的結構。 藉由此層疊法，2.1×10^1 (PFU)/ml 的登革熱病毒二型可藉由此壓電式生物感測器所測得，其介於頻率變化與病毒濃度的對數從 2.1×10^6 至 2.1×10^1 PFU/ml 呈線性相關。

關鍵字：壓電式生物感測器、奈米金球、病原菌、大腸桿菌 O157:H7、登革熱病毒

Establishing a Circulating-flow System of Piezoelectric Biosensor for In-time Detection of Pathogen *Escherichia coli* O157:H7 and Dengue Virus

Graduate student: Sz-Hau Chen Advisor: Chih-Sheng Lin Ph.D.

Institute of Biochemical Engineering
College of Biological Science and Technology
National Chiao Tung University

Abstract

Pathogens infections have been a serious problem on the public health aspect. There are many classes of pathogenic microorganisms, including pathogenic viruses, bacteria, fungi, parasites, marine phytoplankton, and cyanobacteria, etc. in our daily lives. The pathogen transmission mechanism use not only environment factors, ex. water, air or soil, but also the food contamination, blood transfusion or contract infection etc… At every country, the deadly pathogens are usually accompanying economy damage and life loss. Hence, how to prevent and early detect pathogen infection and outbreak is important tasks.

Biosensor is a novel technology for rapid detection of biomolecules. In this study, we develop a DNA piezoelectric biosensing method for In-time detection of pathogens or viruses in a circulating flow system. First, the specific probes of a 30-mer oligonucleotide with additional 12 deoxythymidine 5'-monophosphate (12-dT) is designed to solve steric interference on the biosensor system. The addition of 12-dT to the probes as a spacer, significantly enhanced ($P < 0.05$) the hybridization efficiency (H%). The results indicate that the spacer enhanced the H% by 1.4- and 2-fold when the probes are hybridized with 30-mer and 104-mer targets, respectively. The spacer reduced steric interference of the support on the hybridization behavior of immobilized oligonucleotides, especially when the probes hybridized with relatively long oligonucleotide targets. The DNA piezoelectric biosensing system is also applied in the detection of PCR-amplified DNA from real samples of *Escherichia coli* O157:H7. The resultant H% of the PCR-amplified double-strand DNA is comparable to that of the synthetic target T-104AS, a single strand DNA.

Further, a circulating-flow piezoelectric biosensor, based on an Au nanoparticle amplification and verification method, is used for real-time detection of a foodborne pathogen, *E. coli* O157:H7. Continuing the first part study, a second thiolated probe with 12-dT,

complementary to the target sequence, is conjugated to the Au nanoparticles and used as a "mass enhancer" and "sequence verifier" to amplify the frequency change of the DNA piezoelectric biosensor. The PCR products amplifing from concentrations of 1.2×10^2 CFU/ml of *E. coli* O157:H7 are detectable by the DNA piezoelectric biosensor. A linear correlation is found when the *E. coli* O157:H7 detected from 10^2 to 10^6 CFU/ml. The piezoelectric biosensor is also able to detect targets from real food samples.

Besides bacteria detection, virus detection is a challenge in the filed of piezoelectric biosensor. It needs a lot of time to detect viruses by traditional methods. This part of study combined the previously developed In-time and on-line work, with Au nanoparticles layer by layer method for rapid detection of virus. In this study, a pair of universal primers of dengue virus envelope gene conserve region was used to amplify cDNA fragment, and two specific probes for the identification of dengue virus type II common subtypes are developed in Taiwan. According to pervious process, first probe hybridizes with the target to identify dengue virus in DNA piezoelectric biosensor surface, then, second probe conjugates with Au nanoparticles and hybridizes with target to enhance signal and verification. In order to increase more hybridization efficiency, the layer by layer method is recommended for the first probe to conjugate to Au nanoparticles in different sizes and to hybridize with free targets. Further, the second probes are hybridized with targets at other terminals. The structure is like dendritic form via layer by layer hybridization. Following layer by layer method, as low as 2.1×10^1 plaque forming unit (PFU)/ml DENV type 2 can be detected by the DNA piezoelectric biosensor. Linear correlation between frequency change and logarithmic number of virus concentration is found for DENV from 2.1×10^6 to 2.1×10^1 PFU/ml.

Keyword: piezoelectric biosensor, Au nanoparticles, pathogen, *Escherichia coli* O157:H7, dengue virus

Content

List of Figures

List of Tables

1. Literature review

Pathogens infections have been a serious problem from the public health aspect. There are many classes of pathogenic microorganisms classifications, including pathogenic viruses, bacteria, fungi, parasites, marine phytoplankton, and cyanobacteria, etc. in our daily life. The pathogen transmission mechanism not only uses environment factor, ex. water, air or soil, but also the food contamination, blood transfusion or contract infection etc… At every country, the deadly pathogens are usually accompanying economy damage and life loss. However, how to prevent and early detect pathogen infection outbreak are important tasks.

The foodborne pathogen of bacteria is a common cause of diseases due to food product contamination, accounting for 91% of the total outbreaks of foodborne illness in the USA [Beran et al., 1991; Potter et al., 1997]. An estimated 76 million cases of foodborne disease occur each year in the United States. The great majority of these cases are mild and cause symptoms for only a day or two. Some cases are more serious, and CDC estimates that there are 325,000 hospitalizations and 5,000 deaths related to foodborne diseases in the United States each year [CDC, 2005]. The most severe cases tend to occur in the very old, the very young, those who have an illness already that reduces their immune system function, and in healthy people exposed to a very high dose of an organism. Besides, foodborne diseases are extremely costly. The U.S. Department of Agriculture (USDA) Economic Research Service (ERS) estimates that the medical costs and productivity losses associated with five major pathogens *Escherichia coli* O157:H7, non-O157 STEC (Shiga Toxin- Producing *Escherichia coli*), *Salmonella* (non-typhoidal serotypes only), *Listeria monocytogenes* and Campylobacter, is at least $6.9 billion annually [USDA/ERS, 2002].

Conventional microbiological methods have been standard operating procedures for the detection and identification of pathogens in food for nearly one century and continue to be a reliable standard for ensuring food safety. Detecting foodborne pathogen with conventional procedures can take several days by use of specific agar media to isolate and enumerate viable bacterial cells in samples [Meng et al., 2001]. However, conventional methods are time consuming and labor intensive, and are therefore not suitable for modern food quality assurance to make a timely response to possible risks. Based on this reason, over the past 25 years, numerous rapid methods have been developed to reduce the assay time.

Recent detection technology to identify foodborne pathogen are present in **Table 1-1**, including reform method of plating, real-time PCR, ELISA combining with immunomagnetic or nanoparticles, and biosensors platform. These detection methods are usually using

molecular biology technology to rapid detection, include antibody-based methods (immunofluorescence, immunoimmobilization, enzyme-linked immunosorbent assay, immunomagnetic separation, etc.), nucleic acid-based methods (hybridization and polymerase chain reaction [PCR]), biochemical and enzymatic methods (miniaturized microbiological methods and commercial miniaturized diagnostic kits), and membrane filtration methods (hydrophobic grid membrane filter) [Wu et al., 2004]. In recent years, modern biotechniques such as real time PCR [Yoshitomi et al., 2003; Fu et al., 2005], nanoparticles [Zhao et al., 2004; Mao et al., 2006] and biosensing systems (biosensors) [Campbell and Mutharasan, 2005; Simpson et al., 2005; Mao et al., 2006] have been developed for detection of pathogenic microorganisms. Biosensors are devices that detect biological or chemical complexes in the form of antigen-antibody, nucleic acids, enzyme-substrate, or receptor-ligand compounds. Interest in using biosensors to detect foodborne pathogens is on the rise [Hall, 2002; Patel, 2006; Rasooly and Herold, 2006].

2. Pathogen Biosensor

In recent year, there are many analytic methods that have been developing for the pathogen rapid detection. One approach for rapid pathogen detection is the use of biosensors, because the biosensor provided fast and simple detection method, causing its application to expand. Until today, biosensors have gradually become rapid biomolecular recognition tools in analytical biological material. The biosensors are also applied to pathogen contamination detection on food safety.

A biosensor is defined as a device that combines a biological component with a physicochemical detector component for the detection of an analyte. [http://www.biosensors-congress.elsevier.com/about.htm]

It consists 3 parts:

- The sensitive biological element [biological material (eg. tissue, microorganisms, organelles, cell receptors, enzymes, antibodies, nucleic acids, etc), a biologically derived material or biomimic] that can be created by biological engineering.
- The transducer or the detector element (works in a physicochemical way; optical, piezoelectric, electrochemical, etc.) that transforms the signal resulting from the interaction of the analytic with the biological element into another signal (i.e., transducers) that can be more easily measured and quantified;

- Associated electronics or signal processors that is primarily responsible for the display of the results in a user-friendly way.[Cavalcanti A et al. 2008]

Although the biosensors can rapid detection or have higher sensitivity, the limitation still exists. The limitation is from unknown pathogen interference and few cells contamination in the food. Hence, the diagnosis with the biosensor has differentiated between pathogens need pre-enrichment or without enrichment, Based on enrichment step, the biosensors can be differentiated between immunoassay or DNA recognition. The immunosensor usually needs pre-enrichment of pathogen cells before detection. Contrary, the DNA recognition biosensor does not need pre-enrichment, because the polymerase chain reaction (PCR) can substitute for the cell culture. The immunoassay or DNA diagnosis methods have different functions at detection. The immunobiosensor are based on exploiting the specific interaction of antibody with antigen. Typically, immunoassays (such as the widely used enzyme-linked immunosorbent assay technology) employ a label (e.g., enzyme, fluorescent marker) to detect the immunological reaction. On the other hand, the DNA biosensors, commonly, relys on the immobilization of a DNA probe onto the transducer surface, the subsequent hybridization with the DNA target triggering a signal either directly or indirectly.

Based on these detection methods, the biosensors have several classification and numerous biosensors have been developed for detection and enumeration of pathogen and are promising candidates for rapid screening of foods. The biosensors type according to classify on foodborne pathogen detection have electrochemical, photometric, and mass sensitive etc.

2.1 Mass sensitivity biosensor

The mass sensitivity biosensor meant that it used difference inmass to effect biosensor physical characteristic and then accomplishing objective detection, for example: piezoelectric biosensor. The piezoelectric biosensor can be classified into two main groups: (1) surface acoustic wave-based biosensor (SAW) and (2) quartz crystal microbalance (QCM).

SAW biosensors are based on the detection of mechanical acoustic waves and incorporate a biological component. These are mass sensitive detectors, which are operated on the basis of an oscillating crystal that resonates at a fundamental frequency. After the crystal has been coated with a biological reagent (such as an antibody) and exposed to the particular antigen a quantifiable change occurs in the resonant frequency of the crystal, which correlates to mass changes at the crystal surface. The vast majority of acoustic wave biosensors utilize piezoelectric materials as the signal transducers. Piezoelectric materials

are ideal for use in this application due to their ability to generate and transmit acoustic waves in a frequency-dependent manner. The physical dimensions and properties of the piezoelectric material influence the optimal resonant frequency for the transmission of the acoustic wave. The most commonly used piezoelectric materials include quartz (SiO_2) and lithium niobate ($LiTaO_3$). In order to acquire an active surface for use in a piezoelectric biosensor the surface must be stable chemically, contain a high number of the actively immobilized biological elements and the coating surface should also be as thin as possible.

SAW biosensors offer label-free, on-line analysis for antigen–antibody interactions, and also provide the option of several immunoassay formats, which allow increased detection sensitivity and specificity. Other advantages include cost effectiveness combined with ease of use. Disadvantages associated with these sensors include relatively long incubation times for the bacteria and biosensor surface, problems with crystal surface regeneration and the number of wishing and drying steps required.

The QCM is another the most popular mass biosensor in the world. The core of the QCM is a specifically manufactured quartz plate and the cut angel with respect to the crystal lattice would result from different type of resonators. Generally, the AT-cut form, which at a 35.25° angle from the Z-axis exhibit tremendous frequency stability of $\Delta f / f \fallingdotseq 10^{-8}$ [Janshoff et al., 2000], and when the temperature changes from 0 °C to 60 °C, the frequency change is close to zero [O'Sullivan and Guilbault, 1999].

The crystal is excited to resonance and the effect of molecular absorption monitored [Sauerbrey, 1959]. The QCM is comprised of thin film electrodes, usually gold (Au), deposited on each face of a crystal. Voltage is applied across these electrodes to deform the crystal plate, producing relative motion between the two parallel crystal surfaces. The crystal is induced to oscillate at a specific resonant frequency. Changes in the mass of the material on the surface will alter the resonance frequency of the crystal [Marx, 2003]. A linear relationship exists between deposited mass and frequency response for quartz crystals. The resonance frequency decreases linearly with the increase of mass on the QCM electrode at the nanogram level or less. This characteristic of QCM can be exploited to develop bioanalytical tools on a 10^{-10} to 10^{-12} g scale [Zhou et al., 2000]. QCM-based immunoassay has been designed and applied in several different areas [Su et al., 2000; Kurosawa et al., 2003; Su and Li, 2004].

For SAW biosensor, Howe and Harding [2000] are used a dual channel SAW biosensor

to detect two different microorganisms, *Legionella* and *Escherichia coli*, simultaneously. A series of experiments are conducted to optimize the use of the SAW for bacterial detection using a novel protocol of coating bacteria on the sensor surface prior to addition of the antibody. Results are compared with an experiment in which a conventional protocol is utilized, where antibody are coated on the sensor surface prior to exposure to bacteria. The concentration of bacteria that attached to the surface of the SAW device are related to the antibody that specifically bound to it and therefore to frequency in a dose dependent fashion. Unlike conventional microbiological techniques quantitative results can be obtained for *Legionella* and *E. coli* down to 10^6 cells per ml within 3 h. In addition *E. coli* are detected down to 10^5 cells per ml in a modified protocol using sheep IgG as a blocking agent.

Later, Deisingh and Thompson [2000] is report on the amplification by polymerase chain reaction (PCR) of a 509 base sequence unique to *E. coli* O157:H7. Immobilization of a probe for the bacterium on an acoustic wave sensor by the biotin–neutravidin interaction is employed to detect the on-line hybridization of the sequence with the sample obtained from PCR. The limit of detection is to be 10^{-8} M.

In the recent, Olsen et al.[2006] are used biosensor for the rapid detection of *Salmonella typhimurium* in solution, based on affinity-selected filamentous phage prepared as probes physically adsorbed to piezoelectric transducers. Specific-bacterial binding resulted in resonance frequency changes of prepared sensors, which are evaluated using linear regression analysis. Sensors possessed a rapid response time of <180 s, have a low-detection limit of 10^2 cells/ml and are linear over a range of 10^1–10^7 cells/ml with a sensitivity of 10.9 Hz per order of magnitude of *S. typhimurium* concentration.

Besides SAW biosensor, the QCM biosensor is developed too in recently years. Many studies is usually used QCM biosensor in air or liquid phase combined antibody-antigen method to detect several foodbrone pathogen, include *E. coli* O157:H7 [Liu et al., 2007], *L. monocytogenes* [Minunni et al., 1996; Vaughana et al., 2001], *Salmonella spp.* [Park et al., 2000; Wong et al., 2002; Su and Li, 2005], *S. aureus* [Boujday et al., 2008], *B. cereus* [Vaughan et al., 2003] *and P. aertrginosa* [Kim et al., 2004] etc..

Recently, the QCM immunosensor is based on nanotechnology rapid developing and application; the detection limit is more improved. Liu et al. [2007] has shown that using antibody-antigen recognition method to develop and to evaluate for detection of *E. coli* O157:H7 on quartz crystal microbalance (QCM) immunosensor. The immunosensor are fabricated by self-assembling of protein A and affinity-purified anti-*E. coli* O157:H7

antibodies on the gold electrode of an AT-cut piezoelectric quartz crystal. To enhance the sensitivity of the QCM immunosensor, nanoparticle-antibody conjugates, which are prepared using streptavidin-conjugated nanoparticles (145 nm diameter) and biotinylated anti-*E. coli* antibodies, are used for signal amplification. Compared to the direct detection of *E. coli* O157:H7, the binding of the nanoparticle conjugates further resulted in a decrease in resonant frequency and an increase in resonant resistance, and the detection sensitivity are improved by five orders of magnitude by lowering the detection limit from 10^7 to 10^2 CFU/mL.

Mao et al. [2006] using quartz crystal microbalance (QCM) DNA sensor, based on the nanoparticle amplification method, is developed for detection of *Escherichia coli* O157:H7 *eaeA* gene. The hybridization is induced by exposing the ssDNA probe to the complementary target DNA, and results in the mass change and therefore frequency change of the QCM. Streptavidin conjugated Fe_3O_4 nanoparticles are used as "mass enhancers" to amplify the frequency change. The detection limit is low as 10^{-12} M synthesized oligonucleotides and 2.67×10^2 colony forming unit (CFU)/mL *E. coli* O157:H7 cells can be detected. Linear correlation between frequency change and logarithmic number of bacterial cell concentration is found for *E. coli* O157:H7 from 2.67×10^2 to 2.67×10^6 CFU/mL.

2.2 Electrochemical biosensor

Electrochemical biosensors are based on monitoring electro-active species that are either produced or consumed by the action of the biological components (e.g., enzymes and cells). Transduction can be performed using one of several methods under two broad headings: potentiometry and amperometry.

Potentiometric biosensors are based on monitoring the potential of a system at a working electrode, with respect to an accurate reference electrode, under conditions of essentially zero current flow. In operation, potentiometric measurements are related to the analyte activity (of a target species). The use of ion selective and gas sensitive membranes coupled to enzyme systems, linked to the potentiometric sensor, allows the fabrication of a biosensor device specific to the enzyme substrate or product. By measuring either the ions or the gases that are generated or consumed as a result of the enzyme activity, an effective method for measuring the concentration of the target analytic can be realized. Potentiometric biosensors can operate over a wide range (usually several orders of magnitude) of concentrations. The use of potentiometric biosensors for food analysis has not been as widely reported as for

amperometric sensors. Generally, the use of amperometry as the method of transduction has proved to be the most widely reported using an electrochemical approach. Both “one-shot” (disposable) sensors and on-line (multimeasurement) devices have been described, monitoring a wide range of target analytes. In contrast to potentiometric devices, the principle operation of amperometric biosensors is defined by a constant potential applied between a working and a reference electrode. The imposing potential encourages redox reactions to take place, causing a net current to flow. The magnitude of this current is proportional to the concentration of electroactive species present in solution. Both cathodic (reducing) and anodic (oxidizing) reactions can be monitored amperometrically.

Many amperometric biosensors described to date have been based on the use of enzymes. Typically, oxidase enzymes have been the most frequently exploited catalysts used for these biosensor formats. In operation, amperometric biosensors tend to monitor either the oxygen consumed or the hydrogen peroxide generated. Both are electrochemically active; oxygen can be electrochemically reduced, and hydrogen peroxide can be oxidized. The current generated is proportional to the concentration of the enzyme substrate (i.e., the target analytic) present. Biosensor technologists have also adopted other approaches, including the use of mediators ex. ferrocenedicarboxylic acid, N-methylphenazinium cation and tetracyanoquinodimethane radical anion etc.. These compounds are able to replace oxygen as an electron acceptor and to operate at a much lower operating potential, reducing the effects of other electrochemically active species found in many food matrices.

2.3 Optical biosensor

Optical biosensors are a powerful detection and analysis tool that has vast applications in biomedical research, healthcare, pharmaceuticals, environmental monitoring, food safety, and the battlefield. They are immune to electromagnetic interference, capable of performing remote sensing, and can provide multiplexed detection within a single device. Generally, there are two detection protocols that can be implemented in optical biosensing: fluorescence-based detection and label-free detection. In fluorescence-based detection, either target molecules or biorecognition molecules are labeled with fluorescent tags, such as dyes; the intensity of the fluorescence indicates the presence of the target molecules and the interaction strength between target and biorecognition molecules. While fluorescence-based detection is extremely sensitive, with the detection limit down to a single molecule, it suffers from laborious labeling processes that may also interfere with the function of a biomolecule.

Quantitative analysis is challenging due to the fluorescence signal bias, as the number of fluorophores on each molecule cannot be precisely controlled. In contrast, in label-free detection, target molecules are not labeled or altered, and are detected in their natural forms. This type of detection is relatively easy and cheap to perform, and allows for quantitative and kinetic measurement of molecular interaction. Additionally, as discussed later, some label-free detection mechanisms measure refractive index (RI) change induced by molecular interactions, which is related to the sample concentration or surface density, instead of total sample mass. As a result, the detection signal does not scale down with the sample volume. This characteristic is particularly attractive when ultra-small (femtoliter to nanoliter) detection volume is involved and is advantageous over fluorescence-based detection whose signal usually depends on the total number of analytic in the detection volume or on the detection surface. Despite all these differences between fluorescence-based and label-free detection, both protocols are being widely used in optical sensors and provide vital and complementary information regarding interactions among biomolecules, which makes optical sensors more versatile than other types of sensing technologies, such as optical fibers, surface plasmon resonance fluorescence and surface plasmon resonance (SPR).

Fluorescence occurs when a valence electron is excited from its ground state to an excited singlet state. The excitation is produced by the absorption of light of sufficient energy. When the electron returns to its original ground state, it emits a photon at lower energy. Another important feature of fluorescence is the little thermal loss and rapid (<10 ns) light emission taking place after absorption. The emitted light is at a longer wavelength than the absorbed light since some of the energy is lost due to vibrations, this energy gap is termed Stoke's shift, and it should be large enough to avoid cross talk between excitation and emission signals. Antibodies may be conjugated to fluorescent compounds, the most common of which is fluorescein isothiocyanate (FITC) [Li et al., 2004]. There are, however, other fluorescent markers. The use of lanthanides as sources of fluorescence in luminescent assays has very recently been reviewed [Selvin, 2002]. Although lanthanides pose several important advantages (good stability, lowbackground luminescence under normal light conditions and large Stoke's shift) compared to more traditional fluorophores, their use is very restricted due to safety reasons. Fluorescence detection, in contrast to SPR, is also used in combination with established techniques such as PCR and ELISA. Such is the case of a hand-held real-time thermal cycler recently developed [Higgins et al., 2003]. This analyser measures fluorescence at 490 and 525 nm, which enables the simultaneous detection of more

than one microorganism. Although this work claims detection times of 30 min, it should be pointed that overnight culturing is required to achieve best results. Fluorescence resonance energy transfer (FRET) biosensors [Ko and Grant, 2003] are based on the transfer of energy from a donor fluorophore to an acceptor fluorophore.

SPR biosensors [Cooper, 2003] measure changes in refractive index caused by structural alterations in the vicinity of a thin film metal surface. Current instruments operate as follows. A glass plate covered by a gold thin film is irradiated from the backside by p-polarised light (from a laser) via a hemispherical prism, and the reflectivity is measured as a function of the angle of incidence, θ. The resulting plot is a curve showing a narrow dip. This peak is known as the SPR minimum. The angle position of this minimum is determined by the properties of the gold-solution interface. Hence, adsorption phenomena and even antigen–antibody reaction kinetics can be monitored using this sensitive technique (as a matter of fact, SPR is used to determine antigen–antibody affinity constants). The main drawbacks of this powerful technique lay in its complexity (specialized staff is required), high cost of equipment and large size of most currently available instruments (although portable SPR kits are also available commercially, as is the case of Texas Instruments' Spreeta system). SPR has successfully been applied to the detection of pathogen bacteria by means of immunoreactions [Lazcka, et al., 2007].

2.4. Apply to biosensor related nanotechnology

2.4.1. Nanoparticles, nanocarbon tube, and nanowires

A range of nanoparticles (NPs) including nanotubes and nanowires, prepared from metals, semiconductor, carbon or polymeric species, have been widely investigated for their ability to enhance the response of biosensors. NPs can be used in a variety of ways, such as modification of electrode surfaces, or to modify biological receptor molecules such as enzymes, antibodies or oligonucleotides. Their use in biosensors has been reviewed recently. In particular, they have proved extremely useful in the preparation of DNA biosensors. There are also many reports of the methods of enzymes and proteins based on NPs-modified sensor. For electrochemical biosensor application, the enhanced electrochemistry is due to the ability of the small NPs to reduce the distance between the redox site of a protein and the electrode, since the rate of electron transfer is inversely dependent on the exponential distance between them [Lin et al. 2008].

Metal NPs, such as gold, silver and iron, constitute one of the most researched branches

of nanotechnology due to their electronic, optical, catalytic and thermal properties[Guo et al, 2007; Kariuki et al., 2006]. Among those, Ag NPs are known for their antimicrobial activity and have been used in water treatment [Shrivastava et al., 2007; Baker et al., 2005; Sondi and Salopek-Sondi 2004; Morones et al., 2005]. Their bactericidal activity is shape and size dependent, with particles of sizes less than 100 nm showing optimal antibacterial activity. Another application is as oligonucleotide labeling tags in electrochemical DNA sensors [Cai et al., 2002]. For example, Au NPs have been intensively used for signal amplification, as a component of bio-immobilization matrixes in biosensors and in a variety of colorimetric and fluorescence assays. A miniaturized battery operated nanomaterial surface energy transfer (NSET) probe designed for detection and screening of mercury in soil, water and fish, with detection limits in the ppt range is an example of this approach [Darbha et al., 2005]. In the NSET system, AuNPs (acting as an acceptor) were combined with an organic dye (Rhodamine) as a donor. The method is based on the quenching properties of AuNPs through energy- and electron-transfer, providing enhanced sensitivity for the detection of metal ions. Other NPs such as zero valent iron and bimetallic iron NPs coupled to metal catalysts such as Pd, Pt or Ni were used in environmental remediation of chlorinated organics, polychlorinated biphenyls (PCBs) [He and Zhang, 2005], inorganic ions and heavy metal ions such as As(III), Pb(II), Cu(II), Ni(II) and Cr(VI) [Theron et al., 2008].

The use of carbon nanotubes (CNTs) in electrochemical sensors has been reviewed. CNTs can be single-walled or multi-walled. Single-walled nanotubes are formed by rolling up a single graphite sheet into a cylinder; whereas, for multi-walled CNTs, several singlewalled nanotubes of increasing size lie inside one another, like the consecutive skins of an onion. The sidewalls of the CNTs resemble the basal plane of highly orientated pyrolytic graphite (HOPG), a common electrode material, whereas the ends of the tube resemble the edge planes of HOPG. The enhanced electrochemical response at CNTs is due primarily to the large number of edge plane sites, although this may not be the explanation for all experimental observations. CNTs are often purified with oxidizing acids to introduce surface sites with carboxylate groups, suitable for attachment to electrode surfaces, enzymes or other biological receptors. The large number of sites on the CNTs can result in attachment of large numbers of enzyme molecules. Single-walled CNTs can self-assemble onto an electrode surface. If they align vertically, they can act as a molecular wire and allow direct communication between an enzyme active site and electrode, eliminating the need for mediator. CNTs can be used in variety of electrode formats, and as an additive in addition to

other materials (e.g. carbon, in screen printed electrodes or carbon paste electrodes). Direct oxidation of hydrogen peroxide and NADH has been reported at screen-printed carbon–CNT composite electrodes, which gives an inexpensive method of mass fabrication of sensors that can be used with oxidases and dehydrogenases.

Boron-doped silicon nanowires (SiNWs) are reported by Cui et al. [2001] to create highly sensitive, real-time electrically based sensors for biological and chemical species. The amine and oxide-functionalized SiNWs exhibited pH-dependent conductance that is linear over a large dynamic range and can be understood in terms of the change in surface charge during protonation and deprotonation. Biotin-modified SiNWs are used to detect streptavidin down to at least a picomolar concentration range. In addition, antigen-functionalized SiNWs shows reversible antibody binding and concentration-dependent detection in real time. The small size and capability of these semiconductor nanowires for sensitive, label-free and real-time detection of a wide range of chemical and biological species can be exploited in array-based screening and in vivo diagnostics.

The nanoscale size of these new classes of sensors allows for measurements in the smallest of environments such as individual cells. This property provides opportunities for in vivo monitoring of processes within live cells. Cullum et al. [2000] used optical fibers with a distal-end diameter of less than 1 μm, coated with antibodies, to detect the presence of toxic chemicals within single cells. They are able to measure the concentration of benzopyrene tetrol (BPT) within human mammary carcinoma cells and rat liver epithelial cells. Tuan [2002] fabricated nanoprobes with optical fibers pulled down to tips with the distal ends having sizes of approximately 30-50 nm [Tuan, 2002]. Using these nanobiosensors it has become possible to probe chemical species at specific spots. Nanocontrolled release systems have been devised for optical biosensing of peroxide concentration [Choi et al., 2001].

2.4.2. Quantum dots

A group of inorganic fluorophores, including quantum dots, nanocrystals and functionalized nanoparticles have revolutionized fluorescence-based detection methods. The high quantum yields and high resistance to photo degradation of such probes has led to improve sensitivity and multiplexing of assays. Quantum dots are nanocrystalline

semi-conductors that exhibit unique light emitting properties that can be customized by changing the size or composition of the dots. They are typically 2–8 nm in size and are covered with a layer of organic material that allows functionalization of the surface for biomolecule attachment. The narrow emission spectra of nanocrystals give rise to sharper colors and high spectral resolution, which can improve assay sensitivity

2.4.3. Magnetic beads

Magnetic nanoparticles are a powerful and versatile diagnostic tool in biology and medicine. They usually can be prepared in the form of either single domain or superparamagnetic (Fe_3O_4), greigite (Fe_3S_4), maghemite (g-Fe_2O_3), and various types of ferrites (MeO_Fe_2O_3, where Me = Ni, Co, Mg, Zn, Mn, etc.). Bound to biorecognitive molecules, magnetic nanoparticles can be used to separate or enrich the analyte to be detected. Established techniques such as magnetic cell separation use magnetic field gradients to manipulate and isolate magnetically labeled cells. Magnetic immunoassay techniques also have been developed in which a magnetic field generated by the magnetically labeled targets is detected directly with a magnetometer.

A new technique has been introduced for rapid detection of biological targets by using superparamagnetic nanoparticles and a ‘‘microscope’’ based on a high-transition temperature superconducting quantum interference device (SQUID). In this technique, a mylar film with bound targets is placed on the microscope. A suspension of magnetic nanoparticles carrying antibodies is added to the mixture in a well, and 1-spulses of magnetic field are applied parallel to the SQUID. In the presence of this aligning field, the nanoparticles develop a net magnetization, which relaxes when the field is turned off. Unbound nanoparticles relax rapidly by Brownian rotation and contribute no measurable signal. Nanoparticles bound to the target are captured and undergo Neel relaxation, producing a slowly decaying magnetic flux, which is detected by the SQUID. The ability to distinguish between bound and unbound labels allows anyone to run homogeneous assays, which do not require separation and removal of unbound magnetic particles. Magnetic nanoparticles or microspheres have been reviewed in detail by [Chen et al., 2004].

Besides forward description, **Table 2-1** summarizes the most relevant examples of advanced nanomaterials and nanostructures, their characteristics and potential applications reported in literature.

3. Piezoelectric biosensor

3.1 Piezoelectric effect

The word Piezoelectricity comes from Greek and means “electricity by pressure” (Piezo means pressure in Greek). This name is proposed by Hankel in 1881 to name the phenomenon discovered a year before by the Pierre and Jacques Curie brothers [Curie and Curie,1880]. They observed that positive and negative charges appeared on several parts of the crystal surfaces when comprising the crystal in different directions, previously analysed according to its symmetry. **Figure 3-1A** shows a simple molecular model; it explains the generating of an electric charge as the result of a force exerted on the material. Before subjecting the material to some external stress, the gravity centres of the negative and positive charges of each molecule coincide. Therefore, the external effects of the negative and positive charges are reciprocally cancelled. As a result, an electrically neutral molecule appears. When exerting some pressure on the material, its internal reticular structure can be deformed, causing the separation of the positive and negative gravity centres of the molecules and generating little dipoles **(Figure 3-1B)**. The facing poles inside the material are mutually cancelled and a distribution of a linked charge appears in the material’s surfaces **(Figure 3-1C)**. That is to say, the material is polarized. This polarization generates an electric field and can be used to transform the mechanical energy used in the material’s deformation into electrical energy.

The Curie brothers verified, the year after their discovery, the existence of the reverse process, predicted by Lippmann [1881]. That is, if one arbitrarily names direct piezoelectric effect, to the generation of an electric charge, and hence of an electric field, in certain materials and under certain laws due to a stress, there would also exist a reverse piezoelectric effect by which the application of an electric field, under similar circumstances, would cause deformation in those materials.

3.2 Piezoelectric quartz crystal

Piezoelectric quartz crystal is a reverse piezoelectric material. A prerequisite for the occurrence of piezoelectricity in crystal is an inversion center. The quartz crystal may provide a large variety of different resonator types depending on the cut angle with respect to the crystal lattice **(Figure 3-2).** The cut angle determines the mode of induced mechanical

vibration. Resonators operating in the thickness shear mode, face shear mode or flexural mode can be obtained from the mother crystal with eigenfrequencies ranging from 5×10^2 to 3×10^8 Hz. AT-cut crystals, which are predominately used for quartz crystal microbalance (QCM) devices, operate in the TSM and are prepared by slicing a quartz wafer with an angle of 35¼° to the optical *z*-axis. AT-cut quartz crystals show a tremendous frequency stability of $\Delta f/f \doteq 10^{-8}$ and a temperature coefficient which is close to zero between 0 and 50°C, rendering this particular cut the most suitable for QCM sensors. The technique determines the mass of very thin surface bound layers and simultaneously gives information about their viscoelastic properties [Fredriksson et al., 1998; Fu et al., 2003; Ebarvia et al., 2004; D'Souza et al., 2005]. This offers new opportunities to study conformational changes in layers formed on the sensor surface. Moreover, the technique takes into account water coupled to hydrated layers, in contrast to optical mass measurements, obtained from methods such as surface plasmon resonance and ellipsometry. These unique properties make piezoelectric quartz an invaluable tool for studying macromolecules at surfaces and an important complement to existing techniques.

Many polymers, ceramics, and molecules such as water are permanently polarized: some parts of the molecule are positively charged, while other parts of the molecule are negatively charged. When an electric field is applied to these materials, these polarized molecules will align themselves with the electric field, resulting in induced dipoles within the molecular or crystal structure of the material. Furthermore, a permanently-polarized material such as quartz or barium titanate ($BaTiO_3$) will produce an electric field when the material changes dimensions as a result of an imposed mechanical force. These materials are piezoelectric, and this phenomenon is known as the piezoelectric effect. When a stress is applied to a piezoelectric material, an electric field is generated within it [Lee et al., 2004; Li et al., 2004]. Conversely, if an electric field is applied to the material it undergoes a spontaneous strain. Crystals which acquire a charge when compressed, twisted, or distorted are said to be piezoelectric. This provides a convenient transducer effect between electrical and mechanical oscillations. Conversely, an applied electric field can cause a piezoelectric material to change dimensions. This phenomenon is known as electrostriction, or the reverse piezoelectric effect. Quartz demonstrates this property and is extremely stable **(Figure 3-3)**.

3.3 Quartz crystal microbalance

Piezoelectric biosensor, known as quartz crystal microbalance (QCM), combines high sensitivity to mass on the surface of the quartz crystal with the high specificity of a bioreaction. It has been extensively applied as a transducer in hybridization based on DNA biosensors for the detection of gene mutation [Tombelli et al., 2000; Su et al., 2004], genetically modified organisms [Mannelli et al., 2003], and foodborne pathogens [Ryu et al., 2001; Mo et al., 2002; Wu et al. 2007]. In this study, we utilized QCM as sensing device [Yun et al., 1998; Zhou et al., 1999]. QCM sensors **(Figure 3-4)** have been widely studied and developed as detecting tools for humid, biomedical, and environmental monitoring in recent years. They are popular because of its high sensitivity , fast response, small size, low power consumption, low cost, and simplicity of use.

A piezoelectric quartz crystal resonator [Wieliczka et al., 1996; Wegener et al., 1999; Willner et al., 1999] is a precisely cut slab from a natural or synthetic crystal of quartz. A QCM consists of a thin quartz disk with electrodes plated on it **(Figure 3-4B)**.

Pierre and Marie Curie showed in 1880 that crystals of Rochelle salt could produce electricity when pressure is applied in certain crystallographic directions. Later they also showed the converse effect i.e. production of strain by application of electricity. These findings are the discovery of the piezoelectric effect. Piezoelectricity did not receive lot of interest in the beginning and a more detailed study of piezoelectricity is not started until 1917 when it is showed that quartz crystals could be used as transducers and receivers of ultrasound in water. In 1919 several devices of everyday interest based on the piezoelectricity of Rochelle salt is described i.e. loudspeakers, microphones and sound pick-ups. In 1921 the first quartz crystal controlled oscillator is described. These first quartz crystal controlled oscillators are based on XT-cut crystals, which have the drawback of being very temperature sensitive. Therefore, the XT-cut crystals are nowadays used in applications where the large temperature coefficient is of little importance, such as transducers in space sonars. The dominance of the quartz crystal for all kind of frequency control applications started in 1934 when the AT-cut quartz crystal is introduced [Lasky et al., 1990; Lassalle et al., 2001; Lee et al., 2002]. The advantage with the AT-cut quartz crystal is that it has nearly zero frequency drift with temperature around room temperature. From the very beginning of using quartz crystal resonators as frequency control elements it is common to increase the frequency of the resonator by drawing pencil marks on the electrodes, or decreasing the frequency by rubbing of some electrode material with an eraser. The understanding of this mass induced frequency shift is only known on a qualitative basis. However, in 1959 Sauerbrey published

a paper that showed that the frequency shift of a quartz crystal resonator is directly proportional to the added mass. Sauerbreys [Barraud et al., 1993; Ben-Dov et al., 1997; Bandyopadhyay et al., 1998; Bizet et al., 1998; Abdelmaksoud et al., 2004] work is generally taken as the breakthrough and the first step towards a new quantitative tool to measure very small masses i.e. the QCM. Hence, one can describe the QCM to be an ultra-sensitive mass sensor. The heart of the QCM is the piezoelectric AT-cut quartz crystal sandwiched between a pair of electrodes. When the electrodes are connected to an oscillator and an AC voltage is applied over the electrodes the quartz crystal starts to oscillate at its resonance frequency due to the piezoelectric effect. This oscillation is generally very stable due to the high quality of the oscillation. If a rigid layer is evenly deposited on one or both of the electrodes the resonant frequency will decrease proportionally to the mass of the adsorbed layer according to the Sauerbrey equation [Anzai et al., 1998; Bidan et al., 2000; Bizet et al., 2000; Bernhard et al., 2002; Aizawa et al., 2003]:

$$\Delta F = -\frac{2 f_0^{\,2} \Delta m}{A(\rho_q \mu_q)^{1/2}}$$

Where: measured frequency shift = ΔF, resonant frequency of the fundamental mode of the crystal = f_0, mass change per unit area (g/cm^2) = Δm, piezo-electrically active area = A, density of quartz, 2.648 g/cm^3 = ρ_q, shear modulus of quartz, 2.947 × 1011 g/cm s^2 = μ_q

There are situations where the Sauerbrey equation does not hold, for example, when the added mass is a) not rigidly deposited on the electrode surface, b) slips on the surface or c) not deposited evenly on the electrode. Therefore, the Sauerbrey equation is only strictly applicable to uniform, rigid, thin-film deposits. Due to this the QCM is for many years just regarded as a gas-phase mass detector [Ebato et al., 1994; Darder et al., 1999; Gomes et al., 1999]. Not until the beginning of 1980's scientists realized that a quartz crystal can be excited to a stable oscillation when it is completely immersed in a liquid. Much of the pioneering work in liquid phase QCM measurements have been done by Kanazawa and coworkers [Kanazawa and Gordon., 1985], who showed that the change in resonant frequency of a QCM taken from air into a liquid is proportional to the square root of the liquid's density-viscosity product:

$$\Delta F = -f_u^{\,2/3} \sqrt{\frac{\rho_L \eta_L}{\pi \rho_q \mu_q}}$$

Where: measured frequency shift = ΔF, resonant frequency of the unloaded crystal = f_u,

density of liquid in contact with the crystal = ρ_L, viscosity of liquid in contact with the crystal = η_L, density of quartz, 2.648 g/cm^3 = ρ_q, shear modulus of quartz, 2.947× 10^{11} g/cm s^2 = μ_q

After it is found out that an excessive viscous loading would not prohibit use of the QCM in liquids and that the response of the QCM is still extremely sensitive to mass changes at the solid-liquid QCMs have been used in direct contact with liquids and/or visco-elastic films to assess changes in mass and visco-elastic properties. Even in air or vacuum, where the damping of layers has been considered to be negligible or small the QCM has been used to probe dissipative processes on the quartz crystal [Okahata et al., 1995; Okahata et al., 1998; Okahata et al., 1999]. This is especially true for soft condensed matters such as thick polymer layers deposited on the quartz surface.

In the early days of electronic communication as a result of the limited number of quartz resonators available-frequency adjustment is accomplished by a pencil mark depositing a foreign mass layer on the crystal. In 1959 Sauerbrey showed that the shift in resonance frequency of thickness-shear-mode resonators is proportional to the deposited mass. This is the starting point for the development of a new generation of piezoelectric mass-sensitive devices.

The development of new measurement techniques represents one of the major driving forces in biotechnology that positively impacts related research areas such as polymer characterization and biochemistry and is critical to the evolution of the pharmaceutical, biotechnology, and biomaterials industries.

Since QCM is a piezoelectric [Sato et al., 1995; Sato et al., 1998], an oscillating electric field applied across the device induces an acoustic wave that propagates through the crystal and meets minimum impedance when the thickness of the device is a multiple of a half wavelength of the acoustic wave. A QCM is a shear mode device in which the acoustic wave propagates in a direction perpendicular to the crystal surface. To make this happen, the quartz crystal plate must be cut to a specific orientation with respect to the crystal axes. These cuts belonging to the rotated Y-cut family, the AT- and BT-cuts are representative.

4. Self assembled monolayer for biosensor application

Considerable attention has been drawn during the last two decades to functionalize noble metal surfaces by forming ordered organic films of few nm to several hundred-nm thickness.

Self-assembled monolayer (SAM) provides one simple route to functionalize electrode surfaces by organic molecules (both aliphatic and aromatic) containing free anchor groups such as thiols, disulphides, amines, silanes, or acids. The monolayer produced by self-assembly allows tremendous flexibility with respect to several applications depending upon their terminal functionality (hydrophilic or hydrophobic control) or by varying the chain length (distance control) (**Figure 4-1A**). For example, SAM of long chain alkane thiol produces a highly packed and ordered surface, which can provide a membrane like microenvironment, useful for immobilizing biological molecules. The high selectivity of biological molecules integrated with an electrochemical, optical, or piezoelectric transduction mode of analyte recognition offers great promise to exploit them as efficient and accurate biosensors. It is demonstrated with suitable examples that monolayer design plays a key role in controlling the performance of these SAM based biosensors, irrespective of the immobilization strategy and sensing mechanism.

The present level of research on new biosensors as well as the development of currently available biosensors e.g. glucose sensors) has increased dramatically over the past decade. The main driving force for this enhanced research activity is the booming demand for miniaturised biosensors, particularly for diagnostic applications. These however, impose rather strict requirements on the size of the device, selective response of the analyte, fast response time and compatibility with the peripheral electronic circuitry. Although the active interest in developing these small sensing devices for biomedical use is growing rapidly, some of the presently available biosensors are inadequate in these respects and several new and improved materials are desired to overcome some of these limitations. Self-assembled monolayers offer several attractive features for these kinds of applications due to various reasons. First, since they use only the bare minimum resources (e.g. a monolayer comprising of 10^{13} molecules/cm^2 or only 10^{-7} moles/cm^2), miniaturisation is easy. Secondly, the high degree of ordered and dense nature of the long chain alkane thiols of SAMs mimics the cellular microenvironment of lipid bilayer structures providing novel substrates for immobilized biomolecules (antibodies, enzymes, nucleic acids) or biological systems (receptors, whole cells). More significantly the easy procedure for SAM formation and compatibility with metal substrates (Au, Ag etc.) for electrochemical measurements enable special benefits for biosensor applications involving current or potential measurements. Lastly, the chemical stability of the monolayer even after its coupling with the immobilizing molecules (with its associated specificity) for biological sensing integrated with an

electrochemical, optical or piezoelectric transducer leads them to work as biosensors and DNA sensors **(Figure 4-1B)** .

5. Pathogen diagnosis

5.1. *Escherichia coli* O157:H7

Escherichia coli O157:H7 has been an important foodborne pathogen in a variety of foods worldwide in the last twenty years. It is classified as an enterohemorrhagic *E. coli* with the ability to cause hemorrhagic colitis which includes symptoms such as bloody diarrhea, hemolytic uremic syndrome, and thrombotic thrombocytopenic purpurea [Doyle et al., 1997]. Centers for Disease Control and Prevention [CDC, 2005] reported that an estimated 73,000 cases of *E. coli* O157:H7 infection and 61 resultant deaths occur in the United States each year. Consumption of as few as ten of *E. coli* O157:H7 cells can result in growth of the pathogen in the intestine and production of shiga toxins in susceptible patients. These toxins can kill the cells of the intestinal lining, destroy the kidneys, and cause blood clots in the brain, as well as seizures, paralysis, and respiratory failure [FDA, 2001; CDC, 2005]. Therefore, it is desirable to develop efficient analytical methods with a high degree of sensitivity and specificity to detect this organism in food.

Detecting *E. coli* O157:H7 with conventional procedures can take several days [Meng et al., 2001]. A variety of rapid methods has been proposed to detect and screen many microorganisms, including *E. coli* O157:H7. These methods include antibody-based methods (immunofluorescence, immunoimmobilization, enzyme-linked immunosorbent assay, immunomagnetic separation, etc.), nucleic acid-based methods (hybridization and polymerase chain reaction [PCR]), biochemical and enzymatic methods (miniaturized microbiological methods and commercial miniaturized diagnostic kits), and membrane filtration methods (hydrophobic grid membrane filter) [Wu et al., 2004]. In recent years, modern bio-techniques such as real time PCR [Yoshitomi et al., 2003; Fu et al., 2005], nanoparticles [Zhao et al., 2004; Mao et al., 2006] and biosensing systems (biosensors) [Campbell and Mutharasan, 2005; Simpson and Lim, 2005; Mao et al., 2006] have been developed for detection of pathogenic microorganisms. Biosensors are devices that detect biological or chemical complexes in the form of antigen-antibody, nucleic acids, enzyme-substrate, or receptor-ligand compounds. Interest in using biosensors to detect foodborne pathogens is on

the rise [Hall, 2002; Patel, 2006; Rasooly and Herold, 2006].

5.2. Dengue virus

Dengue fever is a public health problem in many country, in current years, dengue virus (DENV) has grown dramatically in tropical and subtropical regions of Asia, Africa, and Central and South America, more than 2.5 billion people are at risk of infection and dengue transmission is endemic in more than 100 countries [Wilder-Smith et al., 2005]. Dengue viruses are transmitted by *Aedes mosquitoes* [Wang et al., 2000] and cause infections which leading to clinical symptoms ranging from self-limited, acute, febrile disease called dengue fever (DF) to life-threatening dengue hemorrhagic fever (DHF), and dengue shock syndrome (DSS) [Agarwal et al., 1999]. At infection route, the E protein played important roles in many important processes such as virion assembly [Nowak et al., 1989], receptor binding [Wey et al., 2003], membrane fusion during virus enhances and replication [Gollins SW and Porterfield, 1986; Kimura and Ohyama, 1988; Heinz et al., 1994], they also involved to induce immune responses in flavivirus. Furthermore, the E gene is fewer converses between four dengue serotypes; therefore, it can be used as a marker for differentiation dengue subtype.

For virus detection, the three basic methods routinely practiced by most laboratories are virus isolation and characterization, detection of dengue virus antigen, and detection of genomic sequences by nucleic acid amplification techniques [Guzman and Kouri, 1996; Alcon et al., 2002; Chutinimitkul et al., 2005]. Virus isolation by cell culture is the most traditional method, the process needs more than seven days, and it has generally been unsuccessful owing to the low level of transient viremia associated with the disease process. Using antibody-dependent method as immuno-fluorescence [Zhang et al. 2006; Alves et al. 2007], immuno-immobilization [Drosten et al. 2002; Kwakye S and Baeumner, 2003], enzyme-linked immuno-sorbent assay (ELISA) [Russell et al. 2007; Dos Santos et al. 2007] immunomagnetic separation [Lien et al. 2007; Aytur et al. 2006], etc. can detect dengue virus and the antibody recognize the specific antigen also can differenate dengue virus from four serotype. In current, real-time PCR also the most well-know tool for detecting dengue virus at acute phase, and combining with fluorogenic probes are designed to identify dengue serotype, resulting in high sensitivity and specificity [Laue et al., 1999; Callahan et al., 2001; Houng et al., 2001; Shu et al., 2003]. Although real-time PCR is sensitively, however the fluorescent-labeled probe and detecting by sophisticated optical instrument also restrict this

technology to use universally.

6. Research approaches

Biosensors are devices that detect biological or chemical complexes in the form of antigen-antibody, nucleic acids, enzyme-substrate, or receptor-ligand compounds. Interest in using biosensors to detect clinical diagnosis is on the rise. Piezoelectrical Quartz crystal microbalance (QCM) is novel approaches in biosensors and rapid diagnostic assay. The QCM is microgravimetric sensor that stabilizes resonance frequency change via piezoelectric effect. The QCM is a promising candidate for biosensor applications, and its potential for the detection of DNA hybridization has been demonstrated recently. Although the QCM has a high inherent sensitivity (capable of measuring sub-nanogram levels of mass changes), methods for improving the detection limit of this device are being sought to enable wide application of the technique for DNA hybridization detection. Nanoparticles are effective amplifiers used in the QCM DNA detection because of they have a relatively large mass compared to the DNA targets. In the QCM DNA detection, the nanoparticles offers substantial improvement in the detection limits with sensitivity from 10^{-12} to 10^{-14} M of DNA. The sensitivity can in some cases be improved by using QCM crystals of higher frequencies or by amplification of the nucleic acids to increase the concentration of the analyte DNA by polymerase chain reaction (PCR). However, these two methods have practical limitations, particularly in the development of automated biosensor systems for genetic detection: QCM devices of higher frequencies (> *ca*. 9 MHz) are often difficult to operate in liquids because of frequency stability problems, while use of PCR can be laborious and time consuming and requires a number of manipulations. Amplifications of QCM gene sensors by adsorption of an anti-ds-DNA antibody to the formed ds-DNA complex or using dendritic nucleic acid as sensing probes have been reported. However, application QCM sensor detection real sample is not demonstrate, the major problem is not enough sensitivity.

One of the “nanogold amplifier” methods utilizes DNA-capped gold nanoparticles (AuNPs) for signal amplification. Coupled with the DNA targets, nanoparticles act as “mass enhancers”, extending the limits of QCM DNA detection. A nanoparticle- amplified QCM DNA sensor using the sandwich hybridization of two specific probes has been demonstrated; however, the method used for real sample detection has not previously been described.

In this study, we purpose to develop a real-time circulating- flow DNA sensor by QCM

and improve probe hybridization efficiency with target to detect DNA sequence. Furthermore, AuNPs will be introduces to QCM DNA sensor for amplify signal and reduce the limitation on detection in QCM biosensors. Here, we purpose an approach for the quantification of *E. coli* O157:H7 and dengue virus that combines QCM detection with a DNA chip. The system design for the rapid, sensitive detection of bacterial cells or virus, such as *E. coli* O157:H7 and dengue virus, utilizing AuNPs, functionalization probe and QCM DNA biosensor.

7. Materials and methods

7.1 For *E. coli* O157:H7 detection

7.1.1 Chemicals

The chemicals, 30% hydrogen peroxide (H_2O_2), sodium phosphate (Na_2HPO_4) and hydrogen chloride (HCl) and 98% sulfuric acid (H_2SO_4) were purchased from Merck (Darmstadt, Germany). The chemicals, sodium chloride (NaCl) and sodium hydroxide (NaOH) were purchased from Sigma-Aldrich (St. Louis, MO).

7.1.2 Oligonucleotide primers, probes and targets

All oligonucleotides were designed using Primer Express software (Applied Biosystems, Foster, CA, USA), and synthesized by Applied Biosystems including ssDNA of probes, targets as well as PCR primers **(Table 7-1)**.

In the detection for *E. coli* O157:H7 gene *eaeA* (Genbank U32312) [Call et al., 2001], the specific Probe 1 oligonucleotides modified with thiol-linkered tag [HS-$(CH_2)_6$] at 3' end with or without additional of 12 or 24 deoxythymidine 5'-monophosphates (12 dT or 24 dT; /12T or /24T), including P1-30 (30-mer), P1-30/12T (42-mer), and P1-30/24T (54-mer), were designated. These probes were used for immobilization on the Au surface of the QCM sensor to detect target DNA. The second probes (Probe 2) were used to cap the Au nanoparticles (Sigma-Aldrich) and also to detect and verify the *eaeA* sequences of *E. coli* O157:H7. Probe 2 included P2-30(AS) (30-mer; AS, anti-sense strand, complementary to the target sequences), P2-30/12T (AS) (42-mer), and P2-30(S) (30-mer; S, sense strand,

non-complementary to the target sequences).

The synthesized target (T) sequences included complementary target oligonucleotides, T-104(AS) (104-mer) and non-complementary target oligonucleotides, T-104(S) (104-mer).

For PCR-amplified DNA from real samples, the primer pair (E_{157}eae/F and E_{157}eae/R) specific for the *E. coli* O157:H7 *eaeA* gene was designed and used for amplification of the target DNA fragments (104-bp). Sequences of double strands (ds) of the PCR-amplified DNA were the same as the synthesized target sequences, T-104(AS) and T-104(S).

7.1.3 Culture preparation

E. coli O76:H8 (ATCC 23536), *E. coli* O85:H1 (ATCC 23539), *E. coli* O138:H14 (ATCC 23545), *E. coli* O142:H6 (ATCC 23985), *E. coli* O157:H7 (ATCC 43894), *Listeria monocytogenes* (ATCC 19114), *Salmonella choleraesuis* (ATCC 13311), *Staphylococcus aureus* (ATCC 10832), and *E. coli* K12 (ATCC 15153) were obtained from the American Type Culture Collection (Manassa, VA). *E. coli* O157:H7 and *Listeria monocytogenes* cultures were grown in brain heart infusion broth (Difco Laboratories, Detroit, MI) and the other bacteria were cultured in nutrient agar broth (Difco). Bacterial counts were determined by conventional spread-plating method using tryptic soy agar (Difco).

7.1.4 Food sample studies

Apple juice. *E. coli* O157:H7 cells were artificially inoculated into apple juice, and then 1 ml of the mixture was pipetted into a microtube and centrifuged at 12,000 × *g* for 10 min. The bacteria-containing pellet was suspended in 1 ml of phosphate buffer saline (PBS) and centrifuged again at 12,000 × *g* for 10 min. The pellet was finally resuspended in 1 ml of PBS and used for genomic DNA extraction [Yamaguchi et al., 2003].

Milk. *E. coli* O157:H7 cells were artificially inoculated in 1 ml of pasteurized milk. The bacterial cells were then isolated from the milk and used for genomic DNA extraction. The method reported by Yamaguchi et al. [2003] was used to dispose of lipids and proteins from the milk ingredients to isolate *E. coli* O157:H7. Firstly, proteinase K (Promega, Madison, WI) and 50 µl of 0.1% Triton X-100 were added to 100 µl of milk, and the milk samples were incubated at 37°C for 1 h to eliminate protein and lipid components. After incubation, 900 µl of 150 mM NaCl was added and then the mixture was centrifuged at 12,000 × *g* for 10 min. The pellet containing bacteria cells was collected after the

centrifugation. The pellet was suspended in 1 ml of 150 mM NaCl and centrifuged again at 12,000 × g. The pellet was finally resuspended in 150 mM NaCl and used for genomic DNA extraction.

Ground beef. One g of ground beef was artificially inoculated with the cells of *E. coli* O157:H7. After 30 min of inoculation, the sample was added into a tube containing 10 ml of PBS. Samples in the tube was mixed by vortex and centrifuged at 125 × g for 10 min. The middle layer of solution in the tube was removed and pipetted, and then transferred to a microtube. The sample was centrifuged at 12,000 × g for 10 min and the bacteria-containing pellet was resuspended in PBS for genomic DNA extraction [Yamaguchi et al., 2003].

In addition to the food samples, *E. coli* O157:H7 cells were also inoculated in PBS for bacterial detection as positive controls.

7.1.5. DNA extraction

Total genomic DNA was extracted from *E. coli* O157:H7 using the Wizard™ Genomic DNA Purification Kit (Promega, Madison, WI). For each DNA preparation, a pellet containing approximately 1 x 10^6 CFU/ml cells was resuspended in 600 µl of Nuclei Lysis Solution and incubated at 80°C for 5 min to lyse the cells. Three microliters of RNase Solution was added to the cell lysate and treated for 30 min. Two hundred microliters of Protein Precipitation Solution was added to the RNase-treated cell lysate and the DNA extraction was carried out as according to the manufacturer's protocol for bacteria (Promega). The purified DNA was examined by gel electrophoresis (0.8% agarose) and quantified by determining A260 (OD_{260}) with a SpectraMax 190 spectrophotometer (Molecular Devices Corp., CA).

7.1.6 PCR Conditions

For detection of real samples of *E. coli* O157:H7, a 104-bp DNA fragment within the *E. coli* O157:H7 *eaeA* gene was amplified by the synthetic primers (E_{157}eae/F and E_{157}eae/R) indicated in **Table 7-1**. A PTC-100™ thermal cycler (MJ Research Inc., NV) was used with 10X reaction buffer, dNTP (deoxynucleoside triphosphate) concentrated set solution, and Super Taq DNA polymerase (all obtained from HT Biotechnology Ltd, Cambridge, England).

PCR reactions contained 2 µl of genomic DNA, 2 µl forward and reverse primers (final

concentration was 1 μM for each primer), 5 μl of 10x PCR buffer (100 mM Tris HCl [pH 9.0], 15 mM $MgCl_2$, 500 mM KCl, 1% [v/v] Triton X-100, and 0.1% [w/v] gelatin), 2 μl of 10 mM dNTP, 1 μl of 0.5 U Super Taq DNA polymerase, and 38 μl distilled water in a total volume of 50 μl. PCR conditions were as follows: initial denaturation at 94°C for 5 min, followed by 32 cycles of denaturation at 94°C for 30 s, annealing at 55°C for 30 s, and elongation at 72°C for 30 s, and final extension at 72°C for 3 min. The PCR products were purified in a total volume of 50 μl TE buffer using Wizard™ PCR Preps DNA Purification System (Promega) according to the manufacturer's protocol and then visualized on 2.5% agarose gels stained with ethidium bromide under UV light. The concentration of DNA in the samples was measured by UV-absorption spectrophotometer at a wavelength of 260 nm.

The PCR-amplified DNA was sequenced to confirm the sequence using E_{157}eae/F and E_{157}eae/R as primer. Both strands of the DNA fragment were sequenced using a Taq DyeDeoxy Terminator Cycle Sequencing Kit and ABI Prism 373A DNA Sequencer (Applied Biosystems).

7.1.7 The circulating-flow QCM system

The piezoelectric quartz crystals which consist of a 9 MH_Z AT cut quartz crystal slab with a layer of a gold electrode on each side were (0.091 cm^2 in area on each side; the detection limit of the QCM instrument in liquid = 1 Hz) obtained from ANT Technology Co., Ltd. (Taipei, Taiwan). The flow injection and continuous frequency variation recording were operated using Affinity Detection System (ADS; ANT Technology Co., Ltd.). The system had five main components including electronic oscillation circuit, frequency counter, piezoelectric quartz of fixed biosensor molecule (p-chip), circulating-flow system, and a computer to demonstrate the curve of frequency change (ΔF) in real time (**Figure 7-1A**). The experimental data were analyzed by P-Sensor software in real time. The sensor unit was composed of resolution: 0.1 Hz, sampling period: 1 s, frequency range: 2~16 MHz, temperature range: 4~60°C, and voltage: 110 V, 50~60 Hz. The reaction cell was one sensor signal channel with 30 μl of reaction cell volume. The circulating-flow system consisted of a temperature controller, sample tubes, pipelines, and one tubing pump with a flow rate: 10~200 μl/min and a sample loop volume of 150 μl.

7.1.8 Gold-QCM device preparations

The gold electrode surface of the QCM device was cleaned with distilled water for 2–3 min. The water droplets on the surface of the electrode were then blown dry using an air gun. The gold electrode surface was subsequently cleaned with a piranha solution consisting of H_2O_2 (30%) and H_2SO_4 (98%) in a 1:3 ratio. It was then thoroughly wished with distilled water, dried with the air gun, and used immediately afterwards. The cleaning procedures with piranha solution and distilled water removed organic compounds adhered to the gold surface and enhanced the efficiency of immobilization when the thiolated DNA probes covalently attached to the gold surface [Cho et. al., 2004; Su et. al., 2004].

7.1.9 Immobilization of the oligonucleotide probes and hybridization with oligonucleotide targets

The gold-QCM device was inserted into the flow injection ADS. The importing and exporting pipeline ends were placed in the sample tube to create a circulating-flow system **(Figure 7-1A)**. The phosphate buffer (1 M NaCl and 1 mM Na_2HPO_4, pH 7.4) was flushed through the system at the speed of 50μl/min. With the frequency of the chip steady at 300 s, ΔF within ± 1 Hz/100 s, the solution containing specific probe sequences (5'-thiolated: P-30-SH, P-30/12T-SH or non-thiolated: P-30, P-30/12T; **Table 7-1**) for detecting the *E. coli* O157:H7 gene *eaeA* was added to the sample tube (total volume: 500 μl). The probes were self-assembly immobilized on the gold electrode through the flow-circulation for 30 min. After immobilization of the probes, the sample tube containing the probes was removed. The circulating pipeline was cleaned by flowing through the phosphate buffer for 15 min to remove unbound probes on the gold surface and probe residues in the pipeline. The gold-QCM device was then exposed with the sample flow (total volume: 500 μl) containing target sequence (T-30S, T-30AS, T-104S, or T-104AS; **Table 7-1**). Hybridization of probes and targets in the QCM device was at a flow speed of 50 μl/min for 30 min. The temperature of the QCM system was maintained at 30°C except in the study of temperature effects on the hybridization. The Δ*F* during the hybridization were recorded in a real-time observation.

In these experiments, different concentrations of the probe oligonucleotides (0, 0.25, 0.5, 1.0, and 2.0 μM) were evaluated for the efficiency of immobilization on the gold surface of the QCM device. The influence of varying concentrations of the target oligonucleotids on ΔF and hybridization efficiency (H%) were also compared. The Δ*F* was observed in a real-time continuous reading and reported as the difference between the final value and the

value before the hybridization or immobilization. The H% was calculated by dividing the hybridized target coverage by the immobilized probe coverage [Su et al., 2005]. The mass of immobilized probes as well as hybrid DNA of probes and targets on the QCM device was calculated using Sauerbrey's equation [Kanazawa and Gordon II, 1985],

$$\Delta F = -F_0^{3/2}\left(\frac{\rho_l \eta_l}{\pi \rho_q \mu_q}\right)^{1/2} \qquad (1)$$

where ΔF is the measured frequency shift, F_0 is resonant frequency of the unloaded crystal, ρ_l is the density of liquid in contact with the crystal, η_l is the viscosity of liquid in contact with the crystal, ρ_q is the density of quartz (2.648 g cm^{-3}), and μ_q is the shear modulus of quartz, 2.947 x 10^{11} g cm^{-1}·sec^{-2}. The frequency change of 1 Hz corresponds to a mass change of 0.391 ng.

For detection of PCR-amplified DNA of *E. coli* O157:H7 gene *eaeA*, the thiolated probe, P-30/12T-SH (1 μM), was used. The double-strand sequences of the PCR-amplified DNA were the same as the synthetic sequences of 104 mer targets, T-104AS and T-104S **(Table 7-1)**. Before the PCR-amplified DNA was applied into the circulating-flow QCM system, the DNA was treated in a denaturing solution (TE and 0.5 M NaCl) at 95°C for 5 min. The denatured DNA was then applied to the circulating-flow QCM system following the same procedure used for synthetic target oligonucleotides. Temperature effects (20, 30, 40, 50, and 60°C) on the DNA hybridization (hybridization buffer: 1.0 mM Na_2HPO_4 and 1.0 M NaCl) during the circulating-flow detection were evaluated. In each hybridization, 1 μM of PCR-amplified DNA (equivalent to 1 μM of the target T-104AS) was used to hybridize with the thiolated probes immobilized on the QCM device.

7.1.10 Probe oligonucleotide–nanoparticle conjugates

Suspensions of Au nanoparticles with an average diameter of 20 nm, which were synthesized by reduction of $HAuCl_4$ solution with sodium citrate, were obtained from Sigma-Aldrich. Preparation of probe oligonucleotide-Au nanoparticle conjugates was carried out as previously described [Li et al., 2006; Goodrich et al., 2004; Mirkin et al. 1996]. Briefly, 50 μl of freshly purified 100 μM thiolated oligonucleotides was added to 800 μl of the Au nanoparticle solution in an Eppendorf tube. The tube was then placed in a heat block at 37°C for a minimum of 4 h before the addition of 230 μl of H_2O and 120 μl of 1 M NaCl/100

mM phosphate buffer (Na_2HPO_4, pH 7.4). After aging overnight at 37 °C, excess oligonucleotides were extracted by centrifugation at 9,500 rpm (7,500 × g) for 50 min with the removal of supernatant and resuspension of the Au pellet in 0.1 M NaCl/10 mM phosphate buffer (pH 7.4). These procedures were repeated three times. After the final centrifugation, the Au pellet was resuspended in 0.3 M NaCl/10 mM phosphate buffer (pH 7.4) with a final concentration of 10 nM. This concentration was obtained from UV-vis spectroscopy using an extinction coefficient of 1.94×10^8 /M· cm, as described previously by Goodrich et al. [Goodrich et al., 2004].

7.1.11. Immobilization of different length probe oligonucleotides and hybridization with target sequences

The QCM sensor was inserted into the QCM system. The importing and exporting pipeline ends were placed in the sample tube to create a circulating-flow system. The buffer of 1 M NaCl and 1 mM phosphate (pH 7.4) was flushed through the system at the speed of 50 µl min^{-1}. With the frequency of the sensor steady at frequency change within ± 1 Hz/5 min, the solution containing specific probe sequences (3'-thiolated Probe 1: P1-30, P1-30/12T, and P1-30/24T; **Table 7-2**) for detecting *E. coli* O157:H7 gene *eaeA* was added to the sample tube (total volume of reactive buffer: 500 µl). The probe oligonucleotides were self-assembly immobilized on the Au electrode surface through the flow-circulation for 30 min. After immobilization of the probes, the probe solution in the sample tube was removed. The circulating pipeline was cleaned by flowing through the buffer for 15 min to remove unbound probes on the Au surface and probe residues in the pipeline. The QCM sensor was then exposed with the sample flow (500 µl) containing target oligonucleotides T-104(S), T-104(AS), or PCR-amplified DNA (**Table 7-2**). The sample flow was circulated for about 30 min with a flow speed of 50 µl min^{-1} allowing hybridization of probes and targets on the QCM sensor. Temperature of the QCM system during DNA hybridization was maintained at 30 °C. Before applying the PCR-amplified DNA, it was heat-denatured at 95°C for 5 min and then immediately introduced into the sample tube of QCM system for detection. The frequency shift during the hybridization was recorded in a real-time observation.

7.1.12 Sandwich hybridization by oligonucleotides capped with Au nanoparticles

The PCR-amplified DNA was prepwered in the buffer of 1 M NaCl and 1 mM phosphate

(pH 7.4), heat-denatured, and then applied onto the Probe 1 (**Table 7-2**) immobilized QCM sensor for DNA hybridization. After 30 min of DNA hybridization, frequency of the QCM sensor was steady (frequency change within ± 1 Hz/5 min), excess PCR-amplified DNA in the sample tube was removed and the circulating pipeline was cleaned by circulating buffer for 15 min to remove unhybridized DNA in the pipeline. The QCM sensor was then exposed with the sample flow (total volume: 500 μl) containing the 1.0 μM of Probe 2-capped (**Table 7-2**) with Au nanoparticles. Sandwich hybridization of the DNA immobilized on the QCM sensor was performed for 20~30 min with a flow speed of 50 μl min^{-1}. The frequency change during the hybridization was recorded in a real-time observation. The temperature of the QCM system was maintained at 30°C.

7.1.13 Data analysis

The experimental data were analyzed by P-Sensor software of the ADS system in real time. Each experiment was repeated 5 times using five different QCM devices to test the reproducibility of the QCM sensor. All data were presented as the mean ± standard deviation (SD). Differences between groups were evaluated by a two-tailed Student's *t*-test. *P*-values less than 0.05 were considered to be statistically significant differences.

7.2 For dengue virus detection

7.2.1 Chemicals and reagents

The chemicals and reagents used in the study were purchased from Merck (Darmstadt, Germany) and Sigma-Aldrich (St. Louis, MO, USA). These included 30% hydrogen peroxide (H_2O_2; Merck), 98% sulfuric acid (H_2SO_4; Sigma-Aldrich), sodium chloride (NaCl; Sigma-Aldrich), sodium phosphate (Na_2HPO_4; Merck), hydrogen chloride (HCl; Merck), sodium citrate ($C_6H_5Na_3O_7 \cdot 2H_2O$; Merck), chloroauric acid ($HAuCl_4$; Sigma-Aldrich), and sodium hydroxide (NaOH; Sigma-Aldrich).

7.2.2 Oligonucleotide primers, probes and targets design

All of oligonucleotides were designed using Primer Express software (Applied Biosystems, Foster, CA, USA), and synthesized by Applied Biosystems. The characteristics of the synthesized oligonucleotides were listed in **Table 7-3**, which includes single-stranded

DNA of probes (P), target (T) and primers for reverse transcription (RT) and PCR. For the detection of gene sequence encoding envelope (E) protein of DENV2 (GenBank DQ341195), the specific probe sequences, DENV2-P1 and DENV2-P2 that were modified with thiol-linkered tag (HS-$(CH_2)_6$; -SH) and with additional 12 deoxythymidine 5'-monophosphate (12-dT) at 3' terminus and 5' terminus were synthesized, respectively. The synthesized target oligonucleotide was the sequence being complementary to the probe oligonucleotides. In order to amplify the E gene fragment from all of four dengue serotypes, DENV serotype 1 (DENV1), DENV2, DENV serotype 3 (DENV3) and DENV serotype 4 (DENV4). A pair of universal primer (DENV-UF and DENV-UR) was designed at the conserve domains of E gene among the dengue serotypes. A target DNA fragment in length of 130 bp could be obtained by RT-PCR amplification with DENV-URT as RT primer, and DENV-UF and DENV-UR as PCR primer pair. The internal sequences of amplified DNA fragments (i.e., target sequences) from four DENV serotypes, DENV1-4, were diverse; therefore, the specific probe sequences designed according to this diverse domain could be used to differentiate their complementary target sequences from the four DENV serotypes via DNA hybridization.

7.2.3 Culture preparation of dengue virus

The DENV was transfected and amplified in mosquito cell, *Aedes albopictus* cells C6/36 (ATCC number CRL 1660™) that was obtained from Food Industry Research and Development Institute (Hsinchu, Taiwan). C6/36 cells were grown in minimum essential medium (MEM) (Gibco, Grand Island, NY, USA) and supplemented with 10% fetal bovine serum (FBS) (Gibco, Grand Island, NY, USA) at 27°C in a humidified incubator with 5% CO_2. The parental PL046 DENV, DENV2, was originally obtained from Prof. Huan-Yao Lei (National Cheng Kung University, Tainan, Taiwan). Stock of PL046 DENV was amplified in C6/36 cells, concentrated via ultracentrifugation, and titrated by plaque assays as previously described [Chen et al., 2001; Shresta et al., 2004]. The virus titers were adjusted to 2×10^6 PFU/mL in MEM with 10% FBS. The virus concentrate was stored at -80°C before use.

7.2.4 Plaque forming unit assay of DENV

Viral PFU assay was performed in BHK-21 cells (ATCC number CCL-10™) [Liu et al. 2008]. BHK-21 cells (3×10^5/mL) suspended in MEM were seeded into each 6-well culture

plate (Nalge Ncnu, Rochester, NY, USA) and incubated at 37°C in a humidified incubator with 5% CO_2. The cells were cultured overnight before virus adsorption. A series of viral dilutions made in the culture medium at 0.4 mL were adsorbed onto the monolayer of BHK-21 cells for 1 hour at 37°C, and every 30 min wavered slightly to make virus adsorption on BHK-21 uniformly. Each virus-infected culture well was overlaid with 4 mL of 1.1% carboxylmethyl cellulose containing 5% FBS for an additional 6 days. The plaque-forming wells were fixed with 3.7% formalin for 30 min followed by staining with 0.5% crystal violet in 3.7% formalin. Results were calculated by counting plaques on the four replicate wells.

7.2.5 Dengue virus RNA extraction

DENV RNA was extracted by ALS Viral Nucleic Acid Extraction System (ALS, Kaohsiung, Taiwan). For each RNA preparation, 150 μL supernatant of DENV infected cells were mixed with 570 μL VRE buffer and incubated at room temperature for 10 min to lyse the virus. Thirty microliters of 400 U/μL DNase solution was added to the lysate and treated for 30 min, and then the viral RNA extraction was carried out according to the manufacturer's protocol for virus (ALS). For each preparation, a total of 50 μL of viral RNA was eluted from the RNA purified column and quantified by determining OD_{260} with a SpectraMax 190 spectrophotometer (Molecular Devices Corp., Sunnyvale, CA, USA). The viral RNA was stored at -80°C until use.

7.2.6 Dengue virus cDNA preparation

The DENV cDNA was prepared by RT using ReverTra Ace (TOYOBO, Osaka, Japan). Ten microgram of DENV RNA was used as template to prepare cDNA and synthesized oligonucleotide, DENV-URT, as primer. The RT reaction was carried out in PTC-100™ thermal cycle (MJ Research 171 Inc., Watertown, MA, USA) with the following program: extension at 52°C for 30 min and followed by inactivating RT enzyme at 99°C for 5 min.

7.2.7 Asymmetric PCR amplification

For detecting the DNA sequences of DENV E gene, asymmetric PCR was used to amplify the target DNA (130 bp) for direct hybridization detection [Giakoumaki et al., 2003]. The ratio of forward primer (DENV-UF) and reverse primer (DENV-UR) concentration was

5:1, and the lower concentrated reverse primer acted as a “limiting primer”. Double-stranded target DNA fragments were produced when both primers were present in PCR mixture at the beginning steps of reaction. However, after the limiting primer was consumed, the remaining primer (forward primer) continued to amplify the target DNA, which resulted in the PCR products predominantly being single-stranded E gene fragments. The PCR reaction was carried out in PTC-100^{TM} thermal cycle (MJ Research 171 Inc.) with the following program: DENV cDNA was initially denatured at 95°C for 3 min, followed by 40 cycles of 30 sec denaturation at 95°C, 20 sec annealing at 53°C, 30 sec extension at 72°C, and 5 min final extension 72°C. One microliter of DENV cDNA (1 μg), 1 μL forward (25 μM), 1μL reverse primers (5 μM) and other components were added for the 50 μL PCR reaction mixture followed the instruction of PCR reagent (BerTaq DNA Polymerase, Bertec, Taipei, Taiwan). Following amplification, the PCR products were purified by Wizard^{TM} PCR Preps DNA Purification System (Promega, Madison, WI, USA) according to the manufacturer’s protocol and then performed electrophoresis follow by visualizing through UV transilluminator (Apices Scientific Co., Ltd, MA, USA). The DNA concentration of PCR-amplified products was determined spectrophotometrically (Agilent Technologies, Palo Alto, CA, USA) at 260 nm.

7.2.8 The circulating-flow QCM system

The circulating-flow QCM system was applied as our previous reports [Wu et al., 2007; Chen et al., 2008]. The piezoelectric quartz crystals, which was consisted of a 9 MHZ AT cut quartz crystal slab with a layer of a gold electrode on each side were (0.091 cm^2 in area on each side; the detection limit of the QCM instrument in liquid = 1 Hz) obtained from ANT Technology (Taipei, Taiwan). The flow injection and continuous frequency variation recording were operated using Affinity Detection System (ADS; ANT Technology). The experimental data were analyzed by P-Sensor software in real-time. The sensor unit was composed of resolution as 0.1 Hz, and sampling period as 1 sec. The oscillatory frequency change (ΔF) of 1 Hz corresponds to a mass change of 0.391 ng.

Before experiments, the gold electrode surface of QCM chip was pretreated with hot piranha solution (concentrated H_2SO_4 and 30% of H_2O_2, 3:1 v/v). After an incubation period of 1 min with piranha solution, the QCM chip was thoroughly rinsed with distilled water and air-dried subsequently [Fohlerová Z et al. 2006]. This procedure was repeated twice and immersed in distilled water [Cho et al., 2004; Su et al., 2004].

7.2.9 AuNPs preparation and oligonucleotide-modification

The colloidal gold was prepared by reduction of 0.01% $HAuCl_4$ with 38.8 mM sodium citrate aqueous solution, while the monodispersed AuNPs of different sizes (5, 13, 20, and 50 nm in diameter) were obtained by the same procedure with different amounts of sodium citrate [Link and El-Sayed, 1999; Li et al ., 2005]. The sizes of AuNPs were checked by scanning electron microscopy (SEM) images with a JEM 100 CX electron microscope (JEOL Co. Ltd., Tokyo, Japan) at 25 kV and the AuNPs average diameter was estimated by dynamic laser scattering (DLS) (TPCL, Chu-Pei, Taiwan). The AuNPs were functionalized with DENV2-P1 or DENV2-P2 at 37°C for 60 min [Sarah et al., 2006]. To steady the AuNPs-probes and increase the probe oligonucleotides loading onto the AuNPs, the concentration of NaCl was increased to 0.3 M using phosphate buffer (1 M NaCl and 10 mM Na_2HPO_4, pH 7.4). The process was, add 20 μL of 0.05, 0.1, 0.2 and 0.3 M NaCl diluted step by step from PBS buffer (1 M NaCl, 1 mM Na_2HPO_4, pH 7.4) for 6 h, respectively., Then, the AuNPs-probe solution was dispelled for 10 sec by vortex when every 6-hour incubation period at 4°C. To remove excess oligonucleotides, the AuNPs-probes were centrifuged and the supernatant was removed. The precipitated AuNPs-probes then were resuspended in 0.3 M phosphate buffer.

7.2.10 Immobilization of probes, hybridization, and signal amplification by AuNPs-probes

Figure 7-1A shows schematic illustration of the procedures of probe oligonucleotides immobilization, DNA hybridization of probes and targets, and signal amplification of detection in the DNA-QCM system by layer-by-layer AuNPs-probes via target sequences. In the procedure, the phosphate buffer was firstly flushed through the QCM chip at a flow speed of 50 μL/min and began the study while the frequency of the chip steady within ΔF within ± 1 Hz/300 sec. The solution containing specific probe sequences (3'-thiolated DENV2-P1; **Table 7-3**) for detecting the sequences of DENV E gene was added to the sample tube (total volume: 500 μL). The probe oligonucleotides were self-assembly immobilized onto the gold surface of QCM chip through the flow-circulation for 10 min. After probe immobilization, the probe solution was removed and then the solution containing target sequences was added. Hybridization of probe and target sequences on the QCM chip was at

a flow speed of 50 μL/min for 10 min. The temperature of the QCM system was maintained at 30°C. The ΔF during the hybridization was recorded in a real-time observation. After target-probe hybridization, the 1st layer of AuNPs-DENV2-P2 (the AuNPs conjugated with DENV2-P2; the sequences of DENV2-P2 were complementary with 3' terminus of the target sequences) was added to enhance the mass on the QCM chip. Following, the AuNPs-DENV2-P1 (the AuNPs conjugated with DENV2-P1; the sequences of DENV2-P1 were complementary with 5' terminus of the target sequences) was added to specifically link the surplus (not hybridized) target sequences in the reaction. The 2nd layer of AuNPs was formed as AuNPs-DENV2-P2/ Target/ AuNPs-DENV2-P1 conjugant to amplify the detection signal.

8. Part I:

Real-time detection of *E. coli* O157:H7 sequences using a circulating- flow system of quartz crystal microbalance

8.1 Abstract

A DNA piezoelectric biosensing method for real-time detection of *Escherichia coli* O157:H7 in a circulating flow system is developed in this study. Specific probes [a 30-mer oligonucleotide with or without additional 12 deoxythymidine 5'-monophosphate (12-dT)] for the detection of *E. coli* O157:H7 gene *eaeA*, synthetic oligonucleotide targets (30 mer and 104 mer) and PCR amplified DNA fragments from the *E. coli* O157:H7 *eaeA* gene (104 bp), are used to evaluate the efficiency of the probe immobilization and hybridization with target DNA in the circulating-flow quartz crystal microbalance (QCM) device. It is found that thiol modification on the 5' end of the probes is essential for probe immobilization on the gold surface of the QCM device. The addition of 12-dT to the probes as a spacer, significantly enhanced ($P < 0.05$) the hybridization efficiency (H%). The results indicate that the spacer enhanced the H% by 1.4- and 2-fold when the probes are hybridized with 30-mer and 104-mer targets, respectively. The spacer reduced steric interference of the support on the hybridization behavior of immobilized oligonucleotides, especially when the probes hybridized with relatively long oligonucleotide targets. The QCM system is also applied in the detection of PCR-amplified DNA from real samples of *E. coli* O157:H7. The resultant H% of the PCR-amplified double-strand DNA is comparable to that of the synthetic target T-104AS, a single strand DNA. The piezoelectric biosensing system has potential for further applications. This approach lays the groundwork for incorporating the method into an integrated system for rapid PCR-based DNA analysis.

Keywords: *E. coli* O157:H7, quartz crystal microbalance, DNA biosensor, foodborne pathogens

8.2 Introduction

Escherichia coli O157:H7 has been an important foodborne pathogen in a variety of foods worldwide in the last twenty years. It is classified as an enterohemorrhagic *E. coli* with the ability to cause hemorrhagic colitis which includes symptoms such as bloody diarrhea, hemolytic uremic syndrome, and thrombotic thrombocytopenic purpurea [Doyle et al., 1997]. Centers for Disease Control and Prevention [CDC, 2005] reported that an estimated 73,000 cases of *E. coli* O157:H7 infection and 61 resultant deaths occur in the United States each year. Consumption of as few as ten of *E. coli* O157:H7 cells can result in growth of the pathogen in the intestine and production of shiga toxins in susceptible patients. These toxins can kill the cells of the intestinal lining, destroy the kidneys and cause blood clots in the brain, as well as seizures, paralysis, and respiratory failure [FDA, 2001; CDC, 2005]. Therefore, it is desirable to develop efficient analytical methods with a high degree of sensitivity and specificity to detect this organism in food.

Detecting *E. coli* O157:H7 with conventional procedures can take several days [Meng et al., 2001]. A variety of rapid methods has been proposed to detect and screen many microorganisms, including *E. coli* O157:H7. These methods include antibody-based methods (immunofluorescence, immunoimmobilization, enzyme-linked immunosorbent assay, immunomagnetic separation, etc.), nucleic acid-based methods (hybridization and polymerase chain reaction [PCR]), biochemical and enzymatic methods (miniaturized microbiological methods and commercial miniaturized diagnostic kits), and membrane filtration methods (hydrophobic grid membrane filter) [Wu et al., 2004]. In recent years, modern bio-techniques such as real time PCR [Yoshitomi et al., 2003; Fu et al., 2005], nanoparticles [Zhao et al., 2004; Mao et al., 2006] and biosensing systems (biosensors) [Campbell and Mutharasan, 2005; Simpson et al., 2005; Mao et al., 2006] have been developed for detection of pathogenic microorganisms. Biosensors are devices that detect biological or chemical complexes in the form of antigen-antibody, nucleic acids, enzyme-substrate, or receptor-ligand compounds. Interest in using biosensors to detect foodborne pathogens is on the rise [Hall, 2002; Patel, 2006; Rasooly and Herold, 2006].

DNA probes (i.e. an oligonucleotide sequence immobilized on a fixed support able to hybridize the complementary strand present in solution) are powerful molecular tools for monitoring and detecting specific microorganisms in the environment or in food [Marx, 2003; Mann and Krull, 2004]. The standard method of detecting nucleic acid hybrids is by labeling the probe with radioactive nucleotides, chemiluminescent dye, or various hapten

molecules, such as biotin. Piezoelectric mass-sensing devices based on quartz crystal microbalance (QCM) enable the label free detection of molecules, such as ligands, peptides, and nucleic acids [Marx, 2003].

The core of the QCM is a specifically manufactured quartz plate with a fundamental resonance frequency in the range of 5-30 MHz. The crystal is excited to resonance and the effect of molecular absorption monitored [Sauerbrey, 1959]. The QCM is comprised of thin film electrodes, usually gold (Au), deposited on each face of a crystal. Voltage is applied across these electrodes to deform the crystal plate, producing relative motion between the two parallel crystal surfaces. The crystal is induced to oscillate at a specific resonant frequency. Changes in the mass of the material on the surface will alter the resonance frequency of the crystal [Marx, 2003]. A linear relationship exists between deposited mass and frequency response for quartz crystals. The resonance frequency decreases linearly with the increase of mass on the QCM electrode at the nanogram level or less. This characteristic of QCM can be exploited to develop bioanalytical tools on a 10^{-10} to 10^{-12} g scale [Zhou et al., 2000]. QCM-based immunoassay has been designed and applied in several different areas [Su et al., 2000; Kurosawa et al., 2003; Su and Li, 2004]. Using QCM sensing, with an appropriate DNA probe immobilized on the sensor surface, it is possible to detect a specific target sequence without additional labeling procedures. The DNA-based sensors can be coupled with the PCR to increase the sensitivity of the systems and offer a viable alternative to gel electrophoresis and other traditional DNA sequences detection methods that require labeled probes. Currently, some QCM devices are capable of detecting label-free oligonucleotides and/or PCR-amplified DNA fragments [Deisingh and Thompson, 2001; Mo et al., 2002; Mannelli et al., 2003; Mao et al., 2006]. However, a DNA biosensing system for real-time detection of pathogens such as *E. coli* O157:H7 in food has yet to be fully developed.

The objective of the study is to develop a DNA piezoelectric biosensor, QCM, in a circulating-flow system for real-time detection and identification of *E. coli* O157:H7 sequences. We evaluated the enhancement of hybridization efficacy by adding an oligonucleotide spacer to the 5' end of a 30-mer probe. The specificity of the QCM system for synthesized targets of varying lengths (30 mer and 104 mer) and PCR-amplified DNA fragments (104 bp) from real samples of *E. coli* O157:H7 is explored.

8.3 Results and discussion

8.3.1 The QCM system and detection

In the circulating-flow QCM system, real-time frequency shift is recorded. The frequency decreased gradually with addition of oligonucleotides, reflecting immobilization of the probes, or hybridization of probes and targets on the gold surface of QCM. **Figure 7-1** shows an example of the real-time detection of the QCM system performed in our study. There is a 58 Hz decrease in series resonant frequency for immobilization of probes P-30-SH (30 mer), while probes P-30/12T-SH (42 mer) yielded a decrease of 75 Hz. There are decreases in series resonant frequency of approximately 42 and 51 Hz when complementary strands (T-30AS) are introduced and hybridized with P-30-SH and P-30/12T-SH, respectively.

In our circulating-flow QCM system, the thiolated probes are circulated constantly to ensure continuous interaction with the gold surface on QCM device thereby enhancing the efficiency of probe immobilization and the hybridization of probes and targets. The flow circulation also limits non-specific binding, recirculating unattached probes for immobilization.

8.3.2 Immobilization of synthesized oligonucleotide probes

In fabricating a DNA sensor, maximizing the immobilization of DNA on the sensor's surface is crucial. Therefore, various concentrations (0, 0.25, 0.5, 1.0, and 2.0 μM) of thiolated probes, with or without the addition of 12-dT [P-30-SH (30 mer) and P-30/12T-SH (42 mer)], are used to evaluate immobilization efficiency on the gold surface of QCM devices. The results showed that ΔF increased almost linearly with the increase of probe concentrations up to concentrations of 1.0 and 2.0 μM. Probe concentrations of 1.0 and 2.0 μM yielded the greatest covalent attachment to the gold surface compared with other concentrations ($P < 0.01$) (**Figure 8-1**). There is no significant difference between ΔF at concentrations of 1.0 and 2.0 μM ($P > 0.05$), indicating saturation of the immobilization sites on the gold surface of the QCM device. Therefore, the probe concentration of 1.0 μM is selected for the following experiments.

In general, the thiolated probes with additional 12-dT (P-30/12T-SH) showed greater ΔF ($P < 0.05$) than thiolated probes without additional 12T (P-30-SH) among the various concentrations tested (**Figure 8-1**). This is because the weight of P-30/12T-SH per single

molecule (13,155 g mol^{-1}) is larger than that of P-30-SH (9504 g mol^{-1}). According to the calculation by Sauerbrey's equation, the molecule densities of P-30-SH and P-30/12T-SH immobilized onto the gold surface of the QCM device are 1.7 ± 0.1 and 2.1 ± 0.2 (ssDNA/10 nm^2), respectively, when 1.0 μM of probes is used in the immobilization. These molecule density values show no significant differences ($P > 0.05$). Therefore, the efficiency of immobilization of P-30-SH and P-30/12T-SH onto the gold surface of the QCM is similar.

8.3.3 Detection of the short (30 mer) synthesized target oligonucleotides

Different concentrations (0, 0.25, 0.5, and 1.0 μM) of the short synthesized target oligonucleotides (T-30AS, 30 mer) complementary to the probes immobilized on the gold surface of QCM device are compared for the ΔF and H% in the circulating-flow QCM system. The ΔF due to hybridization increased with increasing concentrations of the targets up to 0.5 μM ($P < 0.01$) (**Figure 8-2A**). At concentrations ≥1 μM, the frequency shift is less sensitive, indicating the saturation of the probe hybridization sites (**Figure 8-2A** and data not shown). The H% also increased with increasing concentrations of the targets (**Figure 8-2B**). The H% of target T-30AS at 0.25 μM and 0.5 μM hybridized with the probe P-30/12T-SH are significantly higher ($P < 0.01$) than those of the target hybridized with probe P-30-SH. Results indicate the addition of 12-dT to the probes increased the H% in the QCM system.

According to the ΔF results, the probes are able to hybridize with their complementary sequences. The probes with the spacer (12-dT) influenced the hybridization with the target oligonucleotides [Shchepinov et al., 1997], and increased the hybridization efficiency in our circulating-flow QCM system. During DNA hybridization, spacers have been shown to reduce steric interference, making the probe end closet to the surface of the device more accessible [Shchepinov et al., 1997; Southern et al., 1999]. Spacers such as 12-dT also reduce steric hindrance in three-dimensional space and increase of molecule collision to increase H%.

8.3.4 Specificity of the QCM detection

We evaluated the DNA hybridizations among four probes (P-30-SH, P-30/12T-SH, P-30, and P-30/12T; 1 μM) and two targets (T-30AS and T-30S; 0.5 μM) (**Table 7-1.**). We compared the probes with or without thiol-linkered tag modification on the 5' end for

influencing the efficiency of probe immobilization on the gold surface of the QCM device and subsequent hybridization. The results indicate that non-thiolated probes (P-30 and P-30/12T) fail to attach covalently to the gold surface ($\Delta F < 2$Hz for 30 min), preventing the subsequent hybridization of probes and targets (**Figure 8-3A**). Non-specific binding is investigated using T-30S (a sense strand to the probe sequences, non-complimentary strand). The thiolated probes (P-30-SH, P-30/12T-SH) are covalently immobilized on the gold surface and specifically hybridized to the complementary targets (T-30AS), but not to the non-complementary targets (T-30S) (**Figure 8-3**). The target T-30S, as the negative control of hybridization in our QCM system did not yield a measurable frequency shift when applied to the probe-immobilized QCM device. Hybridization of surface-bound ssDNA is dependent on surface coverage and materials. The thiolated ssDNA has a more profound effect on surface coverage, such as with the gold in our system, than non-thiolated ssDNA [Herne and Tarlov, 1997; Levicky et al., 1998]. The hybridization of P_{157}30/12T-SH and T_{157}30AS showed greater ΔF ($P < 0.01$) (**Figure 8-3A**) and higher H% (**Figure 8-3B)** than the hybridization of P_{157}30/SH and T_{157}30AS, reflecting the reduction of steric hindrance in the three-dimensional space and the increase in molecule collisions caused by the additional 12-dT.

8.3.5 Detection of the long (104 mer) synthesized target oligonucleotides

The 104-mer synthesized targets (T-104AS and T-104S) are applied in the QCM system and the ΔF and H% are evaluated. Within the target of T-104AS, only the 30 mer sequences are complementary to the probes, P-30-SH and P-30/12T-SH (**Table 7-1**). As shown previously, no measurable frequency shift is detected when the targets are applied to the immobilized probes without thiol-linkered tag modification. Using T-104S, a non-complementary strand to the probes, non-specific binding is investigated. No measurable ΔF is detected when T-104S is applied to the probe-immobilized QCM. The ΔF (due to the hybridization), and the H% significantly increased ($P < 0.05$ or $P < 0.01$) with increasing concentrations (0.5 and 1 μM) of the target T-104AS (**Figure. 8-4A and 4B**). However, the frequency shift decreased when a relatively high concentration of T-104AS (2 μM) is applied for the hybridization with P-30/12T-SH, indicating the upper limit of hybridization and saturation of the probe hybridization sites.

In **Figure 8-2**, the results show that the 12-dT spacer enhanced the ΔF and H% by

approximately 1.4-fold when the probes hybridized with the 30-mer target T-30AS (0.5 μM). In **Figure 8-4**, the ΔF has a 2-fold increase when the 104-mer target T-104AS hybridized to the probe P-30/12T-SH instead of to the probe P-30-SH ($P < 0.01$). This phenomenon indicates that the 12-dT spacer has greater effects on the 104-mer targets than on the 30-mer targets in reducing steric interference during DNA hybridization. This result is confirmed by previous reports which showed that the addition of spacers to probes has a greater increase in hybridization efficacy when the probes hybridized to a longer rather than shorter target sequence [Herne and Tarlov, 1997; Levicky et al., 1998]. We infer that it is easier to form a bent sequence and generate surface inhibition on the gold surface of the QCM device when the target T-104AS molecules hybridize to the probe P-30-SH than to the probe P-30/12T-SH. This occurrence may obstruct entrance of other target sequences for hybridization (**Figure 8-6**).

Interestingly, the values of H% (20-25%) in the hybridization of the probe P-30/12T-SH with the 104-mer targets are significantly lower ($P < 0.05$) than those in the hybridization of the 30-mer targets at optimal conditions (85-95%) (**Figure 8-2B** and **Figure 8-3B**). This indicates that free fragments extending from the complementary region of the target obstructed the hybridization of the target sequences to their probes. In addition, long target oligonucleotides may produce the secondary structures due to hairpin formation in the hybridization conditions we used. Even though H% is reduced to 20-25% in the hybridization of the probe P-30/12T-SH and the 104-mer targets, the detectable ΔF reached 70-80 Hz, indicating that the sensitivity of our QCM system is sufficient to detect sequences such as the 104-mer targets that hybridized to the 30-mer probes.

8.3.6 Detection of PCR-amplified DNA of *E. coli* O157:H7 gene *eaeA*

The PCR-amplified DNA fragment is 104 bp and is located within the respective region of *E. coli* O157:H7 *eaeA* gene (**Figure 8-5A**). The PCR products are detected in real-time by the circulating-flow QCM system. The temperature effects on the hybridization of P-30/12T-SH and PCR-amplified DNA are indicated in **Figure 8-5B**. The results show that the ΔF equaled 70 ± 4 Hz when the system temperature is maintained at 30°C and is significantly higher ($P < 0.01$) than when the system is maintained at 20, 40, 50, and 60°C. The frequency shift of the QCM system for detecting PCR-amplified products is equivalent to that for detecting the synthetic target oligonucleotides, T-104AS.

The piezoelectric biosensor detected the presence of *E. coli* O157:H7 when the DNA strand is complementary to the immobilized probes with synthetic oligonucleotides. The system will be further applied in the detection of field samples or other sequences by employing various probes to be immobilized on the gold surface of the crystal. In conjunction with PCR application, the QCM sensor labeled with DNA probes can be used as a quantitative and highly sensitive assay. The optimal conditions of our QCM system use to detect the PCR-amplified DNA from the real sample has relative standard deviation values (% RSD) as low as 5.3%, which are considered acceptable among established analytical techniques [Skoog et al., 1998]. Our QCM device may be use to detect a single sequence, a single organism, or an entire community of environmental and food microorganisms with selectivity controlled by the choice of primers and primer annealing temperature for the PCR procedures.

8.3.7 Conclusions

We developed a DNA piezoelectric sensor for the real-time detection of *E. coli* O157:H7. Synthetic probe oligonucleotides are self-assembly immobilized on the sensor surface of the QCM device and the hybridization between the immobilized probes and the complementary sequences of the targets in solution is monitored in real-time. A spacer (12-dT) linked to the probes enhanced the detection signals because the spacer molecules reduced the steric interference of the support on the hybridization behavior of the immobilized oligonucleotides. The QCM system is also used to detect the PCR-amplified DNA from real samples. Our results suggest that the DNA piezoelectric sensor has potential for further applications in detecting *E. coli* O157:H7 as well as other microorganisms in food, water, and clinical samples. This approach lays the groundwork for incorporating the method into an integrated system for rapid PCR-based DNA analysis.

9. Part II:

Using oligonucleotide-functionalized Au nanoparticles to rapidly detect foodborne pathogens on a piezoelectric biosensor

9.1 Abstract

A circulating-flow piezoelectric biosensor, based on an Au nanoparticle amplification and verification method, is used for real-time detection of a foodborne pathogen, *Escherichia coli* O157:H7. A synthesized thiolated probe (Probe 1; 30-mer) specific to *E. coli* O157:H7 *eaeA* gene is immobilized onto the piezoelectric biosensor surface. Hybridization is induced by exposing the immobilized probe to the *E. coli* O157:H7 *eaeA* gene fragment (104-bp) amplified by PCR, resulting in a mass change and a consequent frequency shift of the piezoelectric biosensor. A second thiolated probe (Probe 2), complementary to the target sequence, is conjugated to the Au nanoparticles and used as a "mass enhancer" and "sequence verifier" to amplify the frequency change of the piezoelectric biosensor. The PCR products amplified from concentrations of 1.2×10^2 CFU/ml of *E. coli* O157:H7 are detectable by the piezoelectric biosensor. A linear correlation is found when the *E. coli* O157:H7 detected from 10^2 to 10^6 CFU/ml. The piezoelectric biosensor is able to detect targets from real food samples.

Keywords: Au nanoparticle, piezoelectric biosensor, *E. coli* O157:H7

9.2 Introduction

Enterohemorrhagic *Escherichia coli* O157:H7 is first recognized as a foodborne pathogen in 1982 during an investigation into an outbreak of hemorrhagic colitis associated with consumption of hamburgers from a fast food chain restaurant [Riley et al., 1983]. Since then, numerous cases have been reported around the world including a recent *E. coli* O157:H7 outbreak in spinach [CDC, 2006; FDA, 2006]. *E. coli* O157:H7 has become a global public health problem, causing symptoms such as bloody diarrhea, hemolytic uremic syndrome, and thrombotic thrombocytopenic purpurea [Doyle et al. 1997]. The US Centers for Disease Control and Prevention reported that an estimated 73,000 cases of *E. coli* O157:H7 infection and 61 resultant deaths occur in the United States each year [CDC, 2006].

Many methods are available for the detection of *E. coli* O157:H7. In the conventional culture method, Sorbitol-MacConkey agar has been used in a direct plating method to isolate *E. coli* O157:H7 from samples [FDA, 2001]. The conventional methods are reliable but time-consuming and laborious, further studies are needed to develop rapid and objective methods for foodborne pathogen detection. These methods include antibody-based methods, nucleic acid-based methods, and biochemical and enzymatic methods. Interest in using biosensors to detect foodborne pathogens is on the rise [Hall et al., 2002; Patel, 2006, Rasooly and Herold, 2006]. Among these, DNA sensors integrated with a PCR-based DNA system have shown great potential for the specific detection of pathogenic microorganisms. Many techniques are currently available, such as optical DNA detection using fluorescence-labeled oligonucleotides [Heng and Tsui, 2006], application of surface plasmon resonance [Mariotti et al., 2002], direct electrochemical assay [Korri-Youssoufi et al., 1997], and piezoelectric quartz crystal microbalance (QCM) targeting DNA [Wu et al., 2007]. However, the detection limit of these methods is still needed to be improved before the methods are applied for detecting pathogenic microorganisms in real food or filed samples.

QCM has been extensively investigated as a transducer in hybridization based DNA biosensors for the detection of gene mutation [Su et al., 2004; Tombelli et al., 2000], genetically modified organisms [Mannelli et al., 2003], and foodborne pathogens [Mo et al., 2002; Ryu et al., 2001] including the application of QCM sensors to the detection of *E. coli* O157:H7 [Deisingh and Thompson, 2001; Mao et al., 2006; Wu et al., 2007]. To improve the sensitivity of QCM sensors, many methods have been developed including optimizations of probe immobilization [Caruso et al., 1997; Tombelli et al., 2002; Zhou et al., 2001] and various signal amplification strategies using non-specific amplifiers of anti-dsDNA antibodies

[Bardea et al., 1999], liposomes [Patolsky et al., 2002], enzymes [Patolsky et al., 2001], and nanoparticles [Mao et al., 2006]. Nanoparticles are effective amplifiers used in the QCM DNA detection because of they have a relatively large mass compared to the DNA targets. In the QCM DNA detection, the nanoparticles offers substantial improvement in the detection limits with sensitivity from 10^{-12} to 10^{-14} M of DNA [Zhou et al., 2000; Zhao et al., 2001].

One of the "nanogold amplifier" methods utilizes DNA-capped gold nanoparticles for signal amplification [Lin et al., 2000; Zhao et al., 2001; Zhou et al., 2000; Weizmann et al., 2001; Liu et al., 2003; Mao et al., 2006]. Coupled with the DNA targets, nanoparticles act as "mass enhancers", extending the limits of QCM DNA detection. A nanoparticle-amplified QCM DNA sensor using the sandwich hybridization of two specific probes has been demonstrated by Mo et al. [2005]; however, the method used for foodborne pathogen detection has not previously been described. Therefore, a QCM DNA sensor based on nanoparticle amplification for detection and verification of *E. coli* O157:H7 is designed and reported in the present study. The target DNA is captured by the single-stranded DNA (ssDNA) of Probe 1 which self-assembled on the QCM sensor surface. The signal is then amplified using the sequence specific probe (Probe 2) conjugated to Au (gold) nanoparticles, resulting in highly sensitive detection of *E. coli* O157:H7. The sensitivity and specificity of the QCM system are evaluated. The application of the QCM system is tested in real food samples (apple juice, milk, and ground beef).

9.3 Results

9.3.1 The QCM system and detection

Piezoelectric QCM, quartz crystal microbalance, has been extensively applied as mass biosensor for the detection of specific proteins and nucleic acids. In our circulating-flow QCM system, the oscillation frequency of QCM chip decreased when the weight of QCM surface increased, which would be real-time recorded (**Figure 9-1**). The frequency decreased gradually with addition of oligonucleotides, reflecting immobilization of the first *E. coli* O157:H7 specific probes, hybridization of the probes with the *E. coli* O157:H7 targets on the Au surface of QCM, and sandwich hybridization by the second *E. coli* O157:H7 specific probes which are capped onto Au nanoparticles. **Figure 9-1** shows the typical frequency shift of real-time detection of the QCM system performed in this study. A frequency decrease of approximately 80 Hz is observed after Probe 1, P1-30/12T (1.0 μM), is self-assembly immobilized, which suggested that the Au surface is successfully functionalized. Subsequent association of complementary target oligonucleotides, T-104(AS) (0.5 μM) introduced for the DNA hybridization resulted in an additional frequency decrease of approximately 70 Hz. Additional treatment of the DNA hybridized QCM sensor with Probe 2-capped Au nanoparticles, P2-30/12T(AS), resulted in an amplification and a large frequency shift of approximately 300 Hz.

In our circulating-flow QCM system, the thiolated probes, target sequences and oligonucleotide-functionalized Au nanoparticles are circulated constantly to ensure continuous interaction with the Au surface on QCM sensor thereby enhancing the efficiency of the probe immobilization and DNA hybridizations.

9.3.2 Immobilization of synthesized probe oligonucleotides

The first step of preparation of the QCM DNA sensor is to immobilize the probe sequences onto the surface of the QCM sensor. The thiol-linkered tag [HS-$(CH_2)_6$] modified probes (1.0 μM), i.e., Probe 1, are applied in the QCM system. The frequency changes of immobilization by P1-30, P1-30/12T and P1-30/24T are 69.5 ± 5.3, 80.4 ± 4.2 and 79.1 ± 7.7 Hz, respectively (**Figure 9-2A**). The increases in mass due to the immobilization of P1-30, P1-30/12T and P1-30/24T on the Au surface of QCM are calculated as approximately 27, 32 and 31 ng, respectively. The thiolated probes with additional 12 dT (P1-30/12T) and 24 dT

(P1-30/24T) showed significantly greater frequency change than the probe without additional dT (P1-30) ($P < 0.05$). However, the frequency change*s* are similar between P1-30/12T and P1-30/24T.

The increases in mass when P1-30/12T or P1-30/24T is applied are larger than when P1-30 is applied because the single molecule weights of P1-30/12T (1.31×10^4 g mole^{-1}) and P1-30/24T (1.67×10^4 g mole^{-1}) are larger than that of P1-30 (9.42×10^3 g mole^{-1}). According to the calculation, the molecule densities of P1-30, P1-30/12T and P1-30/24T immobilized onto the Au surface on QCM sensor are 1.73×10^{12}, 1.47×10^{12} and 1.11×10^{12} (ssDNA cm^{-2}), respectively.

9.3.3 Hybridization of synthesized target oligonucleotides to probes immobilized QCM sensor

The frequency change of synthesized target oligonucleotides T-104(AS) [104-mer; 30 mer within the sequences is complementary to the probes immobilized on the Au surface of QCM sensor] and T-104(S) [104-mer; non-complementary to the probes] (**Table 7-2**) applied in the circulating-flow QCM system are also determined. The frequency change is 50.2 ± 3.5, 81.4 ± 5.2 and 86.6 ± 5.7 Hz when 0.5 μM of T-104(AS) oligonucleotides hybridized with P1-30, P1-30/12T and P1-30/24T, respectively (**Figure 9-2B**). The target oligonucleotide T-104(S) (0.5 μM), as the negative hybridization control in our QCM system, did not yield a measurable frequency change (< 3 Hz) when applied to the probe-immobilized QCM sensor. Note that the oligonucleotide T-104(S) is essentially complementary to T-104(AS). Thus, the lack of frequency change upon interaction of the Probe 1 with T-104(S) indicates that non-specific oligonucleotide binding is negligible on the interface. The frequency change due to target DNA hybridization with probes in the P1-30/12T or P1-30/24T immobilized QCM sensors is significantly greater ($P < 0.01$) than that in the P1-30 immobilized QCM sensor (**Figure 9-2B**), even though the probe density of P1-30 on the Au surface of the QCM sensor is high. This indicates that the probes with spacer segments (additional 12 dT) influence hybridization with the target sequences.

9.3.4 Detection of PCR-amplified DNA of *E. coli* O157:H7 gene *eaeA*

The probe-immobilized QCM sensors are also used for detection of amplified target

DNA by PCR. The DNA fragment is 104-bp and located within the respective region of *E. coli* O157:H7 *eaeA* gene. The amplified DNA fragment is identified by DNA sequencing. The double strand sequences of the PCR-amplified DNA are the same as the sequences of the synthesized 104-mer targets, T-104(AS) and T-104(S) (**Table 7-2**).

Before the PCR-amplified DNA is applied to the circulating-flow QCM sensor, the amplified DNA isolated from *E. coli* O157:H7 is denatured and immediately added to the circulating flow QCM system for DNA hybridization. In each hybridization, 1 μM of PCR amplified DNA (equivalent to 0.5 μM of the target T-104AS) is used to hybridize with the thiolated probes immobilized the QCM sensor. The results show that the frequency shifts are 44.6 ± 2.7, 72.8 ± 3.9 and 66.8 ± 5.4 Hz when the PCR-amplified DNA hybridized with P1-30, P1-30/12T and P1-30/24T, respectively (**Figure 9-2B**).

Similar to the results of the synthesized target oligonucleotides, the frequency change in the P1-30/12T or P1-30/24T immobilized QCM sensors is significantly greater than that in the P1-30 immobilized QCM sensor. However, the frequency change in the PCR-amplified DNA applied on the three probe-immobilized QCM sensors is less than those of parallel detections in the synthesized target oligonucleotides, T-104(AS).

In comparison of PCR-amplified DNA and synthesized oligonucleotides T-104(AS) as target sequences applied in the QCM system, the frequency change in the PCR-amplified DNA applied on the three probe-immobilized QCM sensors is less than those of parallel detections in the synthesized target oligonucleotides (**Figure 9-2B**). The hybridization results hint that the denatured strands of PCR-amplified DNA can hybridize with complementary strands other than the probe oligonucleotides immobilized on the QCM sensor and/or the coexisted sequences (sense and antisense strands) may interfere with the hybridization of complementary targets and probe oligonucleotides.

9.3.5 Detection of PCR-amplified DNA of E. coli O157:H7 using oligonucleotide -functionalized Au nanoparticles

As shown in **Figure 9-1**, the detection signal, frequency shift, of the PCR-amplified DNA from *E. coli* O157:H7 genomic DNA is amplified by the specific oligonucleotide-functionalized Au nanoparticles in our QCM system. In the process, the Au nanoparticles are firstly capped with the thiolated probes (designated Probe 2), P2-30(S) (30-mer; a non-complementary oligonucleotide to the target sequences that are hybridized to

the Probe 1 immobilized on the QCM sensor), P2-30(AS) (30-mer; a complementary oligonucleotide to the target sequences at the 5' end), or P2-30/12T(AS) (30-mer with an additional 12 dT). When the Au nanoparticles or P2-30(S)-capped Au nanoparticles are applied to the P1-30/12T-immobilized QCM sensor which is hybridized the target sequences, a negligible frequency change is recorded (< 3 Hz). In contrast, the frequency change markedly decreased when the P2-30(AS)- or P2-30/12T(AS)-capped Au nanoparticles are applied (**Figure 9-3**). The value of frequency change in the treatment with P2-30/12T (AS)-capped Au nanoparticles (292 ± 17 Hz) is significantly larger than that with the P2-30(AS)-capped Au nanoparticles (168 ± 13 Hz) ($P < 0.01$). The 12 dT spacer segment adapted to Au nanoparticles could enhance hybridization efficiency (**Figure 9-3**).

9.3.6 Specificity of the QCM system in detecting *E. coli* O157:H7

Several bacterial strains, including *E. coli* O157:H7, *L. monocytogenes*, *S. choleraesuis*, *S. aureus* and *E. coli* K12 are applied to the PCR and QCM system for testing the specificity of the method for *E. coli* O157:H7. Except *E. coli* O157:H7, the primer pair (E_{157}eae/F and E_{157}eae/R) is failure to amplify the DNA fragments from the genomic DNA isolated from bacterial cells of *L. monocytogenes*, *S. choleraesuis*, *S. aureus* and *E. coli* K12 (data not shown). The solutions of PCR reaction from these bacteria are also applied in the QCM detection; however, the results show the frequency changes at background level except *E. coli* O157:H7.

The genomic DNA isolated from the O serotypes of *E. coli*, including O76:H8, O85:H1, O138:H14 and O142:H6, are also used in the PCR and QCM detection. Although the *eaeA* gene presents in these pathogenic strains, the primers which are designed for specifically amplifying the DNA fragment within *E. coli* O157: H7 *eaeA* gene could not successfully amplify the DNA fragments from the *E. coli* O76:H8, O85:H1, O138:H14 and O142:H6 genomic DNA (data not shown). Therefore, none of the PCR-amplified DNA fragments of the *E. coli* O76:H8, O85:H1, O138:H14 and O142:H6 could be detected in the QCM sensor. These results suggest that the QCM system established in this study may be specifically used in the *E. coli* O157:H7 detection.

9.3.7 Quantitation of the QCM detection of PCR-amplified DNAs

Genomic DNA is extracted from different concentrations of serially diluted *E. coli*

O157:H7 (1.2×10^1 to 1.2×10^8 CFU/ml) using the protocol described in the experimental section. PCR is carried out using the DNA extract from each concentration of cells. The gel electrophoresis detection of PCR products is shown in **Figure 9-4A**. Electrophoresis confirmed the successful amplification of PCR products with the correct size, 104-bp. The PCR-amplified DNAs for *E. coli* O157:H7 are detected by the P1-30/12T immobilized QCM sensors using P2-30/12T-capped Au nanoparticles as an amplifier and verifier. The time-dependent frequency changes are shown in **Figure 9-4B**. The frequency change of the sensor is enhanced as the cell concentrations of the PCR products increased. The blank control (PCR products using purified water as the PCR template) is also tested and yielded a frequency change < 3 Hz.

The responses of the QCM sensor to differentiate PCR samples with/without amplification by oligonucleotide-functionalized Au nanoparticles are shown in **Figure 9-5**. The measurements are highly reproducible for all concentrations of *E. coli* O157:H7 (n = 3, RSD < 8.3%). In the detection of PCR-amplified DNA with and without probe P2-30/12T-capped Au nanoparticles, linear relationships are found between the frequency change *vs.* log (CFU/ml of *E. coli* O157:H7) from 1.2×10^2 to 1.2×10^6 CFU/ml ($y_1 = -19.8x + 134.9$, $R^2 = 0.986$) in the samples treated with P2-30/12T-capped Au nanoparticles and from 1.2×10^4 to 1.2×10^8 CFU/ml ($y_2 = -10.5x + 82.0$, $R^2 = 0.993$) in the samples without the Au nanoparticle amplification (**Figure 9-5**). Our results show that the *E. coli* O157 cell concentration is positively relative to the response of the frequency change indicating it is possible to enumerate *E. coli* O157:H7 using the QCM DNA sensor.

The threshold for detection limit of the QCM system is defined by the signal-to-noise (S/N) characteristics as S/N > 3; hence, the detection limit of our system is assessed as 1.2×10^2 CFU/ml and 1.2×10^4 CFU/ml in the tests with and without P2-30/12T-capped Au nanoparticles as the amplifier, respectively.

9.3.8 Detection of *E. coli* O157:H7 in food samples

For real food detection, the cells of *E. coli* O157:H7 is artificially inoculated in apple juice, milk, or ground beef samples to reach the concentrations of 5.3×10^2 CFU/ml or CFU/g. These mixtures are used for the detection of *E. coli* O157:H7 without pre-enrichment by the QCM circulating system with Au nanoparticles for signal amplification. As shown in **Figure 9-6**, the QCM frequency changes detected in the food samples containing 5.3×10^2

CFU/ml or CFU/g of *E. coli* O157:H7 are significantly larger than those detected in the blank controls ($P < 0.01$). However, the detected frequency changes in the food samples are less than those detected in the parallel detection, i.e., PBS containing 5.3×10^2 CFU/ml of *E. coli* O157:H7. We suggested that the less sensitivity of detecting *E. coli* O157:H7 in the food samples compared with that in the PBS may be related to a few bacterial cells being lost when the *E. coli* O157:H7 cells are isolated from the food samples and it can be also related to inhibitors coming from the food [Bhaduri and Cottrell, 2001]. The results indicate that the established QCM system in the present study is applicable for the detection of *E. coli* O157:H7 in real food samples.

9.4 Discussion

For the detection of *E. coli* O157:H7, methods focusing on rapid and accurate have been investigated, including DNA, immunological and biosensor methods. However, the immunological method for detecting *E. coli* O157:H7 needs significant pre-enrichment or relatively high cell numbers to reach sensing ability [Deisingh and Thompson, 2001]. For this reason, the researches move toward using multiplex PCR and the methods are gradually becoming a major procedure for the detection of *E. coli* O157:H7 [Mukhopadhyay and, Mukhopadhyay 2007]. Among these, DNA sensors integrated with a PCR-based DNA system have shown great potential for the specific detection and easily differentiation of pathogenic microorganisms. In this study, the DNA-based QCM sensor coupled with the PCR not only increases the sensitivity of the systems, but also offers a viable alternative to gel electrophoresis and other traditional DNA sequences detection methods that require labeled probes.

In the present study, we demonstrated a sensitive QCM DNA sensor using the sequence-specifically oligonucleotide-functionalized Au nanoparticles as “mass enhancers” for the detection of *E. coli* O157:H7 (**Figure 9-1**). The method is used to detect the PCR-amplified DNA fragments from the real samples of *E. coli* O157:H7 with a detective limitation as low as 1.2×10^2 CFU/ml and a quantitative relationship is noted between the measured signal and the concentration of *E. coli* O157:H7 cells in a broad range, from 1.2×10^2 to 1.2×10^6 CFU/ml (**Figure 9-4** and **Figure 9-5**). The technique of nanoparticle amplification applied to the DNA sensors resulted in a significant improvement in the detection limit in compared with those of immunosensor methods [Su and Li., 2004; Radke

SM and Alocilja, 2005; Subramanian et al., 2006; Yang et al., 2004]. Moreover, the results are comparable to the detection limit of 2.67×10^2 CFU/ml of *E. coli* O157:H7 in a recent report on the QCM DNA sensor based on a nanoparticle amplification method using non-specifically streptavidin-conjugated Fe_3O_4 nanoparticles for the detection of *E. coli* O157:H7 [Mao et al 2006]. We reasoned that the PCR-based technique integrated into the DNA sensor system increased the target molecules in the detected samples.

The steric effect on oligonucleotide immobilization onto a solid surface and DNA hybridization in a QCM DNA sensor is improved in this study. The addition of 12 dT to the 5' end of the probes increases the hybridization efficiency in our circulating flow QCM system. This confirms the studies that report the poly dT at probes may reduction of steric hindrance in three-dimensional space and the increase of molecule collision caused by the addition of the spacer during DNA hybridization [Mo et al., 2005; Shchepinov et al., 1997]. It is also proposed that spacers may reduce steric interference during DNA hybridization by making the probe end closest to the surface of the device more accessible [Shchepinov et al., 1997; Southern et al., 1999]. Compared to P1-30/12T, however, the probe P1-30/24T showed similar hybridization efficiency in spite of its longer length (**Figure 9-2**). These results are consistent with the hypothesis that the longer probes behave as flexible, coil-like polymer chains which encounter greater steric hindrance, inhibiting effective hybridization at the sensor/solution interface [Steel et al., 2000; Song et al., 2002].

In this study, we could detect 5.3×10^2 CFU/g of *E. coli* O157:H7 in the food samples without pre-enrichment. With current sufficient data presented, we proposed that our QCM system could be realistic in detecting 1 CFU/g of *E. coli* O157:H7 from a mixture of microorganisms in ground beef or other food, such as milk and juice, if an enrichment procedure is applied. Therefore, it can be expected that two log CFU/g of *E. coli* O157:H7 can be enriched within 2-3 hr at initial inoculum of 1 CFU/g when a brief enrichment is used. With the amplification of Au nanoparticles, only a short period of pre-enrichment may be necessary, especially for detection of *E. coli* O157:H7 in food products.

PCR is used for the amplification of target DNA prior to the application of the QCM circulating system, but no enrichment is used in our present study. The total detection time of our current assay on prepared samples is within 3 hr (DNA extraction for 0.5 hr, PCR for 1.5 hr, and real-time QCM detection for 1 hr). Considering the total preparation time from food sampling to results including an enrichment procedure, with the current sensitivity of our assay, the total detection time is approximately 6 hr for ground beef samples using the

standard enrichment with our QCM system (3 hr for enrichment at initial inoculum of 1 CFU/g and 3 hr for QCM detection including PCR application). Our method is compatible to the current commercial PCR based techniques.

9.5 Conclusions

We have demonstrated the use of oligonucleotide-functionalized Au-nanoparticles as amplifying and confirming probes for the microgravimetric QCM DNA-sensing method. By this method, probe immobilization, target hybridization and sandwich hybridization with the oligonucleotide-functionalized Au nanoparticles are successfully completed in a circulating-flow QCM system with real-time monitoring of frequency change.

In the present study, we demonstrated a sensitive QCM DNA sensor using oligonucleotide-functionalized Au nanoparticles as "mass enhancers" and "verifiers" for the detection of *E. coli* O157:H7 in food samples. This use of nanoparticles effectively amplified the signals in frequency change due to their relatively large mass of the nanoparticles compared to DNA targets, and yield increasingly sensitive detection limits for *E. coli* O157:H7 (1.2×10^2 CFU/ml for PCR products) without enrichment of the culture and a quantitative relationship is noted between the measured signal and the concentration of *E. coli* O157:H7 cells in a broad range, from 1.2×10^2 to 1.2×10^6 CFU/ml. Our results suggest that the DNA piezoelectric sensor with specifically oligonucleotide-functionalized Au nanoparticles as amplifiers has potential for additional applications in detecting *E. coli* O157:H7 or other microorganisms in food, water and clinical samples. This approach lays the groundwork for incorporating the method into an integrated system for rapid PCR-based DNA analysis systems for testing food that may be contaminated with pathogenic organisms.

10. Part III:

A method of layer-by-layer gold nanoparticles hybridization in a quartz crystal microbalance DNA sensing system used to detect dengue virus

10.1 Abstract

Dengue virus (DENV) is nowadays the most important arthropod-spread virus affecting humans existing in more than 100 countries worldwide. A rapid and sensitive detection method for the early diagnosis of infectious dengue virus is urged to be developed. In the present study, a circulating-flow quartz crystal microbalance (QCM) biosensing method combining oligonucleotide-functionalized gold nanoparticles (i.e., AuNPs-probes) used to detect DENV has been established. In the DNA-QCM method, two kind of specific AuNPs-probes are linked by the target sequences onto the QCM chip to amplify the detection signal, i.e., oscillatory frequency change (ΔF) of the QCM sensor. The target sequences amplified from DENV genome play as a bridge for the layer-by-layer AuNPs-probes hybridization in the method. Besides as amplifiers of detection signal, the specific AuNPs-probes used in the DNA-QCM method also play a role of verifiers to specifically recognize their target sequences in the detection. The effect of four AuNPs sizes on the layer-by-layer hybridization has been evaluated and found that 13 nm AuNPs collocated with 13 nm AuNPs showed the best hybridization efficiency. According to the nanoparticles application, the DNA-QCM biosensing method is able to detect dengue viral RNA in the virus contaminated serum as plaque titers being 2 PFU/mL and a linear correlation ($R^2 = 0.987$) of ΔF *vs.* virus titration from 2×10^0 to 2×10^6 PFU/mL is found. The sensitivity and specificity of the present DNA-QCM method with nanoparticle technology showed to be comparable to the fluorescent real-time PCR methods. Moreover, the method described herein is shown to non-required precious equipments, label-free and highly sensitivity.

Keywords: dengue virus, gold nanoparticle, quartz crystal microbalance, DNA sensor

10.2 Introduction

Dengue is the most important arbovirosis in terms of numbers of humans affected. It constitutes a serious public health problem in many subtropical and tropical regions where environmental conditions allow the proliferation of insect vectors. *Aedes aegypti* is the main vector of dengue virus (DENV) and is present in most countries between Asia, Africa, and Central and South America, more than 2.5 billion people are at risk of infection and dengue transmission is endemic in more than 100 countries [Shu and Huang, 2004; Wilder-Smith et al., 2005]. DENVs cause infections which leading to clinical symptoms ranging from self-limited, acute, febrile disease called dengue fever (DF) to life-threatening dengue hemorrhagic fever (DHF), and dengue shock syndrome (DSS) [Agarwal et al., 1999; Wang et al., 2002]. An estimated 500,000 cases of DHF require hospitalisation each year, of which very large proportions are children. At least 2.5% of cases die, although case fatality could be twice as high.

Effective vaccines or drugs are still unavailable to prevent or cure the disease caused by DENV. Therefore, a rapid and reliable method for DENV detection is important task, which rapidly focus on the medical treatment for help doctors to save the patients' life as early as possible. Especially in the acute phase of the dengue infection before any specific antibody response directed against the DENV is detectable, only virus detection, either by cDNA detection and/or virus isolation [Laue et al., 1999], will be the matter of choice for the diagnostic. However, virion isolation needed consuming a lot of time for cultivation and identification, usually need three to four workdays [Parida et al., 2005]; only cDNA detection can give quick and reliable results within a few hours via polymerase chain reaction (PCR) . Traditional amplification methods like nested or single-tube multiplex PCR [Lanciotti et al., 1992; Harris et al., 1998] get more and more replaced by real-time, automated RT-PCR assays like the TaqMan or light cycler technique [Laue et al., 1999; Callahan et al.,2001; Drosten et al., 2002]. However, these methods need expensive instruments and professionals to operate and analyze. There is great urgency to develop a novel detection system with high sensitivity, short operation time, handy processing with easy interpretation.

Piezoelectric biosensor, known as quartz crystal microbalance (QCM), combines high sensitivity to mass on the surface of the quartz crystal with the high specificity of a biosensor. Wu and coworkers [Wu et al., 2005] are the pioneers using immuno-QCM biosensor to detect DENV in clinical samples. The authors used monoclone antibodies to recognize DENV envelope protein (E) and non-structure protein 1 (NS-1) and detect the mass increased on the

antibody-modified QCM. Recently, the QCM sensors have been extensively applied as a transducer in hybridization based on DNA biosensors for the detection of gene mutation [Tombelli et al., 2002; Su et al., 2004], genetically modified organisms [Mannelli et al, 2003], and foodborne pathogens [Ryu et al., 2001; Mo et al., 2002; Wu et al., 2007]. Further, gold nanoparticles (AuNPs) are integrated in QCM as effective amplifiers in the DNA detection, because AuNPs have relatively large mass compared with oligonucleotides [Mao et al., 2007, Chen et al., 2008].

Although AuNPs have been used in biotechnology over the last decades as immunocytochemical probes and immuno-conjugates, recent advances in DNA-functionalized AuNPs have paved the way for the development of a series of new and practical bioassay or biosensing systems [Thaxton et al., 2006]. There are several papers revealed that the oligonucleotides-functionalized AuNPs can be used as amplifier in a microgravimetric DNA sensor [Zhou et al., 2000; Zhao et al., 2001; Liu et al., 2004], but rare detection for pathogenic virus has been demonstrated because that lot of procedures, including pretreatment of detection sample, specific probe design and optimal detection processes, should been addressed to develop a DNA-base sensing QCM or cantilever system.

In the present study, we have developed a real-time and circulating-flow QCM combining with oligonucleotides-capped AuNPs (i.e., AuNPs-probes) to specifically detect the DNA fragment, which is amplified from DENV genome by the layer-by-layer hybridization of AuNPs-probes. Using the method, as low as 2 plaque forming unit (PFU)/mL of DENV serotype 2 (DENV2) could be detected. The AuNPs-probes in the DNA-QCM sensor are used not only as amplifiers to enhance the detection sensitivity but also as verifiers to increase the specificity of DNA hybridization.

10.3 Results and discussion

10.3.1 QCM system and detection

Piezoelectric QCM is applied as mass biosensor for the detection of specific DNA sequence reverse transcripted from DENV RNA genome. In the circulating-flow QCM system for DENV detection, the oscillatory frequency of QCM chip decreased when the mass on the surface of QCM chip increased, which the ΔF could be real-time recorded. The frequency decreased gradually with the self-assembly immobilization of probe oligonucleotides, and cDNA hybridization of probe and target sequences on the chip surface of QCM via layer-by-layer AuNPs-probes conjugant. The **Figure 10-1** (lower panel) shows an example of the real-time detection of QCM system performed in the present study. An oscillatory frequency decrease of approximately -45 Hz is observed after the probe DENV2-P1 (1.0 μM) being self-assembly immobilized onto the QCM chip, which suggested that the gold surface of QCM chip is successfully functionalized. Subsequently, the target oligonucleotides, DENV-T (0.5 μM), are introduced for the DNA hybridization and result showed an additional ΔF of approximately -80 Hz. Then, for enhancing the detection signal, the DENV2-P2 functionalized-AuNPs (i.e., AuNPs-DENV2-P2) are applied to the system for playing the first enhancer and confirmer to increase ΔF when the AuNPs-DENV2-P2 hybridized with the target sequences and approximately -200 Hz of ΔF are detected. However, a lot of surplus target oligonucleotides still have not been used in the reaction. In order to make full detection of the target sequences, the DENV2-P1 functionalized-AuNPs (i.e., AuNPs-DENV2-P1) are added into the QCM system. The result shows an -130 Hz of ΔF after AuNPs-DENV2-P1 applied in the system. The AuNPs-DENV2-P1 played a role as a catcher to capture the surplus target sequences in the reaction, and to act the second enhancer to amplify the detection signal via the layer-by-layer AuNPs-probes hybridization until the surplus targets exhausted in the circulating flow QCM system.

10.3.2 Identification of AuNPs size

The AuNPs of 5, 13, 20 and 50 nm in diameter are produced by sodium citrate reduction. Wavelength shifts, ranging from 450 nm to 700 nm, of the AuNPs with different sizes are scanned by spectrophotometer (**Figure 10-2**). The maximum absorbance (λ_{max}) of the prepared 5, 13, 20 and 50 nm AuNPs are about at 515, 520, 524 and 530 nm, respectively. The λ_{max} of 13 nm AuNPs is confirmed by the previous report [Kenneth et al., 2000].

Therefore, the optical spectra can preliminary estimate of AuNPs sizes produced. Further, the SEM and DLS are used to confirm and measure the AuNPs shape and average diameter in a real size. The diameter of 5, 13, 20 and 50 nm AuNPs are 5 ± 1, 13 ± 2, 20 ± 4 and 50 ± 6 nm by DLS assay, respectively. When the probe oligonucleotides are immobilized onto AuNPs, the λ_{max} of oligonucleotides-functionalized AuNPs shifted slightly; it maybe due to the radius of the AuNPs-probes just increases very little. Besides, the high density of probe on the AuNPs caused steric barrier and interfered the hybridization between target and probe. The optimum AuNPs-probe concentration is calculated to provide the better AuNPs-probes stability and DNA hybridization efficiency [Hanauer et al., 2007; Liu et al.,2008], Therefore, the concentration of AuNPs-probe is controlled at 2.6 nM in the circulating-flow QCM system. At this concentration, the hybridization between AuNPs-probes and targets would have better efficiency.

10.3.3 Effect of AuNPs-probe size on ΔF enhancement

The effects of AuNPs-probe size on ΔF are determined (**Figure 10-3**). In the experiments of 5, 13, 20 and 50 nm AuNPs-DENV2-P2 as the 1st layer and 13 nm AuNPs-DENV2-P1 as the 2nd layer enhancers, the ΔF of 5, 13, 20 and 50 nm AuNPs-DENV2-P2 applied are -17 ± 5, -148 ± 48, -103 ± 6 and -50 ± 16 Hz, respectively (**Figure 10-3A**). In the reverse experiments, 13 nm AuNPs-DENV2-P2 as the 1st layer and 5, 13, 20 and 50 nm AuNPs-DENV2-P1 as the 2nd layer enhancers, the ΔF of 5, 13, 20 and 50 nm AuNPs-DENV2-P1 applied are -25 ± 5, -151 ± 30, -86 ± 13 and -37 ± 5 Hz, respectively (**Figure 10-3B**). The results showed that there is the largest efficiency of enhancing ΔF when the 13 nm AuNPs-probes applied as enhancer either for the 1st or 2nd layer enhancer in the detection.

AuNPs-probes deposited onto the QCM chip are dependent on the DNA hybridization efficiency between specific probe and target sequences [Zhao et al., 2001; Liu et al., 2003]. The previous reports showed that the density of DNA on a nanogold-modified surface is directly influenced the hybridization result [Liu et al., 2003] and the ΔF of QCM sensor is decreased accompanied with the increase of AuNPs size applied at static solution [Liu et al., 2003; Nie et al., 2007]. It could be attributed to the steric hindrance effect of nanoparticles. The larger nanoparticles cannot move as freely as the smaller nanoparticles and the larger nanoparticles connected to the target DNAs hindered more of themselves to approach the

target DNAs [Nie et al., 2007]. However, in a circulating-flow condition, our results show that the hybridization rate reaches its maximum value when the average diameter of AuNPs-probes is 13 nm and then decreases with the increasing AuNPs-probe size (**Figure 10-3**). Some speculations could be used to explain the controversial results observed. First, the larger AuNPs could be immobilized with more probe oligonucleotides than the smaller ones, but according to the report by Hurst et al. [Hurst et al., 2006], the larger AuNPs have less number of probes on the same superficial area than smaller ones. Therefore, the larger AuNPs-probes that hybridize with the target sequences are harder than the smaller ones resulting in a decrease of cDNA hybridization efficiency while larger AuNPs-probes used in the cDNA-QCM biosensing system. Second, the flow rate could interfere with the cDNA hybridization efficiency in a flow system [Michalzik et al., 2005]. In the circulating-flow QCM system, the AuNPs-probes in fluid should approach to the chip surface and hybridize with their complementary sequences before they are flowed out the reaction chamber of QCM chip. We proposed that the AuNPs-probes in size of 13 nm may be more suitable applied in the flow condition used in the present system. Third, the AuNPs carry negative charge which could repel each other AuNPs-probes [Sauthier et al., 2002] and the larger AuNPs-probes would have stronger repulsion effect resulting in DNA hybridization efficiency decreasing.

Besides, we supposed that 5 nm AuNPs-probes is easily stayed on the QCM chip to hybridize with the target sequences in the circulating-flow system. Amount of 5 nm AuNPs-probes deposited in the 1st layer may be more than other sizes of AuNPs-probes (the order of deposited efficiency: 5 nm > 13 nm > 20 nm >> 50 nm) in the QCM chip. But considering to the mass effect, the mass of 5 nm AuNPs is about 1/27 folds of 13 nm AuNPs, 1/64 folds of 20 nm AuNPs and 1/1,000 folds of 50 nm AuNPs. Therefore, we conjectured that 5 nm AuNPs-probes with the less efficiency of ΔF enhancement is because of mass effect.

10.3.4 Observation of AuNPs-probes hybridization on QCM chip

The chip surface of QCM sensors is observed with SEM (**Figure 10-4**), where the assembled AuNPs-probes are displayed through DNA hybridization. **Figure 10-4A,** shows the chip surface of immobilized DENV2-P1 probes hybridized with the target sequences on QCM chip without AuNPs-probes applied. The SEM image of the 1st layer of AuNPs-DENV2-P2 (13 nm) deposited onto the QCM chip (**Figure 10-4B**) and of the 2nd

layer of AuNPs-DENV2-P1 (13 nm) added onto the QCM chip via the hybridization with target sequences (**Figure 10-4C**) are shown. In **Figure 10-4B** , the dispersed AuNPs-probes are observed because that the surface of AuNPs-probes is full of negative charge and the AuNPs-probes would repel each other [Bui et al., 2007]. **Figure 10-4C** shows the SEM images of layer-by-layer AuNPs-probes deposited on the QCM chip, i.e., the AuNPs-probes linked by the surplus target sequences and most of two to four AuNPs linked together (close view in **Figure 10-4C**).

10.3.5 Detection of RT-PCR-amplified DNA from DENV2

DENV cDNA is obtained by RT used DENV-URT as primer and then the DNA fragment of DENV E gene is obtained by PCR using the universal primer pair, DENV-UF and DENV-UR (**Figure 10-5**). The PCR-amplified DNA fragment (130 bp) could be obtained from DENV2 and DENV3 which are mixed into the whole blood of human before the RT-PCR performed (lanes 2 and 3 shown in **Figure 10-5A** , respectively). However, only the DNA fragment from DENV2 could be detected in the QCM system and the detected ΔF in the DENV2 sample reached to -115 Hz, the value is 3.4, 4.3 and 4.3 folds compared to those in the DENV3 (38 Hz), C6/36 cells (29 Hz) and whole blood (29 Hz) detected (**Figure 10-5B**). The sequence alignment demonstrated the target sequences between DENV2 and DENV3 are extreme difference (**Figure 10-5C**). It is reason that the DENV2 specific probes can recognize the DENV2 from the other DENV serotypes.

The PCR-amplified DNA from DENV2 cDNA is able to be detected by the DENV2-P1 immobilized QCM chip and detected signal could be amplified by AuNPs-DENV2-P2 and AuNPs-DENV2-P1 hybridization. In addition to the signal amplification, the role of AuNPs-DENV2-P2 and AuNPs-DENV2-P1 is also as sequence verification. In the **Figure 10-5B**, the result demonstrates that the layer-by-layer AuNPs-DENV2 specific probes not only can catch the surplus target sequences but also play a verifier role to provide detection accuracy.

In the present study, only one pair of universal primer is needed to PCR amplify the specific target DNA fragment from four DENV serotypes. The primer pair is selected based on highly conserved regions within DENV genome. The amplified DNA fragment of DENV can be recognized by specific AuNPs-probes in the DNA-QCM biosensing system. Therefore, the developed method could be used to differentiate DENV serotypes via DNA

hybridization.

In an immuno-QCM biosensor developed by Wu et al. [2005], the data showed a high background (10-20 Hz) because serum interference, even though they used a cibacron blue 3GA gel-heat denature (CB-HD) method to pretreat the clinical samples. As the authors mentioned, however, the pretreatment procedures would cause a dramatic decrease in analytical sensitivity. In the nucleic acid-QCM biosensing method developed in this study, the detection targets of nucleic acid would be purified through the procedures of RNA extraction, reverse transcription and PCR amplification. Therefore, the background signal of QCM detection could be lower than 10 Hz. The extraction process is also causing the loss of cellular RNA, but the molecule of detection targets could be largely increased via the procedure of PCR amplification.

10.3.6 Quantitative detection of DENV2 detection in real blood sample

The DNA-QCM sensor used to detect different titers of DENV2 in real blood sample with/without amplification by AuNPs-probes (13 nm) are performed (**Figure 10-6**). The blank control shown the background of $\Delta F = 2 \pm 1$ Hz in the samples without AuNPs-probes and $\Delta F = 7 \pm 1$ Hz in samples with AuNPs-probes application. The ΔF of QCM sensor is increased with the increase of virus concentrations either in the detections with and without AuNPs-probes amplification. The measurements are highly reproducible for all concentrations of DENV2 applied (n = 3 for each detection, RSD < 13.5% in without AuNPs-probes and RSD < 8.7% in with AuNPs-probes amplification). In the detection with the layer-by-layer AuNPs-probes amplification, a linear relationship ($y_1 = -17.646x + 129.3$, $R^2 = 0.9848$) is found between ΔF *vs.* log (PFU/mL of DENV2) from 2×10^0 to 2.0×10^6 PFU/mL. In the detection without the AuNPs-probes amplification, a linear relationship ($y_2 = -11.8x + 51.3$, $R^2 = 0.9981$) is also found, but the relationship is measured from 2×10^2 to 2×10^5 PFU/mL.

Compared with the blank, the results show that as low as 2 PFU/mL of DENV2 could be detected by the QCM system when the AuNPs-probes are applied in the circulating-flow QCM system. However, the detection limit is around 100 PFU/mL of DENV2 without the AuNPs-probes applied. It is indicated that the layer-by-layer AuNPs-probes hybridization can markedly enhance the detection sensitivity by more hundred folds. Beyond the detection limit, the AuNPs-probes can double verify the target sequences; therefore, decrease of the

false-positive in the detection could be expected.

The clinical diagnosis of infectious DENV by the detection of viral nucleic acid, the virus could be immediately detected after virus infection if the detection method being highly sensitive. The detection limit of present method can reach to as low as 2 PFU/mL, it meant that using the DNA-QCM biosensor combining with the technique of layer-by-layer AuNPs-probes hybridization, the DENV in clinical samples can be detected at very initial stage of the virus infection. Comparing with SyBR green or TaqMan real-time PCR methods whose detection limit are around 1-50 PFU/mL of DENV [Kao et al., 2005; Shu et al., 2003], the sensitivity and specificity of the present DNA-QCM biosensing method with nanoparticle technology showed to be comparable to the fluorescent real-time PCR methods. However, the DNA-QCM biosensing method described herein is shown to non-require precious equipments, label-free and higher sensitivity because the specific AuNPs-probes playing as detection amplifiers and verifiers (**Table10-1**).

10.4 Conclusions

DENV is nowadays the most important arthropod-spread virus affecting humans existing in more than 100 countries worldwide [Shu et al., 2004; Wilder-Smith et al., 2005]. In Taiwan, dengue has been a very important infectious disease since 1981 [King et al., 2000]. Effective surveillance and efficient control of the disease is dependent on rapid and sensitive diagnosis. In this study, we have showed a highly sensitive DNA-QCM sensor combined with the method of layer-by-layer of AuNPs-probes amplification. The DNA-QCM sensor is fabricated as a circulating-flow system which could real-time record the ΔF of QCM chip. In the method, the specific oligonucleotide-functionalized AuNPs, AuNPs-probes, play as "mass enhancer" and also "sequence verifier" to increase the detection specificity and limitation. Using the DNA-QCM system, as low as 2 PFU/mL of DENV in the clinical blood samples could be detected and a linear correlation between detection signal and virus titer is found from 2×10^0 to 2×10^6 PFU /mL of DENV. The DNA-QCM biosensing method developed would be useful for the early diagnosis for infectious DENV and great helpful in clarifying the epidemiology patterns of dengue infection. In the future, we will continue to integrate and optimize the detection system and examine clinical specimens or mosquitoes to define a quantitative detection for infectious virus.

11. General conclusions

In this study, we develop DNA QCM biosensor to real-time detection pathogen and compare with three parts, includes: 1. Establishing real-time detection DNA hybridization method by a circulating- flow system of quartz crystal microbalance. 2. Using DNA-AuNPs enhance method to rapidly detection foodborne pathogens on a piezoelectric biosensor. 3. Establishing layer-by-layer gold nanoparticles hybridization method improve detection limit to recognize virus. The conclusions are showed in below, respectively.

11.1 Part 1: Real-time detection of *Escherichia coli* O157:H7 sequences using a circulating- flow system of quartz crystal microbalance

We developed a DNA piezoelectric sensor for the real-time detection of *E. coli* O157:H7. Synthetic probe oligonucleotides are self-assembly immobilized on the sensor surface of the QCM device and the hybridization between the immobilized probes and the complementary sequences of the targets in solution is monitored in real-time. A spacer (12-dT) linked to the probes enhanced the detection signals because the spacer molecules reduced the steric interference of the support on the hybridization behavior of the immobilized oligonucleotides. The QCM system is also used to detect the PCR-amplified DNA from real samples. Our results suggest that the DNA piezoelectric sensor has potential for further applications in detecting *E. coli* O157:H7 as well as other microorganisms in food, water, and clinical samples. This approach lays the groundwork for incorporating the method into an integrated system for rapid PCR-based DNA analysis.

11.2 Part 2: Using oligonucleotide-functionalized Au nanoparticles to rapidly detect foodborne pathogens on a piezoelectric biosensor

We have demonstrated the use of oligonucleotide-functionalized Au-nanoparticles as amplifying and confirming probes for the microgravimetric QCM DNA-sensing method. By this method, probe immobilization, target hybridization and sandwich hybridization with the oligonucleotide-functionalized Au nanoparticles are successfully completed in a circulating-flow QCM system with real-time monitoring of frequency change.

In the present study, we demonstrated a sensitive QCM DNA sensor using oligonucleotide-functionalized Au nanoparticles as “mass enhancers” and “verifiers” for the detection of *E. coli* O157:H7 in food samples. This use of nanoparticles effectively

amplified the signals in frequency change due to their relatively large mass of the nanoparticles compared to DNA targets, and yield increasingly sensitive detection limits for *E. coli* O157:H7 (1.2×10^2 CFU/ml for PCR products) without enrichment of the culture and a quantitative relationship is noted between the measured signal and the concentration of *E. coli* O157:H7 cells in a broad range, from 1.2×10^2 to 1.2×10^6 CFU/mL. Our results suggest that the DNA piezoelectric sensor with specifically oligonucleotide-functionalized Au nanoparticles as amplifiers has potential for additional applications in detecting *E. coli* O157:H7 or other microorganisms in food, water and clinical samples. This approach lays the groundwork for incorporating the method into an integrated system for rapid PCR-based DNA analysis systems for testing food that may be contaminated with pathogenic organisms.

11.3 Part 3: Using layer by layer gold nanoparticles hybridization method to improve detection limit of dengue virus by a circulating-flow quartz crystal microbalance DNA sensing system

Every year, a lot of cases of DHF/DSS occur in epidemic areas and resulted in thousands people deaths. Since there is no effective vaccine to prevent these cases, early diagnosis in the course of the disease may allow for more rapid treatment of cases progressing to DHF/DSS.

In our study, we showed that a sensitive QCM DNA sensor can diagnosed dengue virus in low titer, and combined AuNPs in system as "mass enhancers" for enhancing signal. In previous report, AuNPs-probe always used as enhancers to improve the DNA-sensor sensitivity, and used only one layer AuNPs-probe in their system. In this study, 2nd layer AuNPs-probe are applied not only as enhancer but as played captor. In circulation-system, AuNPs circulate in system and hybridized with surplus target, the target conjugating with AuNPs-probe would move near the QCM chip easily, and QCM system would be more efficient for detection. Using AuNPs-probe effectively amplified the signals in frequency shifts due to their relatively large mass compared to DNA targets, and combined layer by layer AuNPs can step up the surface area of detection and enhance more frequency change in a short time. The circulation system is different from open system, efficiency of different sizes of AuNPs are not similar as Liu et al (2004). In four sizes of AuNPs, 13 nm AuNPs-probe not only on the 1st layer but also on the 2nd layer have the best efficiency to enhance the mass.

Further, layer by layer AuNPs not only enhanced mass, but also increased some surface area, the dendritic surface can interact with surplus target and AuNPs (conjugated with DENV-P1 or DENV-P2) more efficient than flat surface or one layer AuNPs (frequency change within 30 min), specifically when detected low concentration PCR product.

References

Agarwal R, Kapoor S, Nagar R, Misra A, Tandon R, Mathur A, Misra AK, Srivastava KL, Chaturvedi UC. 1999. A clinical study of the patients with dengue hemorrhagic fever during the epidemic of 1996 at Lucknow India. *Southeast Asian Journal of Tropical Medicine & Public Health* 30:735-740.

Alcon S, Talarmin A, Debruyne M, Falconar A, Deubel V, Flamand M. 2002. Enzyme-linked immunosorbent assay specific to Dengue virus type 1 nonstructural protein NS1 reveals circulation of the antigen in the blood during the acute phase of disease in patients experiencing primary or secondary infections. *Journal of Clinical Microbiology* 40:376-381.

Alves FM, Hirata IY, Gouvea IE, Alves MF, Meldal M, Brömme D, Juliano L, Juliano MA. 2007. Controlled peptide solvation in portion-mixing libraries of FRET peptides: improved specificity determination for Dengue 2 virus NS2B-NS3 protease and human cathepsin S. *Journal of Combinatorial Chemistry* 9:627-634.

Andreescu S, Njagi J., Ispas C, Ravalli MT. 2009. JEM Spotlight: Applications of advanced nanomaterials for environmental monitoring. *Journal of environmental monitoring* 11:27-40

Aytur T, Foley J, Anwar M, Boser B, Harris E, Beatty PR. 2006. A novel magnetic bead bioassay platform using a microchip-based sensor for infectious disease diagnosis. Journal of Immunological Methods 314:21-29.

Baker C, Pradhan A, Pakstis L, Pochan DJ and Shah SI. 2005. Synthesis and antibacterial properties of silver nanoparticles. *Journal of nanoscience and nanotechnology* 5:244-249.

Bardea A, Dagan A, Willner I. 1999. Amplified electronic transduction of oligonucleotide interactions: novel routes for Tay-Sachs biosensors. *Analytica Chimica Acta* 385:33-43.

Bassil N, Maillart E, Canva M, Lévy Y, Millot MC, Pissard S, Narwa R, Gooseens M. 2003. One hundred spots parallel monitoring of DNA interactions by SPR imaging of polymer-functionalized surface applied to the detection of cystic fibrosis mutations. *Sensors and Actuators B* 94:313-323.

Bhaduri S and Cottrell B. 2001. Sample preparation methods for PCR detection of *Escherichia coli* O157:H7, *Salmonella typhimurium*, and *Listeria monocytogenes* on beef chuck shoulder using a single enrichment medium. *Molecular and Cellular Probes* 15:267-274.

Bui MPN, Baek TJ, Seong GH. 2007. Gold nanoparticle aggregation-based highly sensitive DNA detection using atomic force microscopy. *Analytical and Bioanalytical Chemistry* 388:1185-90.

Cai H., Xu Y., Zhu N., He P. and Fang Y. 2002. An electrochemical DNA hybridization assay based on a silver nanoparticle label. *Analyst* 127:803-808.

Call DR, Brockman FJ, Chandler DP. 2001. Detecting and genotyping *Escherichia coli* O157:H7 using multiplexed PCR and nucleic acid microarrays. *International Journal of Food Microbiology* 67:71-80.

Callahan JD, Wu SJ, Dion-Schultz A, Mangold BE, Peruski LF, Watts DM, Porter KR, Murphy GR, Suharyono W, King CC, Hayes CG, Temenak JJ. 2001. Development and evaluation of serotype- and group-specific fluorogenic reverse transcriptase PCR

(TaqMan) assays for dengue virus. Journal of Clinical Microbiology 39:4119-4124.

Campbell GA and Mutharasan R. 2005. Detection of pathogen *Escherichia coli* O157:H7 using self-excited PZT-glass microcantilevers. *Biosensors and Bioelectronics* 21:462-473.

Caruso F, Serizawa T, Furlong DN, Okahata Y. 1995. Quartz crystal microbalance and surface plasmon resonance study of surfactant adsorption onto gold and chromium oxide surfaces. *Langmuir* 11:1546-1552.

Caruso F, Rodda E, Furlong DN, Niikura K, Okahata Y. 1997. Quartz crystal microbalance study of DNA immobilization and hybridization for nucleic acid sensor development. *Analytical Chemistry* 69:2043-2049.

Centers for Disease Control and Prevention (CDC), 2005. *Escherichia coli* O157:H7. Available at: http://www.cdc.gov/ncidod/dbmd/diseaseinfo/escherichiacoli_g.htm. Accessed on 13 June, 2006.

Centers for Disease Control and Prevention (CDC), 2006. *Escherichia coli* O157:H7.

Chan V, Graves DJ, and McKenzie SE. 1995. The biophysics of DNA hybridization with immobilized oligonucleotide probes. *Biophysical Journal* 69:2243-2255.

Chen J., Miao Y., He N., Wu X., Li S. 2004. Nanotechnology and biosensors. *Biotechnology Advances* 22:505-518

Chen RF, Yeh WT, Yang MY, Yang KD. 2001. A model of the real-time correlation of viral titers with immune reactions in antibody-dependent enhancement of dengue-2 infections. *FEMS Immunology and Medical Microbiology* 30:1-7.

Chen SH, Wu VCH, Chuang YC, Lin CS. 2008. Using oligonucleotide-functionalized Au nanoparticles to rapidly detect foodborne pathogens on a piezoelectric biosensor. *Journal of Microbiological Methods* 73:7-17.

Cho YK, Kim S, Kim YA, Lim HK, Lee K, Yoon D, Lim G, Pak YE, Ha TH, Kim K. 2004. Characterization of DNA immobilization and subsequent hybridization using in situ quartz crystal microbalance, fluorescence spectroscopy, and surface plasmon resonance. *Journal of Colloid and Interface Science* 278:44-52.

Chutinimitkul S, Payungporn S, Theamboonlers A, Poovorawan Y. 2005. Dengue typing assay based on real-time PCR using SYBR Green I. *Journal of Virological Methods* 129: 8-15.

Curie P. and Curie J. 1880 Développement, par pression, de l'électricité polaire dans les cristaux hémièdres à faces inclines. *Comptes Rendus de l'Académie des Sciences* 91: 294-295.

Darbha G. K., Anandhi Ray A. and Ray P. C., 2007. Gold nanoparticle-based miniaturized nanomaterial surface energy transfer probe for rapid and ultrasensitive detection of mercury in soil, water, and fish. *ACS Nano* 1:208-214.

Deisingh AK and Thompson M. 2001. Sequences of *E. coli* O157:H7 detected by a PCR-acoustic wave sensor combination. *Analyst* 126:2153–2158.

Demers LM, Mirkin CA, Mucic RC, Reynolds RA 3rd, Letsinger R, Elghanian R, Viswanadham G.. 2000. A fluorescence-based method for determining the surface coverage and hybridization efficiency of thiol-capped oligonucleotides bound to gold thin films and nanoparticles. *Analytical Chemistry* 72:5535-5541.

Division of Bacterial and Mycotic Diseases. Atlanta, GA, USA. (http://www.cdc.gov/ncidod/dbmd/diseaseinfo/escherichiacoli_g.htm) Accessed on 13 June, 2006.

Dos Santos FB, Nogueira RM, Lima MR, De Simone TS, Schatzmayr HG, Lemes EM, Harris E, Miagostovich MP. 2007. Recombinant polypeptide antigen-based immunoglobulin G enzyme-linked immunosorbent assay for serodiagnosis of dengue. *Clinical and Vaccine Immunology* 14; 641-643.

Doyle MP, Zhao T, Meng J, Zhao S. 1997. *Escherichia coli* O157:H7. In: Doyle MP, ple and real sample detection. Beuchat LR, Montville TJ(Eds.), *Food Microbiology: Fundamentals and Frontiers*. ASM Press, Ishington D.C., pp. 171-191.

Drosten C, Göttig S, Schilling S, Asper M, Panning M, Schmitz H, Günther S. 2002. Rapid detection and quantification of RNA of Ebola and Marburg viruses, Lassa virus, Crimean-Congo hemorrhagic fever virus, Rift Valley fever virus, dengue virus, and yellow fever virus by real-time reverse transcription-PCR. *Journal of Clinical Microbiology* 40:2323-2330.

Elghanian R, Storhoff JL, Mucic RC, Letsinger RL, and Mirkin CA. 1997. Selective colorimetric detection of polynucleotides based on the distance-dependent optical properties of gold nanoparticles. *Science* 277:1078-1081.

Fohlerová Z, Skládal P, Turánek J. 2006. Adhesion of eukaryotic cell lines on the gold surface modified with extracellular matrix proteins monitored by the piezoelectric sensor. *Biosensors and Bioelectronics* 22:1896-1901.

Food and Drug Administration (FDA), 2001. *Escherichia coli* O157:H7. *Foodborne Pathogenic Miocroorganisms and National Toxins Handbook*. Rockville, MD, USA. (http://www.foodsafety.gov/~mow/chap15.html). Accessed on 1 September, 2006.

Food and Drug Administration (FDA), 2006. FDA announces findings from investigation of foodborne *Escherichia coli* O157:H7 outbreak in spinach. *FDA News*. (http://www.fda.gov/bbs/topics/NEWS/2006/NEW01474.html). Accessed on 30 September, 2006.

Fu Z, Rogelj S, Kieft TL. 2005. Rapid detection of *Escherichia coli* O157:H7 by immunomagnetic separation and real-time PCR. *International Journal of Food Microbiology* 99:47-57.

Giakoumaki E, Minunni M, Tombelli S, Tothill IE, Mascini M, Bogani P, Buiatti M, 2003. Combination of amplification and post-amplification strategies to improve optical DNA sensing. *Biosensors and Bioelectronics* 19:337-344.

Gollins SW and Porterfield JS. 1986. pH-dependent fusion between the flavivirus West Nile and liposomal model membranes. *Journal of General Virology* 67:157-166.

Goodrich G.P, Helfrich MR, Overberg JJ, Keating CD. 2004. Effect of macromolecular crowding on DNA:Au nanoparticle bioconjugate assembly. *Langmuir* 20:10246-10251.

Guo S. and Wang E. 2007. Synthesis and electrochemical applications of gold nanoparticles. *Analytica Chimica Acta*. 598:181-192.

Guzman MG and Kouri G. 1996. Advances in dengue diagnosis. Clinical and Diagnostic *Laboratory Immunology* 3:621-627.

Hall RH. 2002. Biosensor technologies for detecting microbiological foodborne hazards. *Microbes and Infection* 4:425–432.

Hanauer M, Pierrat S, Zins I, Lotz A, Sönnichsen C. 2007. Separation of nanoparticles by gel electrophoresis according to size and shape. *Nano Letters* 7:2881-2885.

Harris E, Roberts TG, Smith L, Selle J, Kramer LD, Valle S, Sandoval E, Balmaseda A. 1998. Typing of dengue viruses in clinical specimens and mosquitoes by single-tube multiplex reverse transcriptase PCR. *Journal of Clinical Microbiology* 36:2634-1639.

He P. and Zhang D. Y. 2005. Preparation and characterizationof a new class of starch-stabilized bimetallic nanoparticles for degradationof chlorinated hydrocarbons in water. *Environmental Science & Technology* 39:3314-3320.

Heinz FX, Stiasny K, Püschner-Auer G, Holzmann H, Allison SL, Mandl CW, Kunz C, 1994. Structural changes and functional control of the tick-borne encephalitis virus glycoprotein E by the heterodimeric association with protein prM. *Virology* 198: 109-117.

Heng HHQ, Tsui LC. 1998. Biosensor technologies for detecting microbiological foodborne hazards. *Journal of ChromatoGraphy A* 806:219-229.

Herne TM and Tarlov MJ. 1997. Characterization of DNA probes immobilized on gold surface. *Journal of the American Chemical Society* 119:8910-8920.

Huang E, Zhou F, Deng L. 2000. Studies of Surface Coverage and Orientation of DNA Molecules Immobilized onto Preformed Alkanethiol Self-Assembled Monolayers. *Langmuir* 16:3272-3280.

Hurst SJ, Lytton-Jean AKR, Mirkin CA. 2006. Maximizing DNA loading on a range of gold nanoparticle sizes. *Analytical Chemistry* 78:8313-8318.

Jaiswal S, Khanna N, Swaminathan S. 2004. High-level expression and one-step purification of recombinant dengue virus type 2 envelope domain III protein in *Escherichia coli*. *Protein Expression and Purification* 33:80-91.

Kanazawa KK and Gordon II JG. 1985. Frequency of a quartz microbalance in contact with liquid. Analytical Chemistry 57:1770-1771.

Kariuki N. Luo N., J., Hassan S. A., Lim I.-Im. S., Wang L. and Zhong C. J. 2006. Assembly of bimetallic gold-silver nanoparticles via selective interparticle dicarboxylate-silver linkages. *Chemistry of Materials* 18:123-132.

Kao CL, King CC, Chao DY, Wu HL, Chang GJ. 2005. Laboratory diagnosis of dengue virus infection: current and future perspectives in clinical diagnosis and public health. *Journal of Microbiology, Immunology and Infection* 38:5-16.

Kenneth RB, Daniel GW, Michael JN. 2000. Seeding of colloidal Au nanoparticle solutions. 2. improved control of particle size and shape. *Chemistry of Materials* 12:306-313.

Kimura T and Ohyama A. 1988. Association between the pH-dependent conformational change of West Nile flavivirus E protein and virus-mediated membrane fusion. *Journal of General Virology* 69:1247-1254.

King CC, Wu YC, Chao DY, Lin TH, Chow L, Wang HT, Ku CC, Kao CL, Chien LJ, Chang HJ, Huang JH, Twu SJ, Hwang KP, Lam SK and Gubler DJ 2000 Major Epidemics of Dengue in Taiwan in 1981-2000: Related to Intensive Virus Activities in Asia. *Dengue Bulletin* (WHO, The South-East Asia and Western Pacific Regions) 24:1-10.

Korri-Youssoufi H, Garnier F, Srivastava P, Godillot P, Yassar A. 1997. Toward bioelectronics: specific DNA recognition based on an oligonucleotide-functionalized polypyrrole. *Journal of the American Chemical Society* 119:7388-7389.

Kurosawa S, Aizawa H, Tozuka M, Nakamura M, Park JW. 2003. Immunosensors using a quartz crystal microbalance. *Measurement Science and Technology* 14:1882-1887.

Kwakye S and Baeumner A. 2003. A microfluidic biosensor based on nucleic acid sequence recognition. *Analytical and bioAnalytical Chemistry* 376:1062-1068.

Lanciotti RS, Calisher CH, Gubler DJ, Chang GJ, Vorndam AV. 1992. Rapid detection and typing of dengue viruses from clinical samples by using reverse transcriptase-polymerase chain reaction. *Journal of Clinical Microbiology* 30:545-551.

Laue T, Emmerich P, Schmitz H. 1999. Detection of dengue virus RNA in patients after primary or secondary dengue infection by using the TaqMan automated amplification system. *Journal of Clinical Microbiology* 37:2543-2547.

Levicky R, Herne TM, Tarlov MJ, Satija SK. 1998. Using self-assembly to control the structure of DNA monolayers on gold: a neutron reflectivity study. *Journal of the American Chemical Society* 120:9787-9792.

Li M, Lin YC, Wu CC, Liu HS, 2005. Enhancing the efficiency of a PCR using gold nanoparticles. *Nucleic Acids Research* 33:e184.

Li Y, Wark AW, Lee HJ, Corn RM. 2006. Single-nucleotide polymorphism genotyping by nanoparticle-enhanced surface plasmon resonance imaging measurements of surface ligation reactions. *Analytical Chemistry* 78:3158-3164.

Lien KY, Lee WC, Lei HY, Lee GB. 2006. Integrated reverse transcription polymerase chain reaction systems for virus detection. *Biosensors and Bioelectronics* 22:1739-1748.

Lien KY, Lin JL, Liu CY, Lei HY, Lee GB. 2007. Purification and enrichment of virus samples utilizing magnetic beads on a microfluidic system. *Lab on a Chip* 7:868-875.

Ligon BL. 2005. Dengue fever and dengue hemorrhagic fever: a review of the history, transmission, treatment, and prevention. *Seminars in Pediatric Infectious Diseases* 16:60-65.

Liu HS, Lin YL, Chen CC. 1997 Comparison of various methods of detection of different forms of dengue virus type 2 RNA in cultured cells. Acta Virologica. 41:317–324.

Lin L, Zhao H, Li J, Tang J, Duan M, Jiang L. 2000. Study on colloidal Au-enhanced DNA sensing by quartz crystal microbalance. *Biochemical and Biophysical Research Communications* 274:817-820.

Link S and El-Sayed MA. 1999 Optical properties and ultrafast dynamics of metallic nanocrystals. *The Journal of Physical Chemistry B* 103:4212-4217.

Lippmann G. 1881 Principe de conservation de l'électricité. *Annales de Physique et de Chimie, 5ª Serie* 24: 145-178.

Liu R, Liew R, Zhou J, Xing B. 2008. A simple and specific assay for real-time colorimetric visualization of beta-Lactamase activity by using gold nanoparticles. *Angewandte Chemie-international Edition English* 47:3081.

Liu T, Tang J, Han M, Jiang L. 2003. A novel microgravimetric DNA sensor with high sensitivity. *Biochemical and Biophysical Research Communications* 304:98-100.

Liu T, Tang J, Jiang L. 2004 The enhancement effect of gold nanoparticles as a surface modifier on DNA sensor sensitivity. *Biochemical and Biophysical Research Communications* 313:3-7

Mann TL and Krull UJ. 2004. The application of ultrasound as a rapid method to provide

DNA fragments suitable for detection by DNA biosensors. *Biosensors and Bioelectronics* 20:945-955.

Mannelli I, Minunni M, Tombelli S, Mascini M. 2003. Quartz crystal microbalance (QCM) affinity biosensor for genetically modified organisms (GMOs) detection. *Biosensors and Bioelectronics* 18:129-140.

Mao X, Yang L, Su XL, Li Y. 2006. A nanoparticle amplification based quartz crystal microbalance DNA sensor for detection of *Escherichia coli* O157:H7. *Biosensors and Bioelectronics* 21:1178-1185.

Mariotti E, Minunni M, Mascini M. 2002. Surface plasmon resonance biosensor for genetically modified organisms detection. *Analytica Chimica Acta* 453:165-172.

Marx KA. 2003. Quartz crystal microbalance: a useful tool for studying thin polymer films and complex biomolecular systems at the solution-surface interface. *Biomacromolecules* 4, 99-120.

Meng JH, Feng P, Doyle MP. 2001. Pathogenic *Escherichia coli*. In: Downes FP, Ito K. (Eds). *Compendium of Methods for the Microbiological Examination of Foods*, 4th ed. American Public Health Association, Ishington D.C., pp. 331-342.

Michalzik M, Wilke R, Büttgenbach S. 2005 Miniaturized. QCM-based flow system for immunosensor application in liquid. *Sensors and Actuators B* 111-112:410-5.

Mirkin CA, Letsinger RL, Mucic RC, Storhoff JJ. 1996. A DNA-based method for rationally assembling nanoparticles into macroscopic materials. *Nature* 382:607-609.

Mo XT, Zhou YP, Lei H, Deng L. 2002. Microbalance-DNA probe method for the detection of specific bacteria in water. *Enzyme and Microbial Technology* 30:583-589.

Mo Z, Wang H, Liang Y, Liu F, Xue Y. 2005. Highly reproducible hybridization assay of zeptomole DNA based on adsorption of nanoparticle-bioconjugate. *Analyst* 130: 1589-1594.

Morones J. R., Elechiguerra J. L., Camacho A., Holt K., Kouri J. b., Ramirei J. P. and Yacaman M. Y. 2005. The bacterial effect of silver nanoparticles. *Nanotechnolgy* 16: 2346-2353.

Mukhopadhyay A and Mukhopadhyay UK. 2007. Novel multiplex PCR approaches for the simultaneous detection of human pathogens: *Escherichia coli* O157:H7 and *Listeria monocytogenes*. *Journal of Microbiological Methods* 68:193-200.

Nie LB, Yang Y, Li S, He NY. 2007. Enhanced DNA detection based on the amplification of gold nanoparticles using quartz crystal microbalance. *Nanotechnology* 18:305501-305505

Nowak T, Färber PM, Wengler G, Wengler G. 1989. Analyses of the terminal sequences of West Nile virus structural proteins and of the in vitro translation of these proteins allow the proposal of a complete scheme of the proteolytic cleavages involved in their synthesis. *Virology* 169, 365-376.

Parida M, Horioke K, Ishida H, Dash PK, Saxena P, Jana AM, Islam MA, Inoue S, Hosaka N, Morita K. 2005. Rapid Detection and Differentiation of Dengue Virus Serotypes by a Real-Time Reverse Transcription-Loop-Mediated Isothermal Amplification Assay. *Journal of Clinical Microbiology* 43:2895-903.

Patel PD. 2006. Overview of affinity biosensors in food analysis. *Journal of AOAC International* 89:805-818.

Patolsky F, Lichtenstein A, Willner AI. 2000. Amplified microgravimetric quartz-crystal-microbalance assay of DNA using oligonucleotide-functionalized liposomes or biotinylated liposomes. *Journal of the American Chemical Society* 122: 418-419.

Patolsky F, Lichtenstin A, Willner I. 2001. Detection of single-base DNA mutations by enzyme-amplified electronic transduction. *Nature Biotechnology* 19:253-257.

Patolsky F, Ranjit KT, Lichtenstein A, Willner I. 2000. Dendritic amplification of DNA analysis by oligonucleotide-functionalized Au-nanoparticles. *Chemical Communications* 10: 1025–1026.

Pena SRN, Raina S, Goodrich GP, Fedoroff NV, Keating CD. 2002. Hybridization and enzymatic extension of au nanoparticle-bound oligonucleotides. *Journal of the American Chemical Society* 124, 7314–7323.

Peterlinz KA, Georgiadis RM, Herne TM, Tarlov MJ. 1997. Observation of Hybridization and Dehybridization of Thiol-Tethered DNA Using Two-Color Surface Plasmon Resonance Spectroscopy. *Journal of the American Chemical Society* 119: 3401–3402.

Radke SM and Alocilja EC. 2005. A high density microelectrode array biosensor for detection of *E. coli* O157:H7. *Biosensors and Bioelectronics* 20:1662-1667.

Rasooly A and Herold KE. 2006. Biosensors for the analysis of food- and waterborne pathogens and their toxins. *Journal of AOAC International* 89:873-883.

Reynolds RAI, Mirkin CA, Letsinger RL. 2000 Homogeneous, nanoparticle-based quantitative colorimetric detection of oligonucleotides. *Journal of the American Chemical Society* 122:3795-3796.

Riley LW, Remis RS, , Helgerson SD, McGee HB, Wells JG, Davis BR, Hebert RJ, Olcott HM, Johnson LM, Hargrett NT, Blake PA, Cohen ML. 1983. Hemorrhagic colitis associated with a rare *Escherichia coli* O157:H7. *The New England Journal of Medicine* 308:681-685.

Russell BJ, Velez JO, Laven JJ, Johnson AJ, Chang GJ, Johnson BW. 2007. A comparison of concentration methods applied to non-infectious flavivirus recombinant antigens for use in diagnostic serological assays. *Journal of Virological Methods* 145:62-70.

Ryu S, Jung S, Kim N, Kim W. 2001. Chemisorption of thiolated Listeria monocytogenes-specific DNA onto the gold surface of piezoelectric quartz crystal. *Agricultural Chemistry and Biotechnology* 44:163-166.

Sarah JH, Lytton-Jean AKR, MirkinCA. 2006. Maximizing DNA Loading on a Range of Gold Nanoparticle Sizes. *Analytical Chemistry* 78:8313-8318.

Sauerbrey G.. 1959. The use of oscillator for weighing thin layers and for microweighting. *Zeitschrift fur Psychosomatische Medizin und Psychotherapie* 155:206-210.

Sauthier ML, Carroll RL, Gorma CB, Franzen S. 2002. Nanoparticle layers assembled throughDNAhybridization: characterization and optimization. *Langmuir* 18:1825-30.

Shchepinov MS, Case-Green SC, Southern EM. 1997. Steric factors influencing hybridisation of nucleic acids to oligonucleotide arrays. *Nucleic Acids Research* 25:1155-1161.

Shresta S, Kyle JL, Beatty PR, Harris E. 2004. Early activation of natural killer and B cells in response to primary dengue virus infection in A/J mice. *Virology* 319:262-273.

Shrivastava S, Bera T, Roy A, Sighn G, Ramachandrarao P, Dash D. 2007. Characterization

of enhanced antibacterial effects of novel silver nanoparticles. *Nanotechnolgy* 18:1-9.

Shu PY, Chang SF, Kuo YC, Yueh YY, Chien LJ, Sue CL, Lin TH, Huang JH. 2003. Development of group- and serotypespecific one-step SYBR green I-based real-time reverse transcription- PCR assay for dengue virus. *Journal of Clinical Microbiology* 41: 2408-2416.

Shu PY and Huang JH. 2004. Current Advances in Dengue Diagnosis. Clinical and Diagnostic *Laboratory Immunology* 11:642-650

Simpson JM and Lim DV. 2005. Rapid PCR confirmation of *E. coli* O157:H7 after evanescent wave fiber optic biosensor detection. *Biosensors and Bioelectronics* 21:881-887.

Skoog DA, Holler FJ, Nieman TA. 1998. Principles of Instrumental Analysis. *Saunders College Publishing*, Philadelphia, PA.

Sondi I. and Salopek-Sondi B. 2004. Silver nanoparticles as antimicrobial agent: a case study on E. coli as a model for Gram-negative bacteria. *Journal of Colloid and Interface Science* 275: 1770-1782.

Song F, Zhou F, Wang J, Tao N, Lin J, Vellanoweth RL, Morquecho Y, Wheeler-Laidman J. 2002. Detection of oligonucleotide hybridization at femtomolar level and sequence-specific gene analysis of the Arabidopsis thaliana leaf extract with an ultrasensitive surface plasmon resonance spectrometer. *Nucleic Acids Research* 30:e72.

Southern E, Mir K, Shchepinov M. 1999. Molecular interactions on microarrays. *Nature Genetics* 21:5-9.

Steel AB, Levicky RL, Herne TM, Tarlov MJ, 2000. Immobilization of nucleic acids at solid surfaces: effect of oligonucleotide length on layer assembly. *Biophysical Journal* 79: 975-981.

Su X, Chew FT, Li SFY. 2000. Design and application of piezoelectric quartz crystal-based immunoassay. *Analytical Sciences* 16:107-114.

Su XL and Li Y. 2004. A self-assembled monolayer-based piezoelectric immunosensor for rapid detection of *Escherichia coli* O157:H7. *Biosensors and Bioelectronics* 19:563-574.

Su X, Wu YJ, Robelek R, Knoll W. 2005. Surface plasmon resonance spectroscopy and quartz crystal microbalance study of streptavidin film structure effects on biotinylated DNA assembly and target DNA hybridization. *Langmuir* 21:348-353.

Su X, Robelek R, Wu Y, Wang G, Knoll W. 2004. Detection of point mutation and insertion mutations in DNA using a quartz crystal microbalance and MutS, a mismatch binding protein. *Analytical Chemistry* 76:489-494.

Subramanian A, Irudayaraj J, Ryan T. 2006. A mixed, self-assembled monolayer-based surface plasmon immunosensor for detection of *E. coli* O157:H7, *Biosensors and Bioelectronics* 21:998-1006.

Sung JH, Ko HJ, Park TH. 2006. Piezoelectric biosensor using olfactory receptor protein expressed in *Escherichia coli*. *Biosensors and Bioelectronics* 21:1981-1986.

Tai DF, Lin CY, Wu TZ, Chen LK. 2005. Recognition of dengue virus protein using epitope-mediated molecularly imprinted film. *Analytical Chemistry* 77:5140-3514.

Takenaka SYK, Takagi M, Uto Y, Kondo H. 2000. DNA Sensing on a DNA probe-modified electrode using ferrocenylnaphthalene diimide as the electrochemically active ligand. *Analytical Chemistry* 72:1334-1341.

Taton TA, Mirkin, CA, Letsinger RL. 2000. Scanometric DNA array detection with nanoparticle probes. *Science* 289:1757-1760.

Thaxton CS, Georganopoulou DG, Mirkin CA. 2006 Gold nanoparticle probes for the detection of nucleic acid targets. *Clinica Chimica Acta* 363:120-126.

Theron J., Walker J. A. and Cloete T. E. 2008. Nanotechnology and water treatment: applications and emerging opportunities. Critical Reviews in *Microbiology* 34:43-69.

Tombelli S, Mascini M, Braccini L, Anichini M, Turner APF. 2000. Coupling of a DNA piezoelectric biosensor and polymerase chain reaction to detect apolipoprotein E polymorphisms. *Biosensors and Bioelectronics* 15:363-370.

Tombelli S, Mascini M, Turner APF. 2002. Coupling of a DNA piezoelectric biosensor and polymerase chain reaction to detect apolipoprotein E polymorphisms. *Biosensors and Bioelectronics* 17:929-936.

Wang E, Ni H, Xu R, Barrett AD, Watowich SJ, Gubler DJ, Weaver SC. 2000. Evolutionary relationships of endemic/epidemic and sylvatic dengue viruses. *Journal of Virology* 74:3227-3234.

Wang WK, Sung TL, Tsai YC, Kao CL, Chang SM, King CC. 2002. Detection of Dengue Virus Replication in Peripheral Blood Mononuclear Cells from Dengue Virus Type 2-Infected Patients by a Reverse Transcription-Real-Time PCR Assay. *Journal of Clinical Microbiology* 40:4472-8

Wei HY, Jiang LF, Fang DY, Guo HY. 2003. Dengue virus type 2 infects human endothelial cells through binding of the viral envelope glycoprotein to cell surface polypeptides. *Journal of General Virology* 84:3095-3098.

Weizmann Y, Patolsky F, Willner I. 2001. Amplified detection of DNA and analysis of single-base mismatches by the catalyzed deposition of gold on Au-nanoparticles. *Analyst* 126:1502:1504.

Wilder-Smith A, Schwartz E. 2005. Dengue in Travelers. *New England Journal of Medicine* 353:2511-2513.

Wolf LK, Gao Y, Georgiadis RM. 2004. Sequence-Dependent DNA Immobilization: Specific versus Nonspecific Contributions. *Langmuir* 20:3357-3361.

Wu TZ, Su CC, Chen LK, Yang HH, Tai DF, Peng KC. 2005. Piezoelectric immunochip for the detection of dengue fever in viremia phase. *Biosensors and Bioelectronics* 21:689-695.

Wu VCH, Gill V, Oberst R, Phebus R, Fung DYC. 2004. Rapid Protocol (5.25 hr) protocol for the detection of *Escherichia coli* O157:H7 in raw ground beef by an immuno-capture system (Pathatrix) in combination with Colortrix and CT-SMAC. *Journal of Rapid Methods and Automation in Microbiology* 12:57-67.

Wu VCH, Chen SH, Lin CS. 2007. Real-time detection of *Escherichia coli* O157:H7 sequences using a circulating-flow system of quartz crystal microbalance. *Biosensors and Bioelectronics* 22:2967-2975.

Yamaguchi N, Sasada M, Yamanaka M, Nasu M. 2003. Rapid detection of respiring *Escherichia coli* O157:H7 in apple juice, milk, and ground beef by flow cytometry. *Cytometry Part A* 54A, 27-35.

Yang L, Li Y, Erf GF. 2004. Interdigitated array microelectrode-based electrochemical impedance immunosensor for detection of *Escherichia coli* O157:H7. *Analytical*

Chemistry 76:1107–1113.

Yong YK, Thayan R, Chong HT, Tan CT, Sekaran SD. 2007. Rapid detection and serotyping of dengue virus by multiplex RT-PCR and real-time SYBR green RT-PCR. *Singapore Medical Journal* 48:662-668.

Yoshitomi KJ, Jinneman KC, Weagant SD. 2003. Optimization of a 3'-minor groove binder-DNA probe targeting the uidA gene for rapid identification of *Escherichia coli* O157:H7 using real-time PCR. *Molecular and Cellular Probes* 17:275-280.

Young PR, Hilditch PA, Bletchly C and Halloran W. 2000. An antigen capture enzyme-linked immunosorbent assay reveals high levels of the dengue virus protein NS1 in the sera of infected patients. *Journal of Clinical Microbiology* 38:1053-1057.

Zhang Y, Bahns JT, Jin Q, Divan R, Chen L. 2006. Toward the detection of single virus particle in serum. *Analytical Biochemistry* 356:161-170.

Zhao HQ, Lin L, Li JR, Tang JA, Duan MX, Jiang L. 2001. DNA biosensor with high sensitivity amplified by gold nanoparticles. *Journal of Nanoparticle Research* 3:321-323.

Zhao X, Hilliard LR, Mechery SJ, Wang Y, Bagwe RP, Jin S, Tan W. 2004. A rapid bioassay for single bacterial cell quantitation using bioconjugated nanoparticles. Proceedings of the National Academy of Sciences of the United States of America 101:15027-15032.

Zhou XC, Huang LQ, Li SFY. 2001 Microgravimetric DNA sensor based on quartz crystal microbalance: comparison of oligonucleotide immobilization methods and the application in genetic diagnosis. *Biosensors and Bioelectronics* 16:85-95.

Zhou XC, O'Shea SJ, Li SFY. 2000. Amplified microgravimetric gene sensor using Au nanoparticle modified oligonucleotides. *Chemical Communications* 16:953-954.

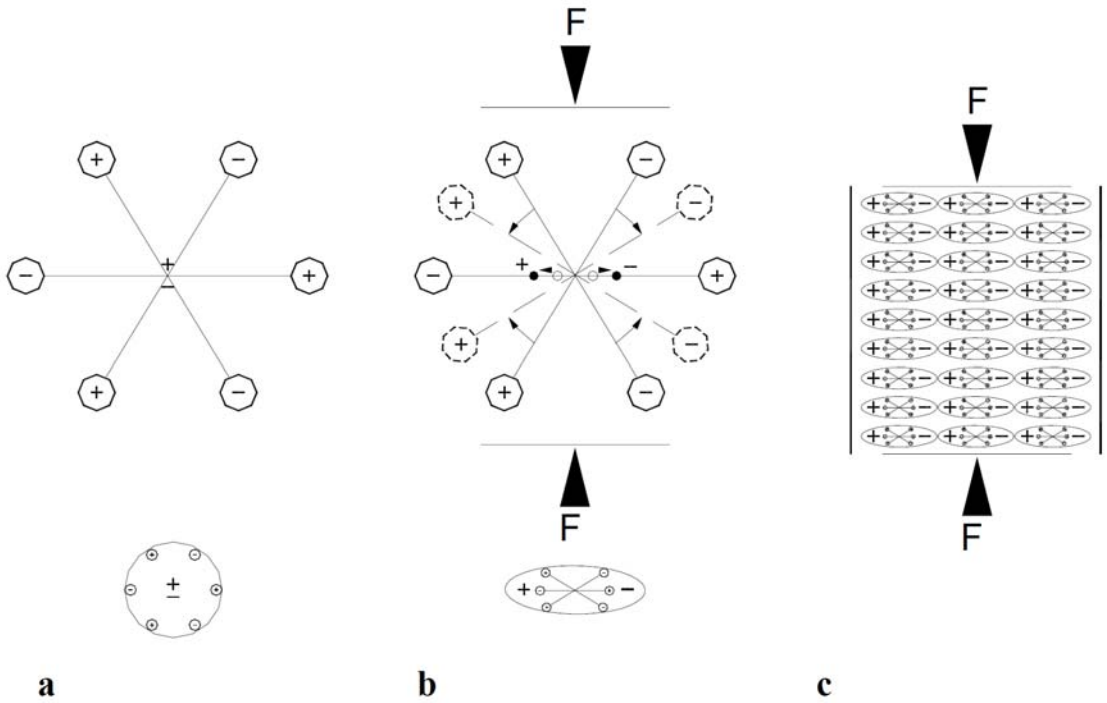

Figure 3-1. Simple molecular model for explaining the piezoelectric effect: **a.** unperturbed molecule; **b.** molecule subjected to an external force, and **c.** polarizing effect on the material surfaces.

A.

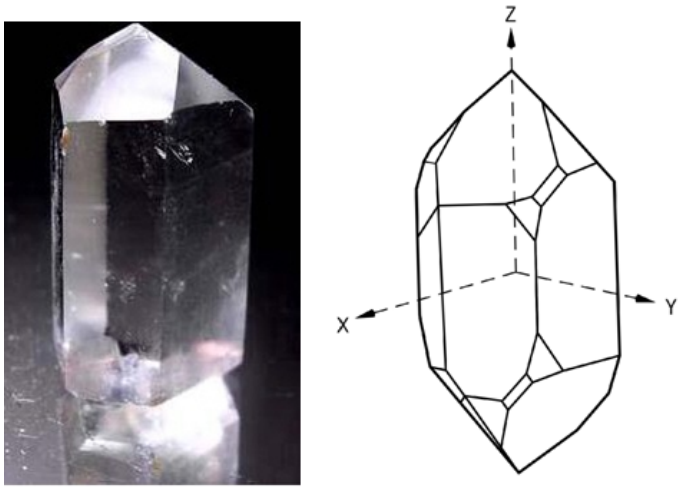

B.

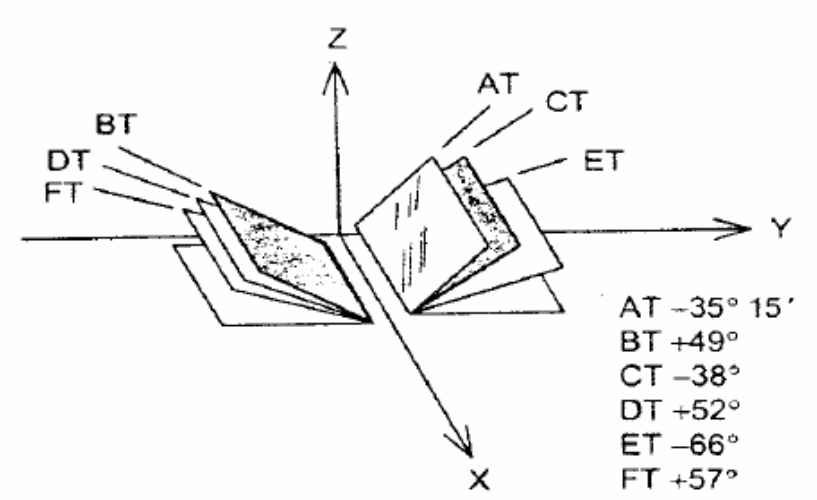

Figure 3-2. Slicing the different angle to the optical z-axis. The quartz crystal may provide a large variety of different resonator types depending on the cut angle with respect to the crystal lattice. The cut angle determines the mode of induced mechanical vibration. AT-cut crystals, which are predominately used for QCM devices, operate in the TSM and are prepared by slicing a quartz wafer with an angle of 35¼° to the optical z-axis**.**

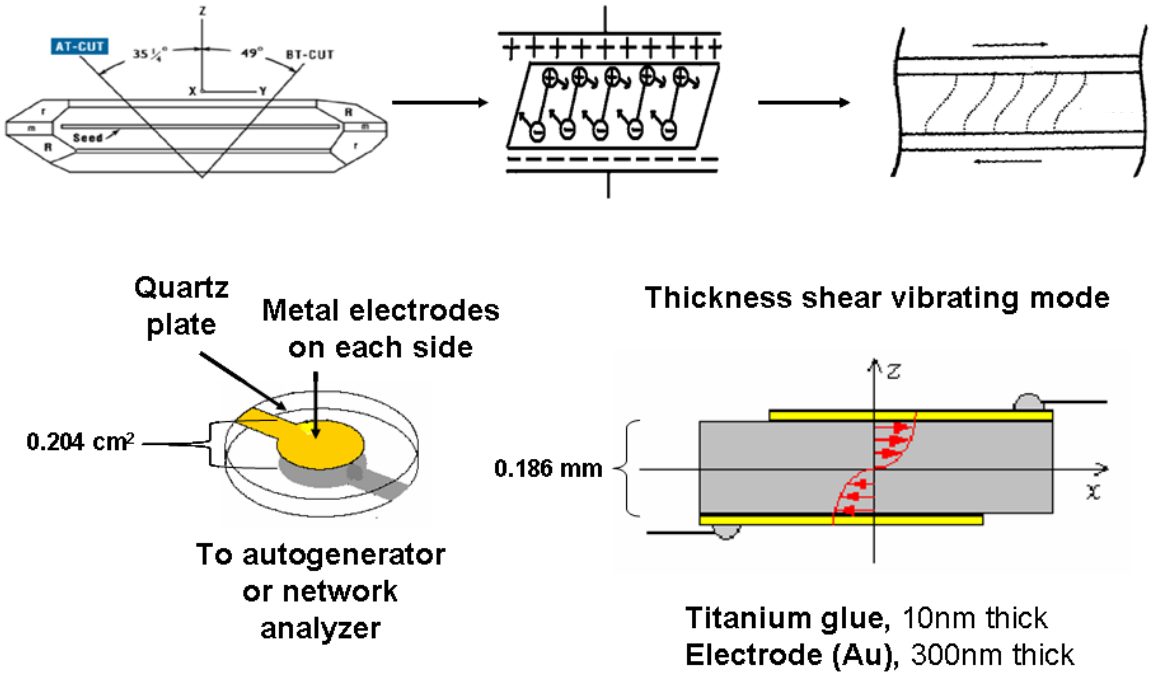

Figure 3-3. Reverse piezoelectric effect on quartz crystal. AT-cut crystals, which are predominately used for quartz crystal microbalance (QCM) devices, operate in the TSM and are prepared by slicing a quartz wafer with an angle of 35¼° to the optical *z*-axis. When electric field is applied to the quartz crystal, the crystals show stability oscillation via electrostriction effect.

A.

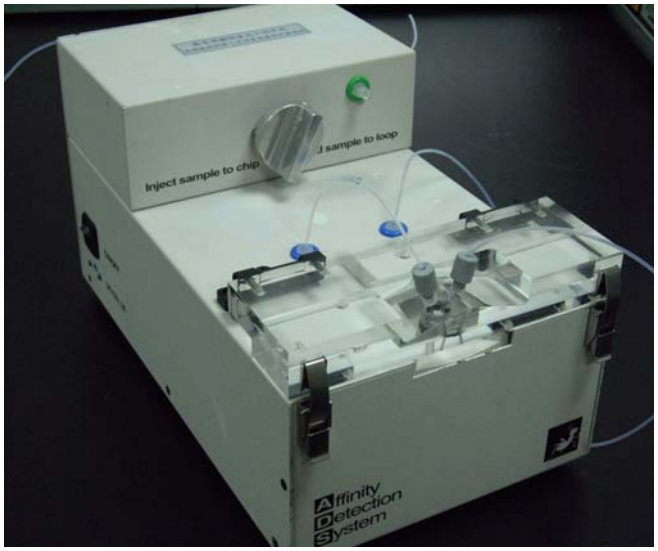

B.

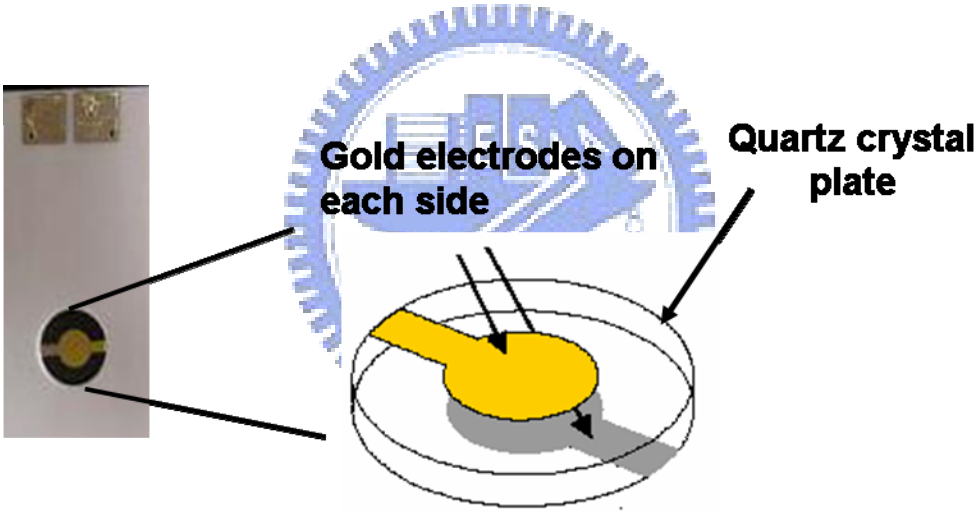

Figure 3-4. Transducer of Quartz Crystal Analyzer. (**A**) ANT-300 is a mass-sensitive detector based on frequency changes of an oscillating quartz wafer. Frequency Range: 1-10 MHz; Resolution: 0.1 Hz; Gate Time: 0.1 sec, 1 sec and 10 sec; Resonant Resistance Range: 10-16 Kohm, 0.1 ohm resolution; Analog Outputs: +/- 10 V, delta-freq = +/- 200 to +/-200 KHz (4 ranges), delta-res= 1/2/4/8/16K ohm ranges. (**B**) AT-cut of a quartz crystal from which the metal coated QCM quartz crystals. (ANT Technology, Taipei, Taiwan)

A.

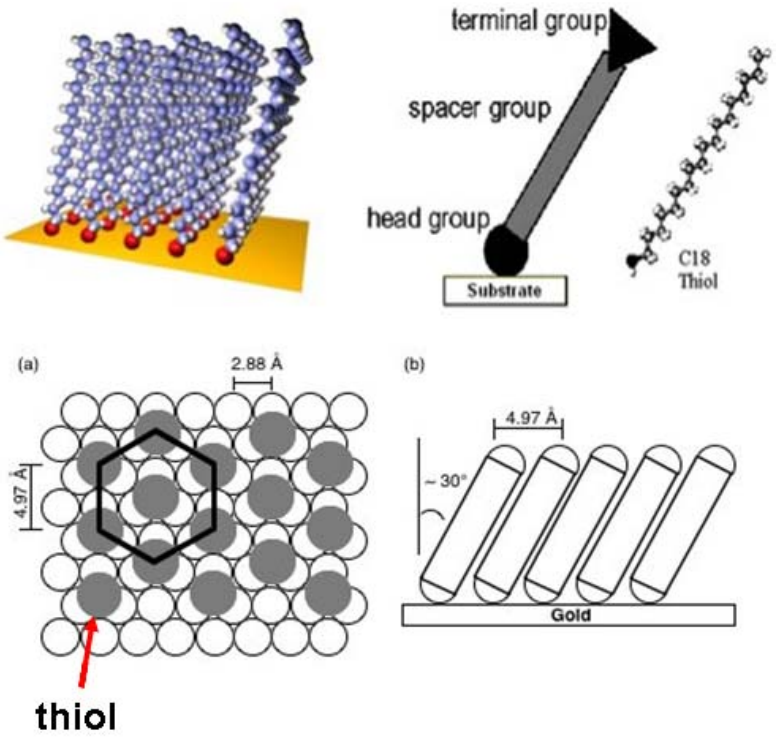

B.

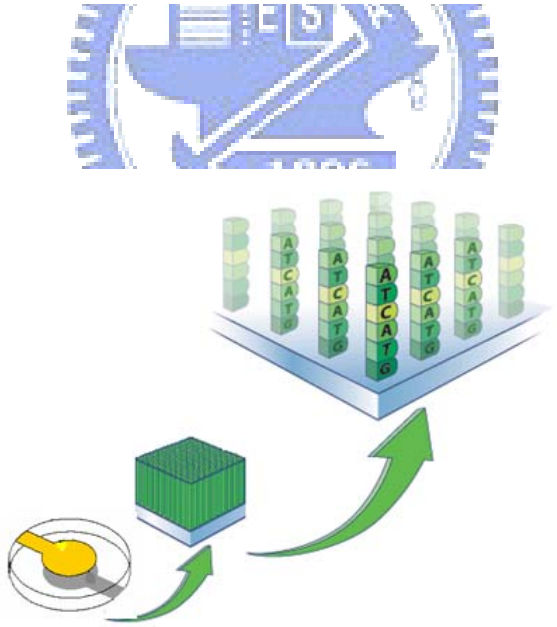

Figure 4-1. Schematic representation of a tightly packed alkanethiol monolayer by SAM. (A) The tilt angle of the individual chains is approximately 30° to the normal degree of the surface. This tilting maximizes the van der Waals interactions between alkane chains. (B) The DNA probes are immobilized gold on Quartz crystal Chip surface by SAM

A.

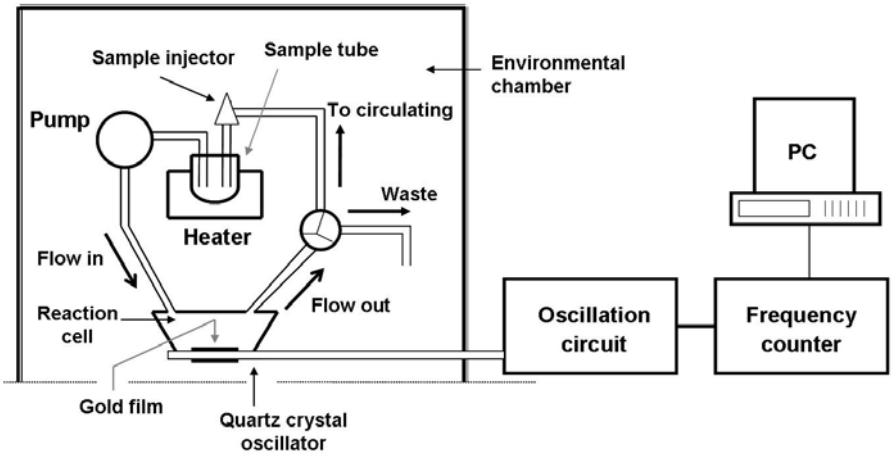

B.

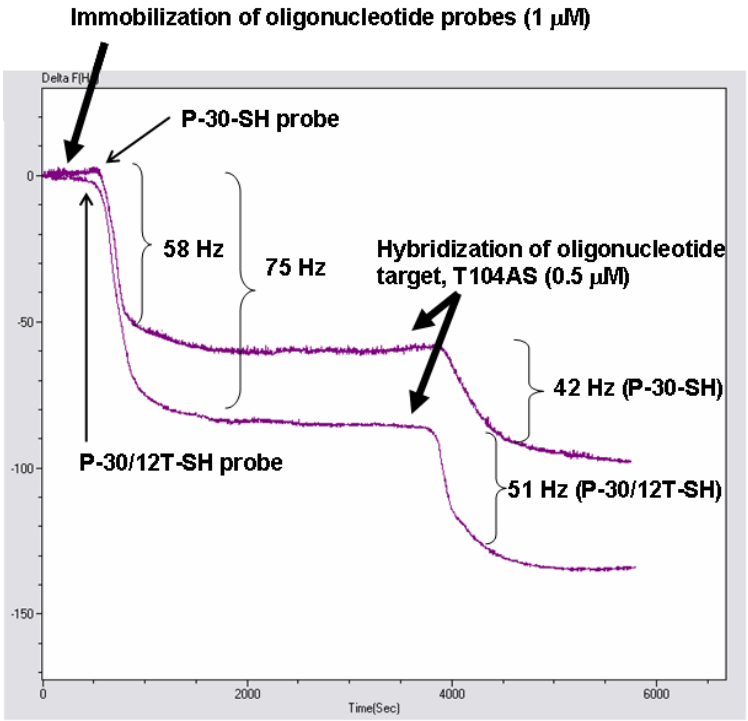

Figure 7-1. The real-time and circulating-flow QCM system. (**A**) a schematic illustration of the real-time and circulating-flow QCM system. The gold films on the quartz crystal oscillator are 3.4 mm in diameter and 0.2 cm^2 in the area of both sides. The volume of the sample tube is 1.5 ml. The volume of the reaction cell is 30 μl and the total volume of the pipeline loop, including flow in and flow out, is 100 μl. (**B**) an example of real-time detection of *E*scherichia *coli* O157:H7 sequences performed in the study using the circulating-flow QCM system.

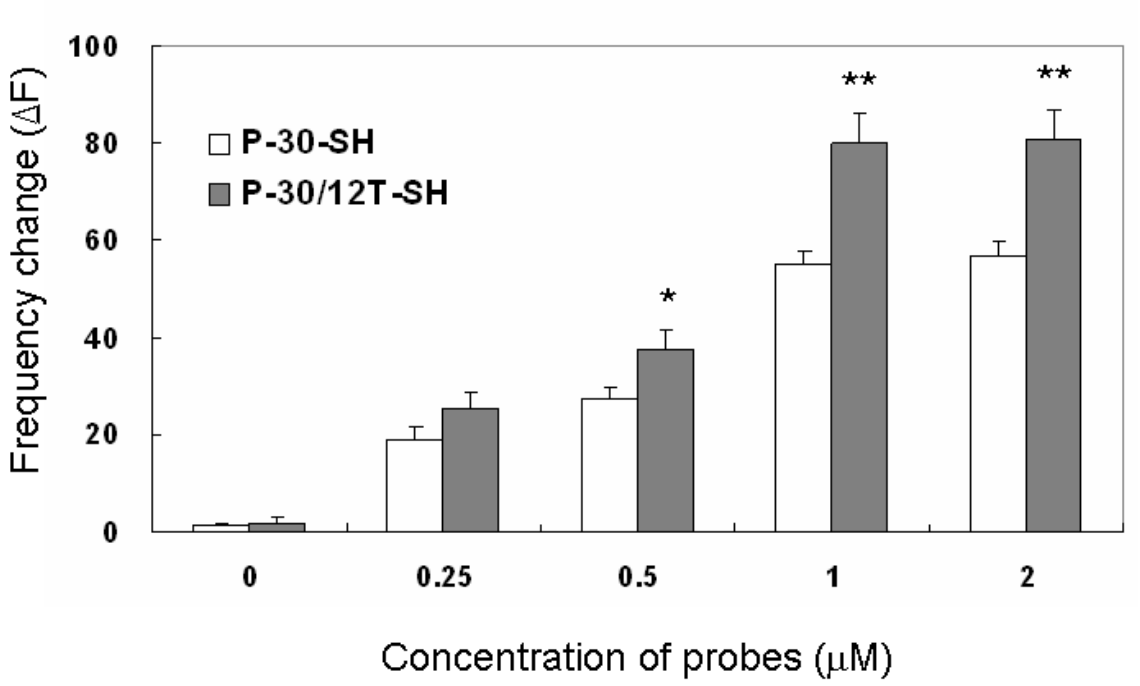

Figure 8-1. Immobilization efficiency of oligonucleotide probes on the gold surface of the QCM device. Frequency change (ΔF) of the QCM device is measured and calculated. Values derived from 5 independent detections, error bars mean standard deviation (SD). * and ** indicate $P < 0.05$ and $P < 0.01$, respectively, vs. P-30-SH.

A.

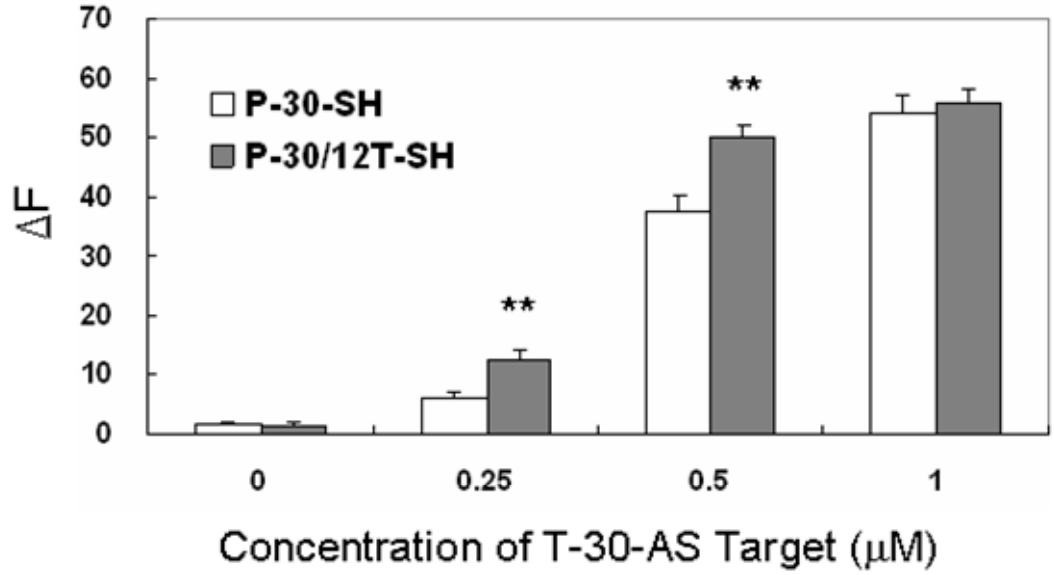

B.

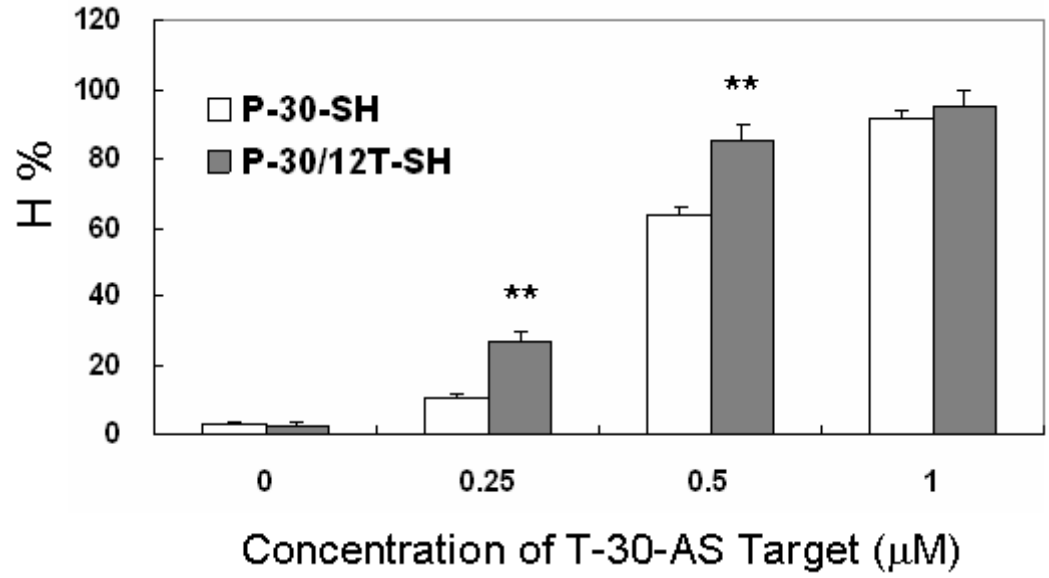

Figure 8-2. Detection of the short target oligonucleotides, T-30-AS, hybridized with the thiolated probes (1.0 μM) immobilized onto the gold surface of the QCM device. Frequency change (**A**) and hybridization efficiency (**B**) are measured and calculated. Values derived from 5 independent detections, error bars mean SD. ** indicates $P < 0.01$ vs. probe P-30-SH.

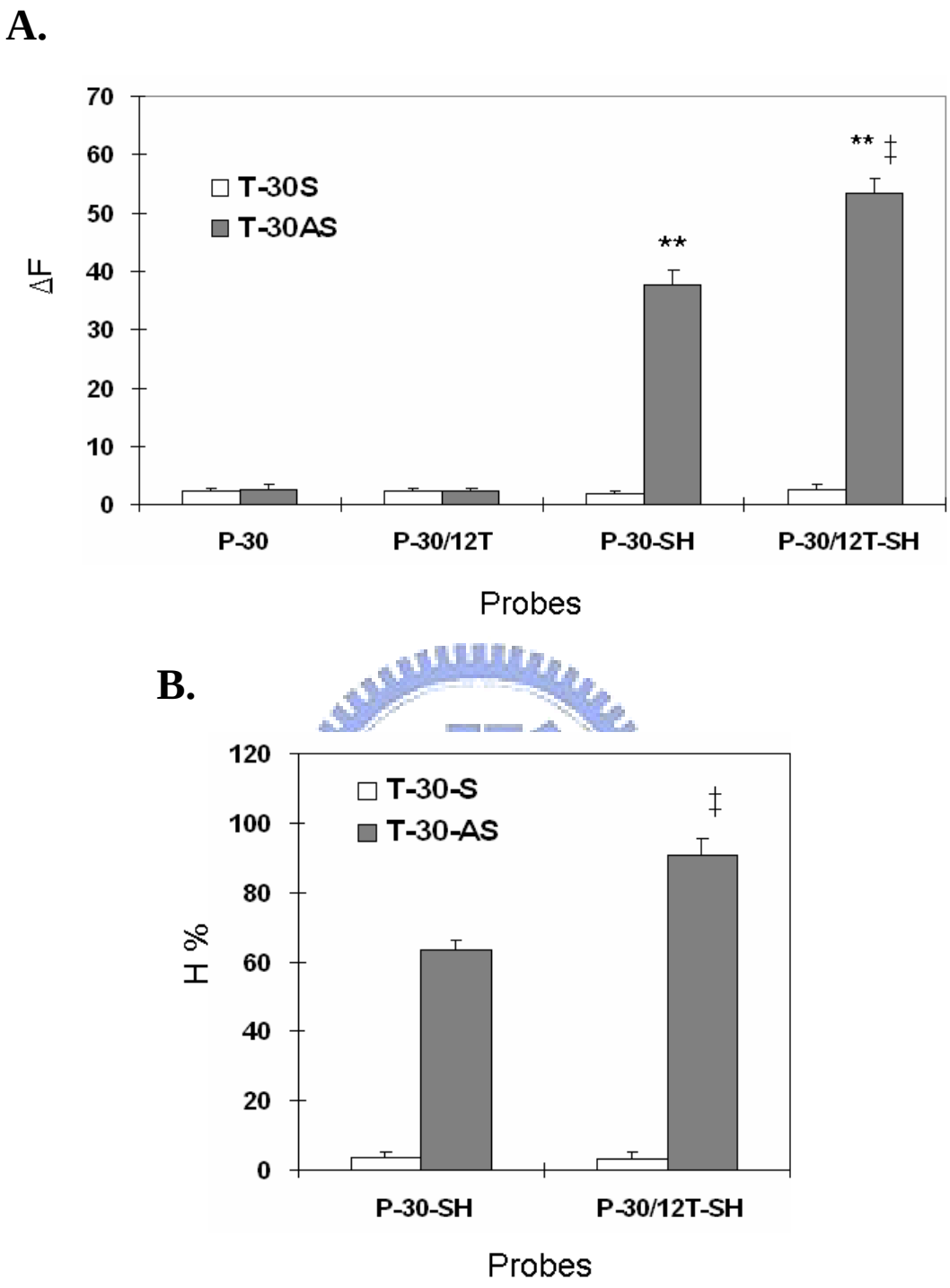

Figure 8-3. Detection specificity of the circulating flow QCM system. Four probes (P-30-SH, P-30/12T-SH, P-30, and P-30/12T; 1 μM) and two targets (T-30AS and T-30S; 0.5 μM) are applied to test the efficiencies of probe immobilization and hybridization of the target to the probe immobilized QCM device. In each treatment, frequency change (**A**) and hybridization efficiency (**B**) are measured and calculated. Values derived from 5 independent detections, error bars mean SD. ** indicates $P < 0.01$ vs. T-30S and ‡ indicates $P < 0.01$ vs. P-30-SH.

A.

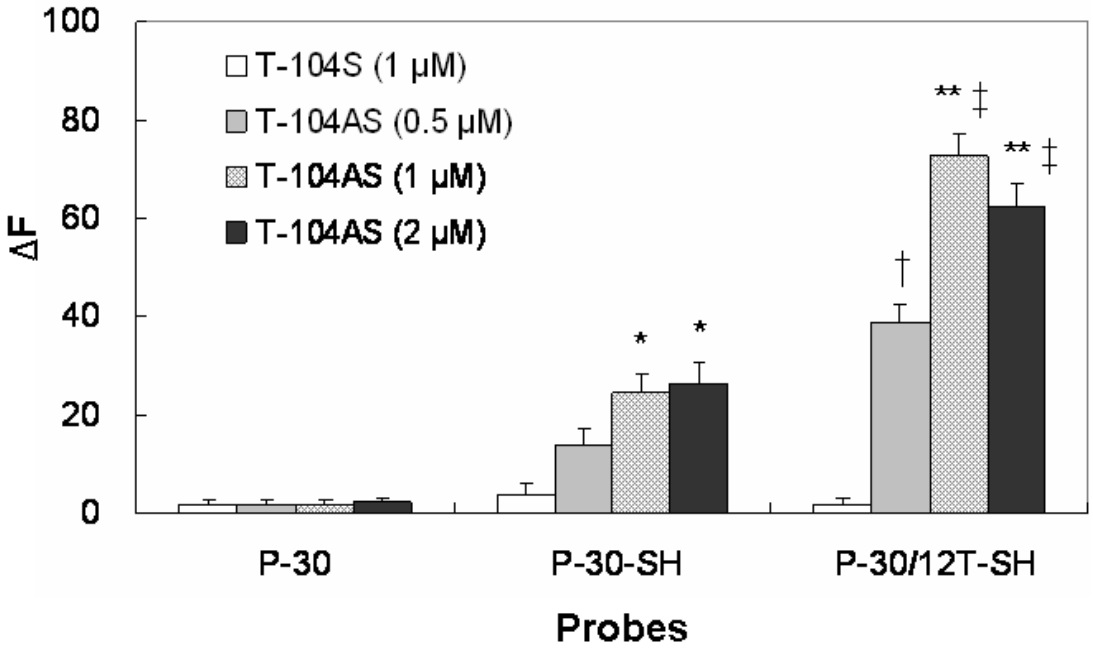

B.

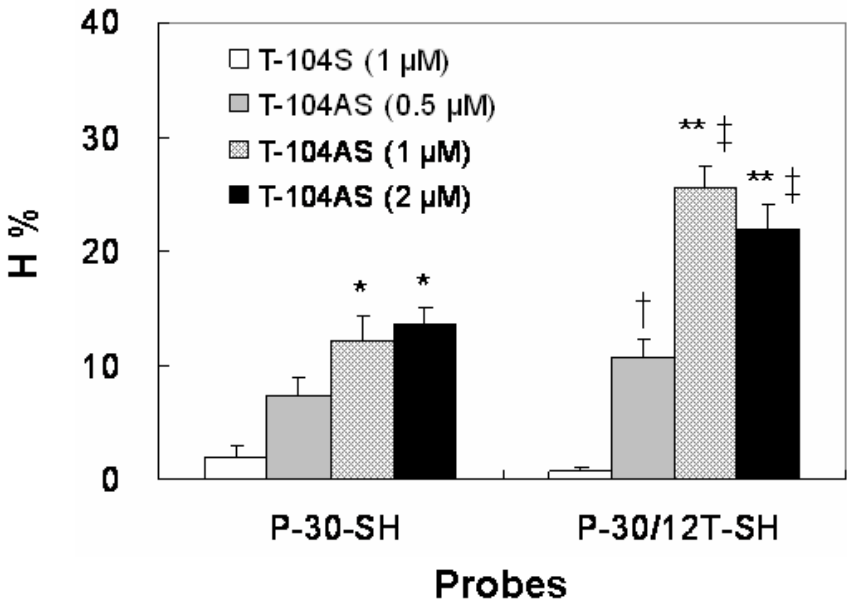

Figure 8-4. Detection of the long oligonucleotide targets, T-104AS and T-104S, hybridized with the probes (1.0 μM) immobilized onto the gold surface of the QCM device. Frequency change (**A**) and hybridization efficiency (**B**) are measured and calculated. Values derived from 5 independent detections, error bars mean SD. * and ** indicate $P < 0.05$ and $P < 0.01$, respectively, vs. target T-104AS (0.5 μM). † and ‡ indicate $P < 0.05$ and $P < 0.01$, respectively, vs. probe P-30-SH.

A. **B.**

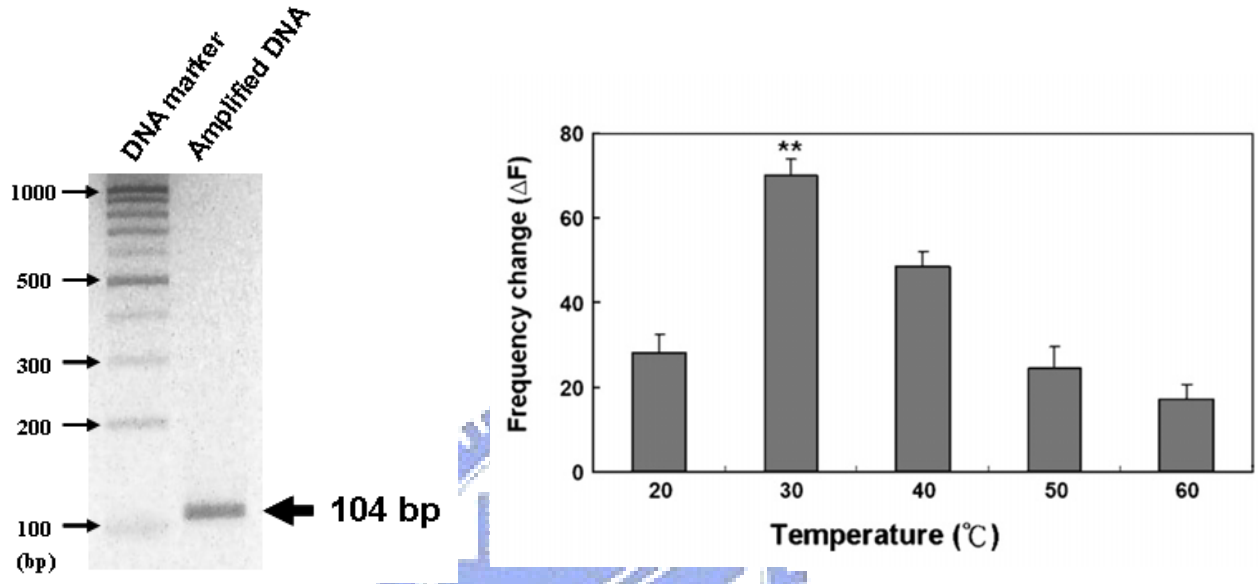

Figure 8-5. Detection of PCR-amplified DNA. (**A**) the 104 bp DNA fragment amplified by PCR from the *eaeA* gene of *E. coli* O157:H7. The amplified sequence is also identified by DNA sequencing and the sequence is " 5'-CAA TTT TTC AGG GAA TAA CAT TGC TGC AGG ATG GGC AAC TCT TGA GCT TCT GTA AAT ATA AAT TTA ATT AAG AGA AAA TAC AAT GTC ATC AAG ATC TGA ACT TT-3' " (This is the sequence of one strand). (**B**) temperature effect on the hybridization of the PCR-amplified DNA fragment from the *eaeA* gene of *E. coli* O157:H7 to the probe P-30/12T-SH. In the hybridization, 2 μM of PCR-amplified DNA (equivalent to 1 μM of target T-104AS) is used to hybridize the thiolated probes immobilized on QCM device. ** indicates $P < 0.01$ vs. other temperature treatments.

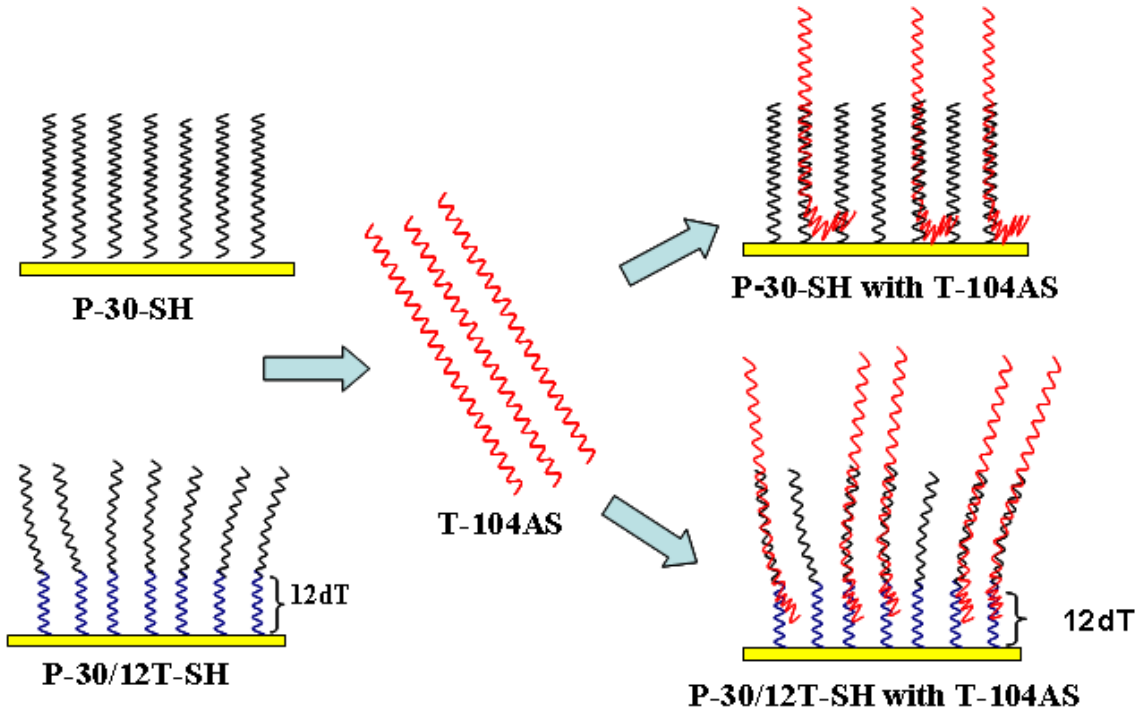

Figure 8-6. Schematic representation of steric hindrance of the probe and target DNA hybridization on the QCM device. The target T-104AS molecules hybridized to the probe P-30-SH easily to form a bent sequences adjacent to the surface of gold film in contrast to the targets hybridized to the probe P-30/12T-SH. This phenomenon may obstruct the entrance of other target sequences for hybridization.

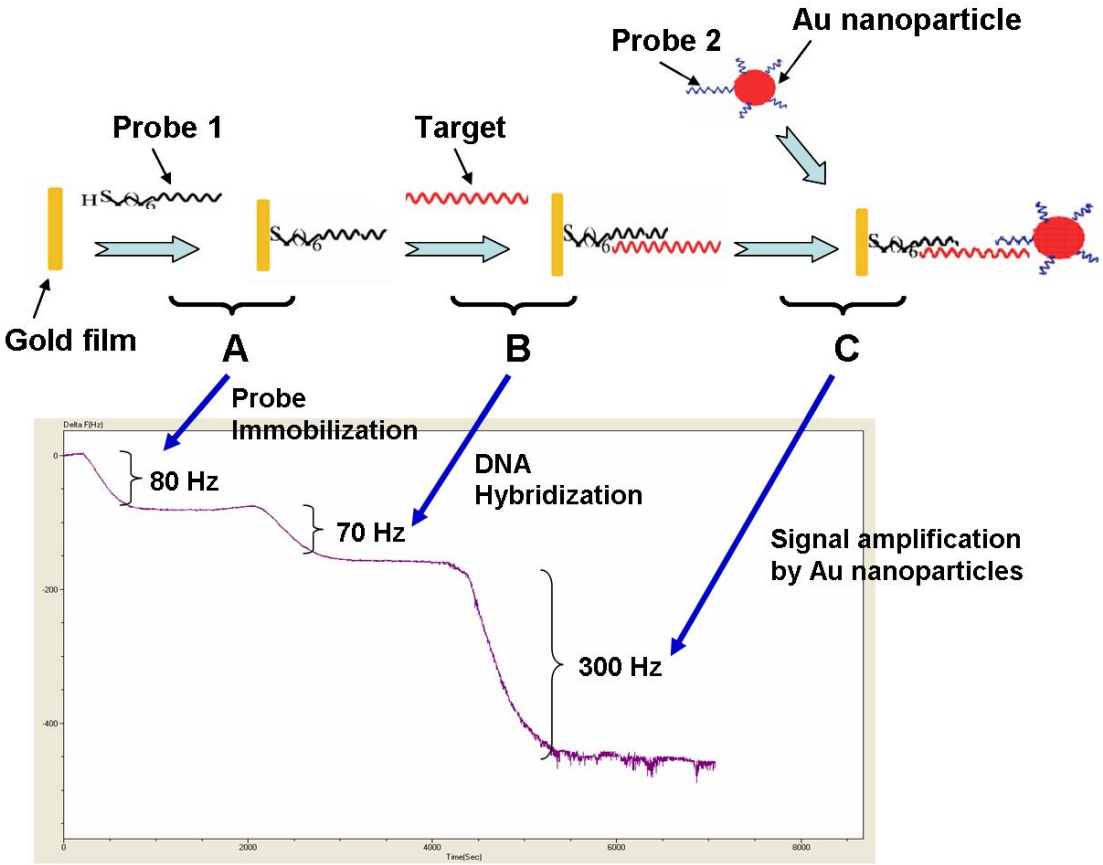

Figure 9-1. Time-dependent frequency changes of the circulating-flow QCM sensor. (**A**) Addition of Probe 1 (1 μM; P1-30/12T) to self-assembly immobilize on the surface of the QCM sensor. (**B**) The complementary target oligonucleotides [0.5 μM; T-104(AS)] are subsequently introduced for DNA hybridization. (**C**) Additional treatment of the DNA hybridized QCM with Probe 2 (P2-30/12T)-capped Au nanoparticles. The sequence of Probe 1 and Probe 2 are complementary to the two ends of the analyte DNA (i.e., target sequences).

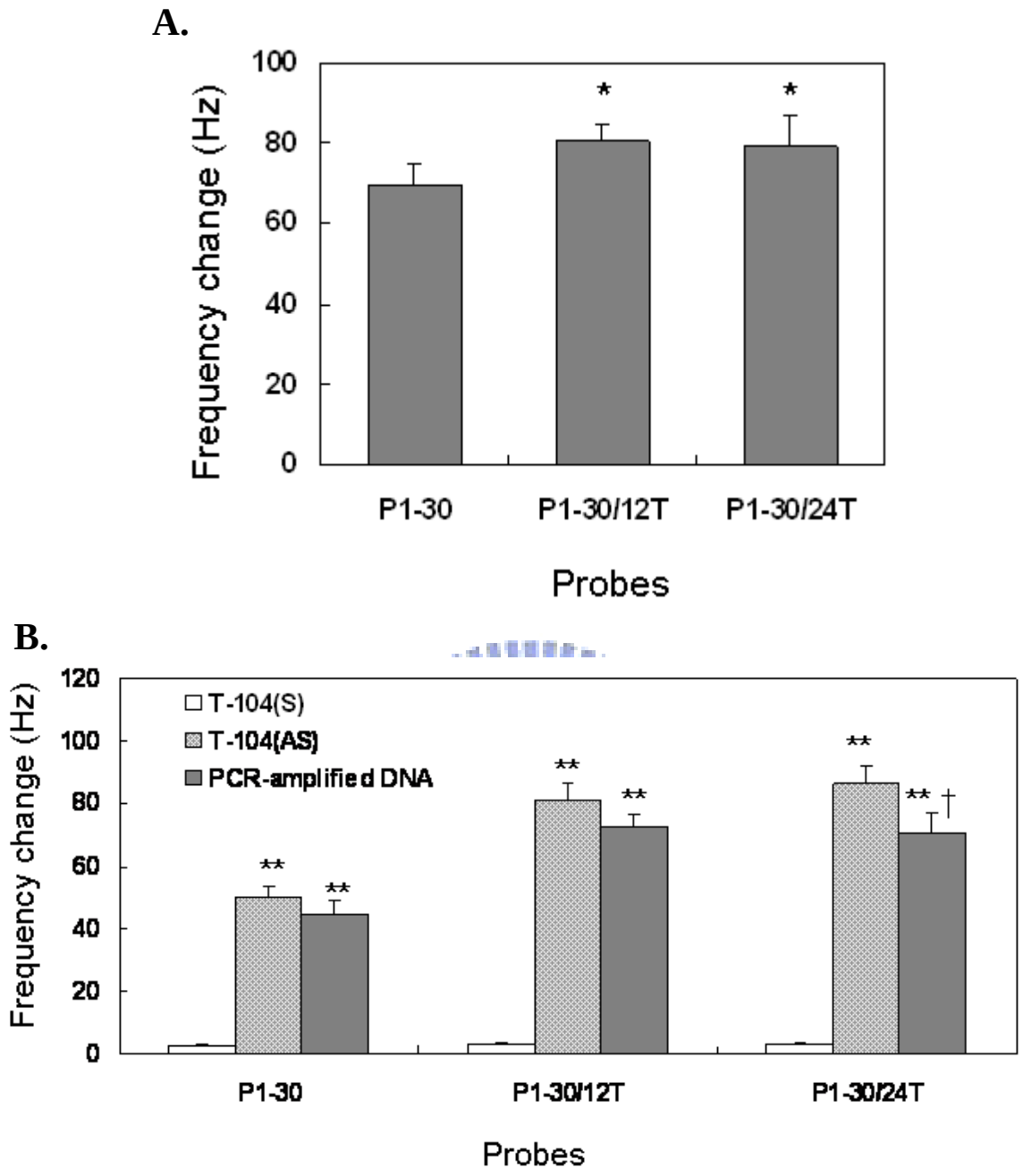

Figure 9-2. Immobilization and hybridization efficiencies in the QCM system. (**A**) The probe oligonucleotides (Probe 1; 1 μM), P1-30, P1-30/12T and P1-30/24T, are immobilized onto the Au surface of QCM sensor and the frequency change of the QCM sensor is measured. * indicates $P < 0.05$ vs. P1-30 probe. (**B**) The target oligonucleotides (0.5 μM), T-104(S) (104-mer; a non-complementary strand to the probes immobilized on the QCM sensor), T-104(AS) (104-mer; a complementary strand), and the PCR-amplified DNA (104-bp; 1 μM) are hybridized with the QCM sensor and the frequency changes are measured. ** indicates $P < 0.01$ vs. T-104(A) and † indicates $P < 0.05$ vs. T-104(AS). Values derived from 3 independent detections, error bars mean SD.

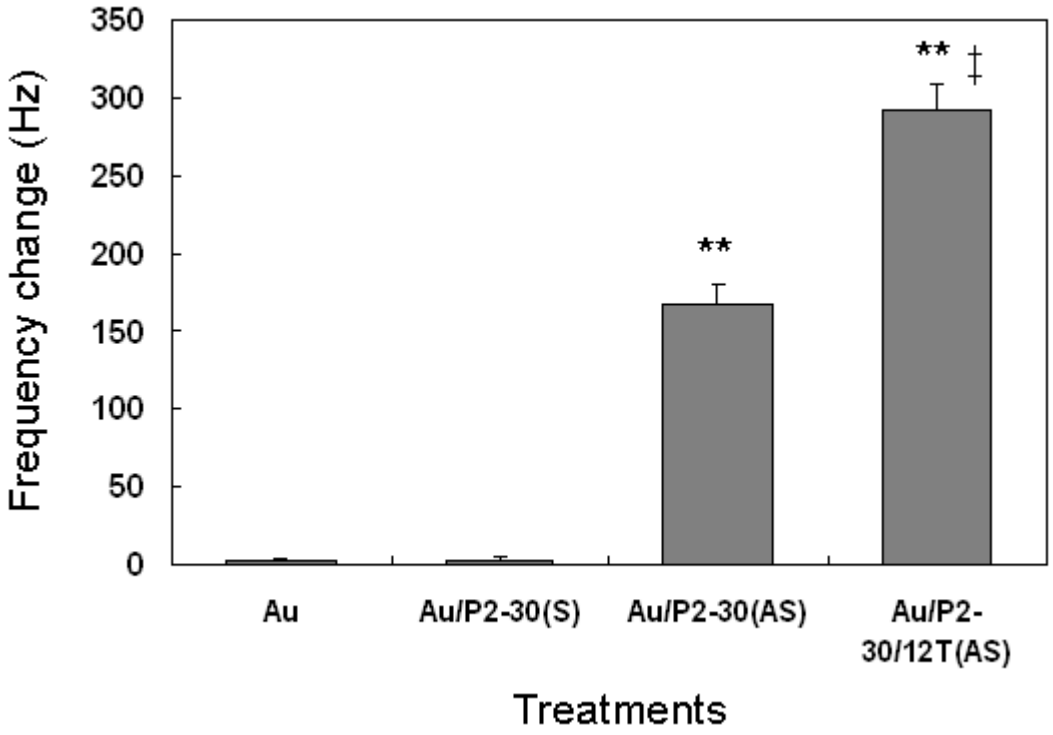

Figure 9-3. Sandwich hybridization using the oligonucleotide-functionalized Au nanoparticles. Au nanoparticles and Probe 2-capped Au nanoparticles, including P2-30(S)-, P2-30(AS)- and P2-30/12T(AS)-capped Au nanoparticles, are applied to hybridize the target sequences that are hybridized to the P1-30/12T probe-immobilized QCM sensors. The frequency changes are measured in each treatment. Values derived from 3 independent detections, error bars mean SD. ** indicates $P < 0.01$ vs. Au nanoparticles and P2-30(S)-capped Au nanoparticles. ‡ indicates $P < 0.01$ vs. P2-30(AS)-capped Au nanoparticles.

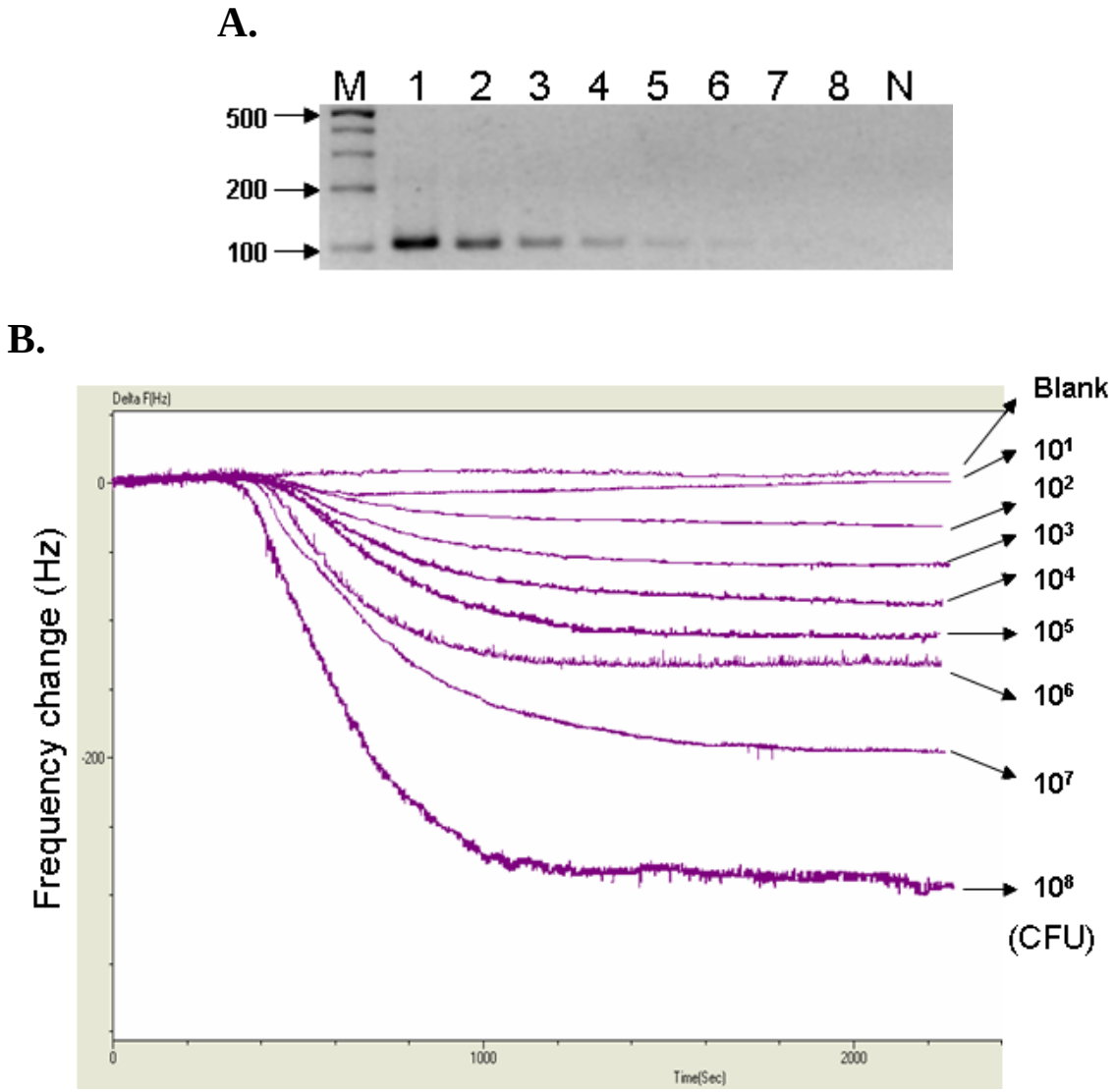

Figure 9-4. Gel electrophoresis and QCM detections of PCR-amplified DNA from *E. coli* O157:H7 *eaeA* gene. (**A**) Gel electrophoresis detection of *E. coli* O157:H7 *eaeA* gene PCR products. M, DNA marker; lane 1–8, 3 μl of the PCR-amplified products (purified and dissolved in 50 μl of TE buffer after PCR) from *E. coli* O157:H7 cells with concentrations from 1.2×10^8 to 1.2×10^1 CFU/ml; N, PCR blank control (water as PCR template). (**B**) Frequency shifts of the DNA sensor as a function of time for different PCR samples (3 μl each). The curves of frequency shift from top and in order are blank; 1.2×10^1 to 1.2×10^8 CFU/ml.

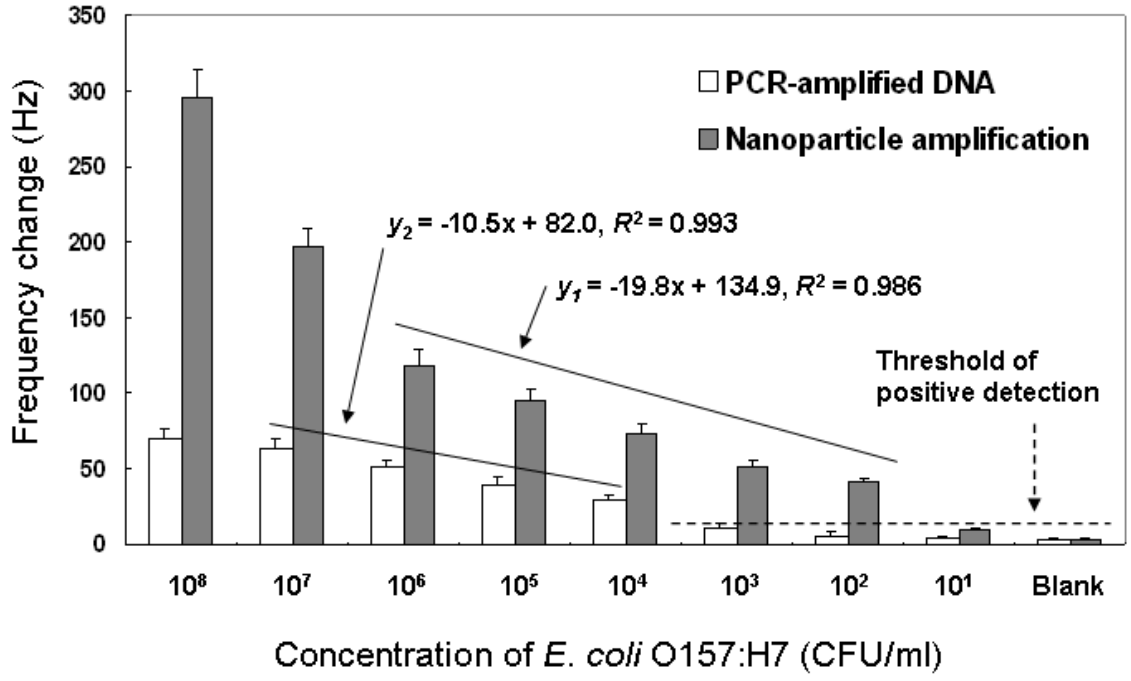

Figure 9-5. The responses of the QCM sensor to the PCR-amplified DNAs isolated from different concentrations of *E. coli* O157:H7. In the detection of PCR-amplified DNA with and without P2-30/12T-capped Au nanoparticle amplification, linear relationships are found between the frequency shift vs. log (CFU/ml of *E. coli* O157:H7) from 1.2×10^2 to 1.2×10^6 CFU (y_1 = -19.8x + 134.9, R^2 = 0.986) and from 1.2×10^4 to 1.2×10^8 CFU/ml (y_2 = -10.5x + 82.0, R^2 = 0.993), respectively. The threshold for the positive detection is set as signal-to-noise (S/N) = 3, and the detection limit is determined as 1.2×10^4 CFU/ml and 1.2×10^2 CFU/ml in the tests without and with Au nanoparticles as the amplifier, respectively. Values derived from 3 independent detections, error bars mean SD.

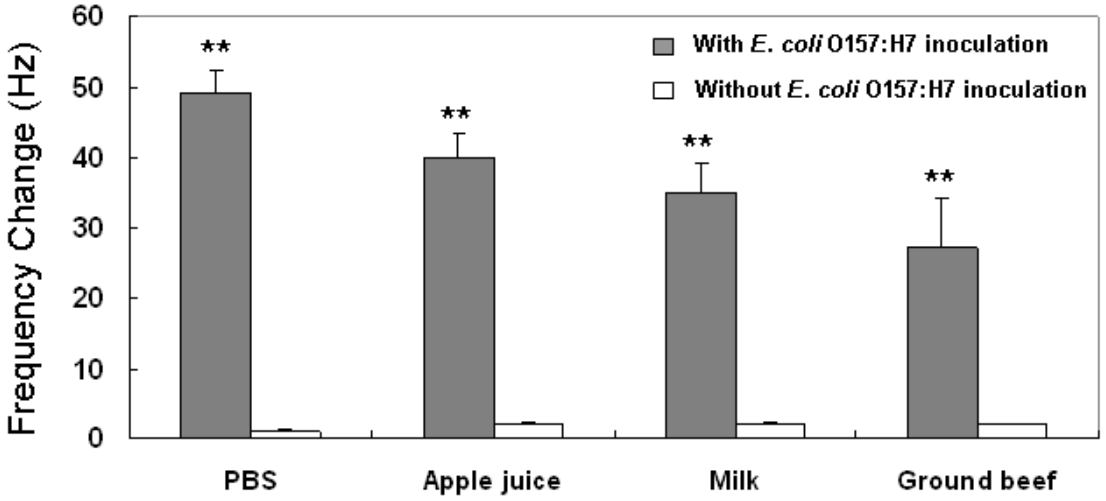

Figure 9-6. Detection of *E. coli* O157:H7 in food samples using the circulating-flow QCM sensor with Au nanoparticles for signal amplification. The food samples inoculated with or without 5.3×10^2 CFU/ml (for apple juice and milk) or CFU/g (for ground beef) of *E. coli* O157:H7 are applied to the detection. *E. coli* O157:H7 cells are also inoculated in PBS (5.3×10^2 CFU/ml) as positive control in the detection. Values derived from 3 independent detections, error bars mean SD. ** indicates $P < 0.01$ *vs.* the sample without *E. coli* O157:H7 cells inoculation.

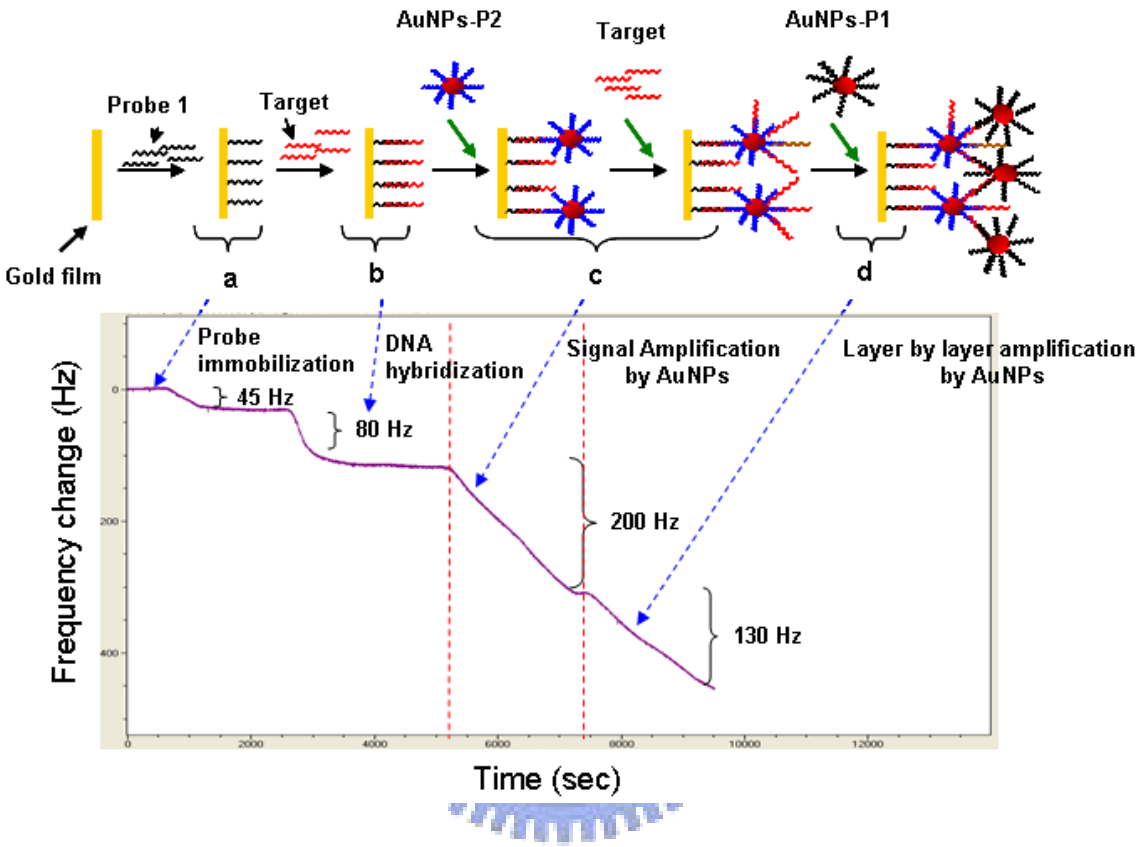

Figure 10-1. Schematic illustration of the steps involved in probe immobilization, probes hybridized with target sequences, and layer-by-layer AuNPs-probes amplification. One example of step by step procedures corresponded to the QCM flowchart and recorded oscillatory frequency change (ΔF) of the detection process is shown. (a) Specific probe (DENV2-P1) immobilized onto the QCM chip. (b) DENV2-P1 probe complement hybridized with the target sequences (partial gene sequences encoding DENV E protein) at 5' terminum. (c) AuNPs-DENV2-P2 complement hybridized with the target sequences at 3' terminum to enhance detection signal, i.e., increasing ΔF. (d) AuNPs-DENV2-P2 linked to AuNPs-DENV2-P1 by the surplus target sequences that play as a bridge for the layer-by-layer AuNPs-probes hybridizes for enhancing ΔF. Specific probes are immobilized onto the chip surface of QCM sensor or AuNPs by thiol (-SH) group.

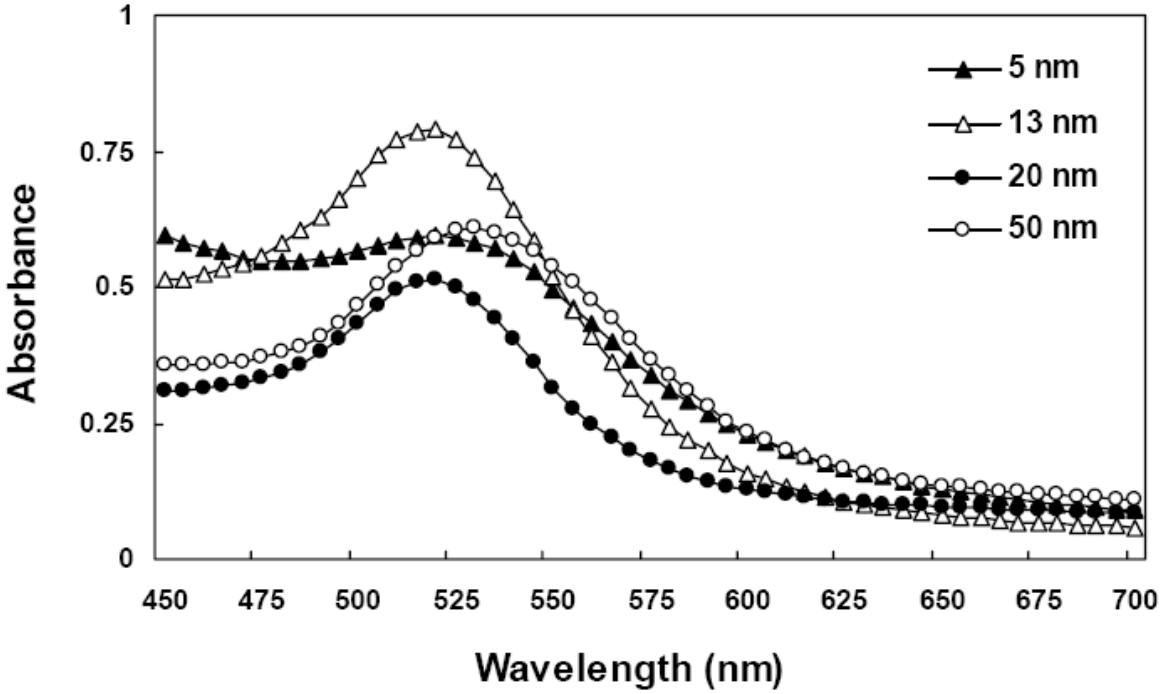

Figure 10-2. UV-Vis absorption spectra of the AuNPs with different diameters. Four sizes of AuNPs in diameter of 5, 13, 20 and 50 nm are measured by UV-Vis absorption spectrophotometer, and they exhibited an absorption maximum at 520-540 nm arising when the AuNPs exhibit noticeable absorption and scattering from the colloid gold localized surface plasmon resonance.

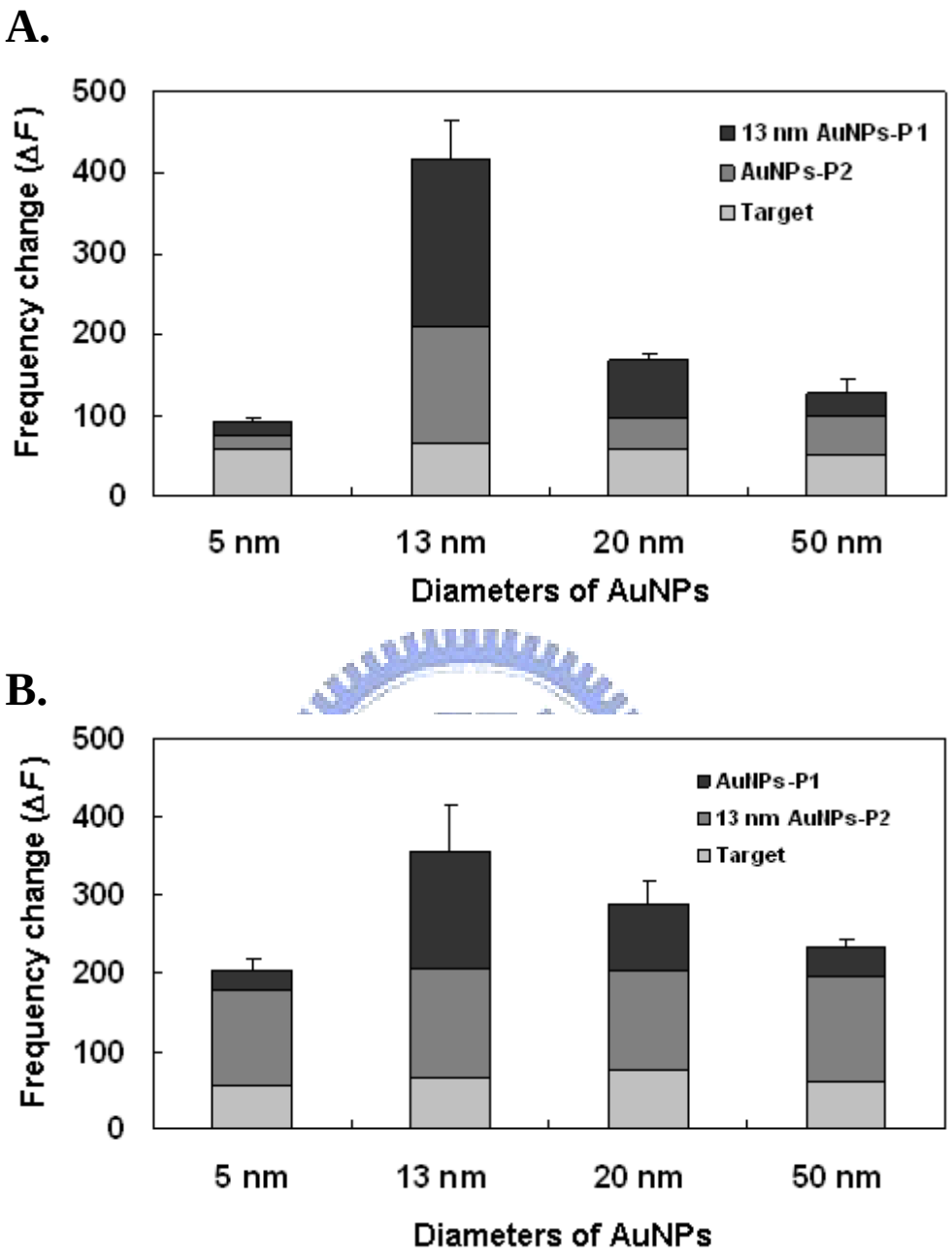

Figure 10-3. The enhancement of detection signal by different sizes of AuNPs-probes. (**A**) In the experiments, 5, 13, 20 and 50 nm AuNPs-DENV2-P2 as the 1st layer and 13 nm AuNPs-DENV2-P1 as the the 2nd layer enhancers. (**B**) In the experiments, 13 nm AuNPs-DENV2-P2 as the 1st layer and 5, 13, 20 and 50 nm AuNPs-DENV2-P1 as the 2nd layer enhancers. Each value is derived from 3 independent detections and error bars mean SD.

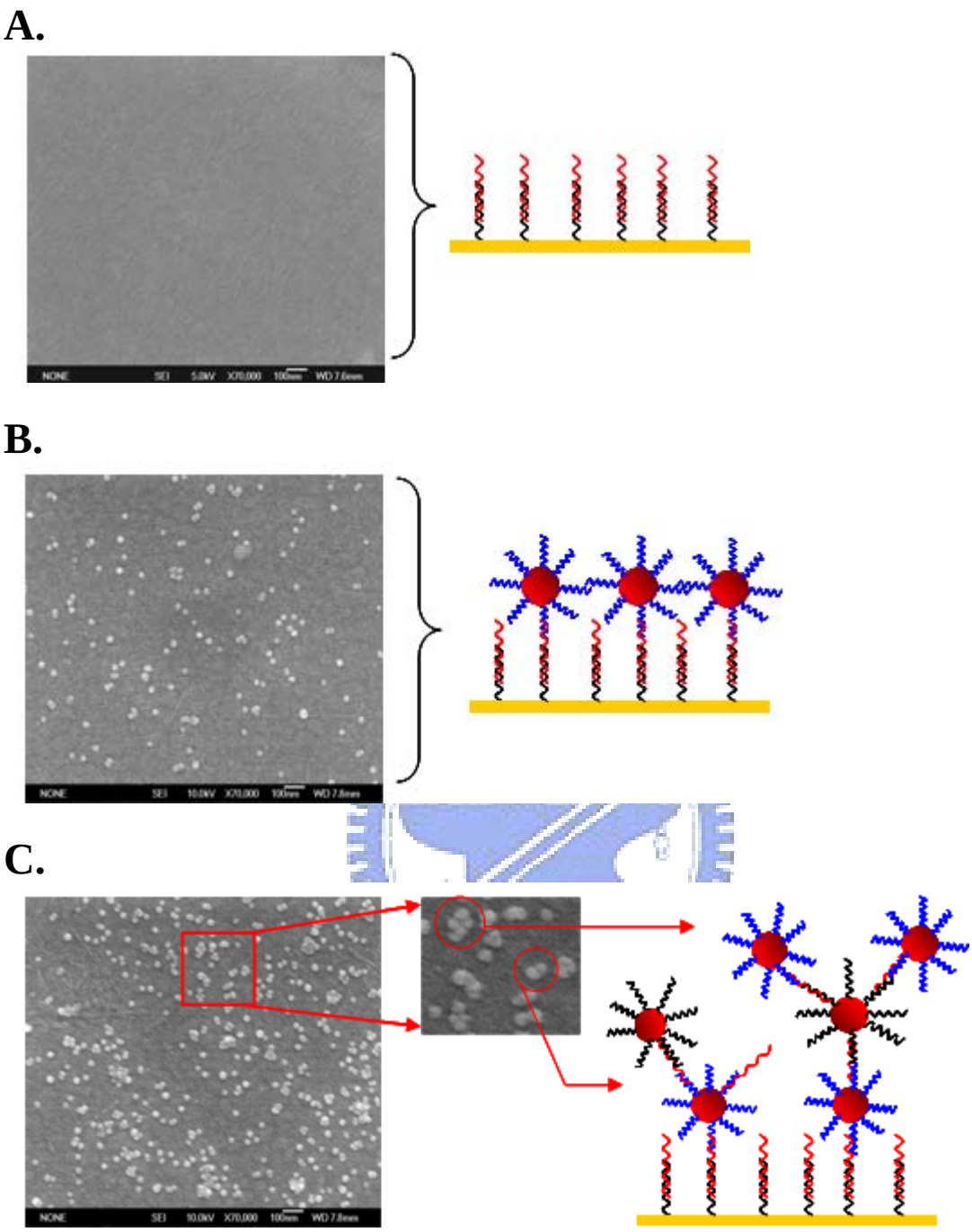

Figure 10-4. SEM images of the chip surface of QCM sensor. (**A**) The chip surface of QCM immobilized DENV2-P1 probes and hybridized target sequences without AuNPs-probes applied. (**B**) The chip surface with the 1st layer of AuNPs-DENV2-P2 (13 nm) adapted onto the QCM chip via the hybridization with target sequences. (**C**) The chip surface with the 2nd layer of AuNPs-DENV2-P1 (13 nm) added onto the QCM chip via the hybridization with target sequences. The close view in the panel c shows the AuNPs-probes linked by the surplus target sequences and most of two to four AuNPs-probes linked together.

A.

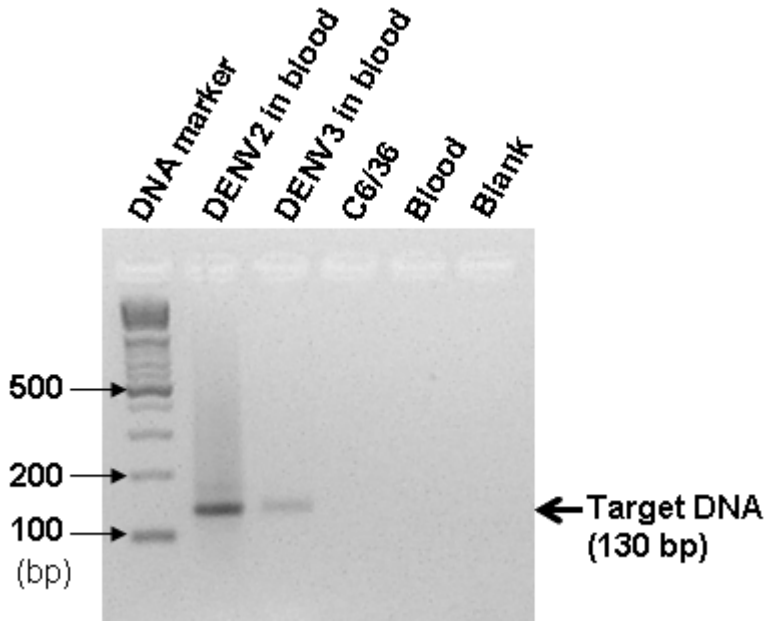
DNA marker
DENV2 in blood
DENV3 in blood
C6/36
Blood
Blank
500
200
100
(bp)
Target DNA
(130 bp)

B.

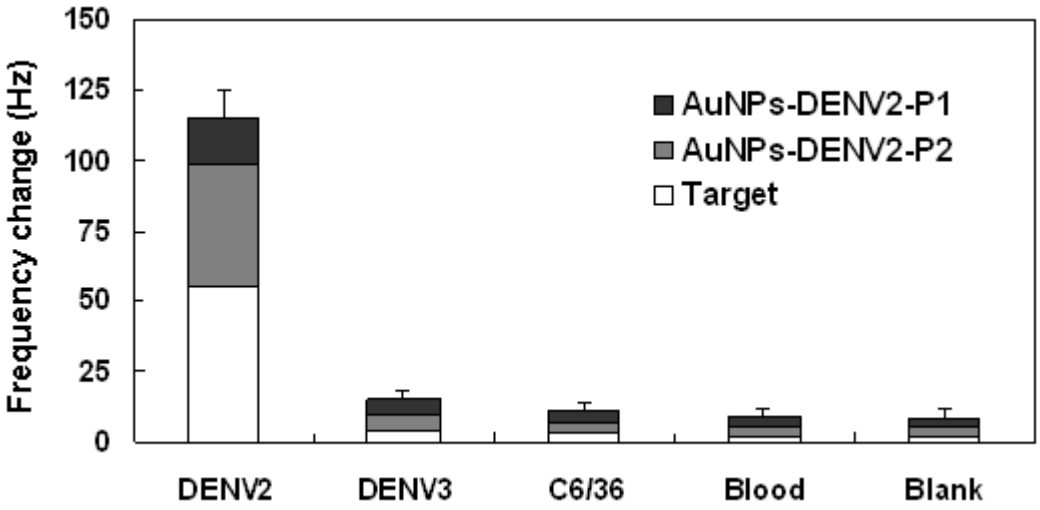
Frequency change (Hz)
150
125
100
75
50
25
0
AuNPs-DENV2-P1
AuNPs-DENV2-P2
Target
DENV2
DENV3
C6/36
Blood
Blank

C.

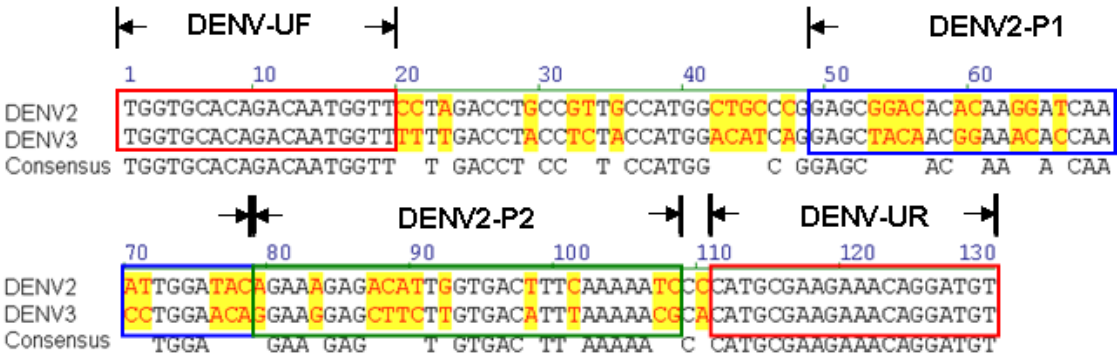
DENV-UF
DENV2-P1
DENV2-P2
DENV-UR
DENV2
DENV3
Consensus
TGGTGCACAGACAATGGTTCCTAGACCTGCCGTTGCCATGGCTGCCGGAGCGGACACACAAGGATCAA
TGGTGCACAGACAATGGTTTTTTGACCTACCTCTACCATGGACATCAGGAGCTACAACGGAAACACCAA
ATTGGATACAGAAAGAGACATTGGTGACTTTCAAAAATCCCCATGCGAAGAAACAGGATGT
CCTGGAACAGGAAGGAGCTTCTTGTGACATTTAAAAACGCACATGCGAAGAAACAGGATGT

Figure 10-5. Specificity of the layer-by-layer AuNPs-probes (13 nm) for the DENV sequence detection. The DENV cDNA is obtained by RT used DENV-URT as primer and then the DNA fragment of DENV E gene is obtained by asymmetric PCR using the universal primer pair, DENV-UF and DENV-UR. (**A**) A representative result of agarose electrophoresis shows that a 130 bp of DNA fragment is obtained in the samples of DENV2 and DENV3 which are mixed into human blood before the RNA is extracted. There are no PCR product is observed in the samples of C6/36 cells and whole blood. (**B**) The results of QCM detection showed that a significant ΔF (-115 Hz) is detected only in the sample of DENV2 in blood. Each value is derived from 3 independent detections and error bars mean SD. (**C**) The sequence alignment show the difference between DENV2 and DENV3 within the target sequences, the sequence similarity of probe 1 and probe 2 recognized region is 53% and 63 %, respectively.

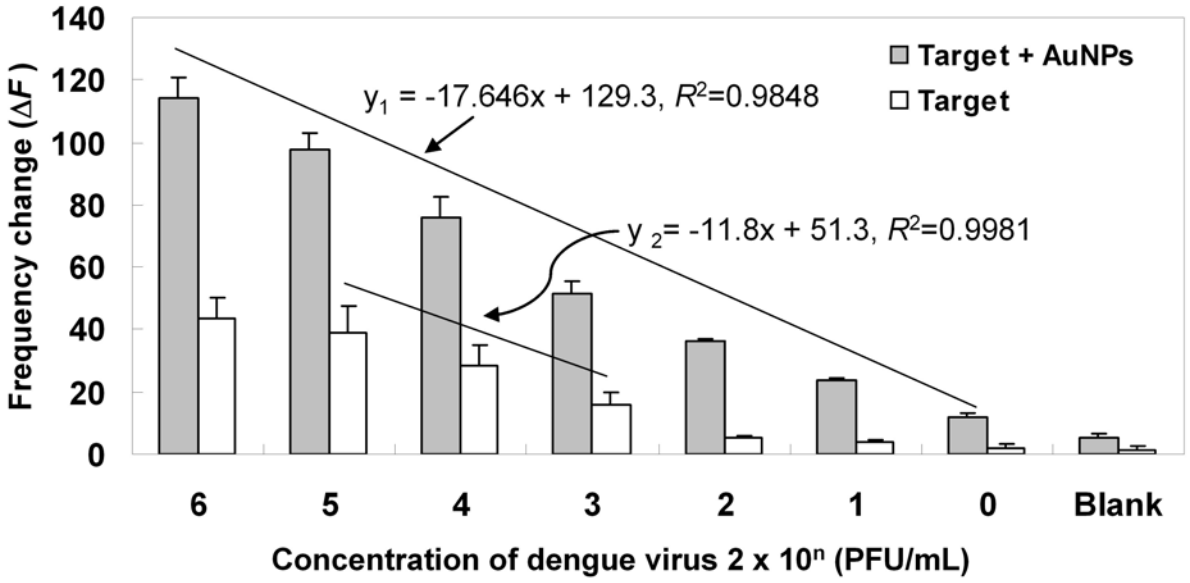

Figure 10-6. Sensitivity of the circulating-flow DNA-QCM sensor combined with the layer-by-layer AuNPs-probes (13 nm) amplification. Different titer of DENV2 (2×10^0 to 2×10^6 PFU/mL) are detected by the QCM system with and without the AuNPs-probes amplification. The blank control showed the background of $\Delta F = 2 \pm 1$ Hz in the samples without AuNPs-probes and $\Delta F = 7 \pm 1$ Hz in samples with AuNPs-probes application. In the detection with the layer-by-layer AuNPs-probes amplification, a linear relationship is found between the ΔF *vs.* log (PFU/mL of DENV2) from 2×10^0 to 2.0×10^6 PFU/mL. In the detection without the AuNPs-probes amplification, a linear relationship is also found, but the relationship is measured from 2×10^3 to 2×10^5 PFU/mL. Each value is derived from 3 independent detections and error bars mean SD.

Table 1-1. Detection technology of foodbrone pathogen

Type of assay	Assistant technology application	Reference
Plating	● Using chromogenic method to detection and enumeration	Reissbrodt R.(2004)
	● The hydrophobic grid membrane filtration method and the spiral plate count method are evaluated as rapid tools for the estimation of pathogen	Brichta-Harhay D.M. (2007)
	● To use immunomagnetic separation method for isolate foodborne pathogen	León L. de(2007)
Real-time PCR	● Using TaqMan real-time PCR assay to rapid detection foodorne pathogen	Kang S.E.(2007); Lambertz S.T. et al. (2008); Liu Y. et al.(2006)
	● To SYBR green real-time PCR method to rapid detect foodborne pathogen	Kim J.S.et al. (2008) Liu Y. et al.(2006)
ELISA	● Comparison of immunomagnetic separation methods for detection foodorne pathogen	Thompson TW(2007)
	● For Serological detection and immunogold localization of cross-reactive antigens shared.	Chakraborty B.N.(2007)
	● Using enzyme-linked immunosorbent assay to identify Staphylococcal enterotoxin in foods.	Bennett R.W.(2005)
Biosensors	● Using piezoelectric biosensor compare with nanoparticles to real-time detection foodorne pathogen	Chen et al. (2008)
	● To use disposable amperometric immunosensing strips fabricated by Au nanoparticles-modified screen-printed carbon electrodes for the detection of foodborne pathogen	Lin et al (2008)
	● Optic biosensor combine with immunoassay to detection foodborne pathogen	Subramanian A et al. (2005); Nanduri V et al. (2006)

Table 2-1. Applications of advanced nanomaterials for environmental monitoring [Andreescu et al., 2009]

Nanomaterials	Types	Properties	Potential application
Carbon nanotubes	Single and multi walled with various diameters and length	Electrocatalytic activity; High adsorption capacity	● Sorbents ● Various types of chemical and biological sensors
Metal nanoparticles	Au, Ag of various shapes and dimensions	Electrocatalytic activity; Ag has antibacterial activity	● Sorbents ● Various types of chemical and biological sensors
Magnetic iron oxide	Fe_2O_3, Fe_3O_4, Fe_3S_4, $MeOFe_2O_3$, (where M= Ni, Co, Zn,. etc.)	Superparamagnetic; Catalytic sites for H_2O_2	● Immunomagnetic separation and concentration of target analytes
Semiconductor metal oxides	TiO_2, ZnO, ZrO_2, CeO_2,	Photocatalytic, antibacterial and electrocatalytic activity	● Photocatalytic damage ● Gas sensing probes and biosensing
Quantum Dots	Inorganic fluorophores with intensity varying with the size and composition	Photoluminexcence; Can be biofuntionalized with enzymes, DNA and Ab	● Detection based on the changes in changes in the photoluminescence intensity
Dendrimer	Hyperbranched nanostructures with different length and nanometre size branches	High surface area with functionalized end groups; High sorption capacity	● DNA microarrays and DNA sensors; ● Composition of filters in waste water treatment

Table 7-1. Sequences of the oligonucleotide probes, targets, and primers used in this study.

Probe sequences for *E. coli* O157:H7 *eaeA*	
P-30-SH	HS-$(CH_2)_6$- 5'-AGC TCA AGA GTT GCC CAT CCT GCA GCA ATG-3' (30 mer)
P-30/12T-SH	HS-$(CH_2)_6$- 5'- TTT TTT TTT TTT AGC TCA AGA GTT GCC CAT CCT GCA GCA ATG -3' (42 mer)
P-30	5'-AGC TCA AGA GTT GCC CAT CCT GCA GCA ATG-3' (30 mer)
P-30/12T	5'- TTT TTT TTT TTT AGC TCA AGA GTT GCC CAT CCT GCA GCA ATG -3'(42 mer)
Short target sequences (30 mer) for *E. coli* O157:H7 *eaeA*	
T-30S	5'- AGC TCA AGA GTT GCC CAT CCT GCA GCA ATG -3'
T-30AS	5'- CAT TGC TGC AGG ATG GGC AAC TCT TGA GCT -3'
Long target sequences (104 mer) for *E. coli* O157:H7 *eaeA*	
T-104S	5'-AAA GTT CAG ATC TTG ATG ACA TTG TAT TTT CTC TTA ATT AAA TTT ATA TTT ACA GAA GCT CAA GAG TTG CCC ATC CTG CAG CAA TGT TAT TCC CTG AAA AAT TG -3'
T-104AS	5'-CAA TTT TTC AGG GAA TAA CAT TGC TGC AGG ATG GGC AAC TCT TGA GCT TCT GTA AAT ATA AAT TTA ATT AAG AGA AAA TAC AAT GTC ATC AAG ATC TGA ACT TT-3'
PCR primers	
E_{157}eae/F	5'-CAA TTT TTC AGG GAA TAA CAT TGC-3'
E_{157}eae/R	5'-AAA GTT CAG ATC TTG ATG ACA TTG-3'

Probe (P) sequences are designed according to the *E. coli* O157:H7 *eaeA* gene and used to detect the sequence of *E. coli* O157:H7. –SH, thiol-linkered tag [HS-$(CH_2)_6$] modification at 5 terminus of probe; /12T, additional 12 mer of dT oligonucleotides to the probes; P-30 (30 mer) and P-30/12T (42 mer), non-thiolated probes with or without additional 12-dT; P-30-SH (30 mer) and P-30/12T-SH (42 mer), thiolated probes with or without additional 12-dT.
Target (T) sequences include complementary target oligonucleotides, T-30AS (30 mer; AS, anti-sense strand to the probe sequence) and T-104AS (104 mer), and non-complementary target oligonucleotides, T-30S (30 mer; S, sense strand to the probe sequence) and T-104S (104 mer). The primer pair is used to amplify the 104 bp DNA fragment of *eaeA* gene from *E. coli* O157:H7 genomic DNA.

Table 7-2. Sequences of the oligonucleotide probes, targets, and primers used in this study.

Probe sequences for *E. coli* O157:H7 *eaeA*		
P1-30	5'-AGC TCA AGA GTT GCC CAT CCT GCA GCA ATG-3' $-(CH_2)_6-$ HS	(30-mer)
P1-30/12T	5'-AGC TCA AGA GTT GCC CAT CCT GCA GCA ATG TTT TTT TTT TTT-3' $-(CH_2)_6-$ HS	(42-mer)
P1-30/24T	5'-AGC TCA AGA GTT GCC CAT CCT GCA GCA ATG TTT TTT TTT TTT TTT TTT TTT TTT -3'$-(CH_2)_6-$ HS	(54-mer)
P2-30(AS)	HS-$(CH_2)_6$-5'-AAA GTT CAG ATC TTG ATG ACA TTG TAT TTT-3'	(30-mer)
P2-30(S)	HS-$(CH_2)_6$-5'-TTT CAA GTC TAG AAC TAC TGT AAC ATA AAA-3'	(30-mer)
P2-30/12T(AS)	HS-$(CH_2)_6$-5'-TTT TTT TTT TTT AAA GTT CAG ATC TTG ATG ACA TTG TAT TTT-3'	(42-mer)
Target sequences (104 mer) for *E. coli* O157:H7 *eaeA*		
T-104(S)	5'-AAA GTT CAG ATC TTG ATG ACA TTG TAT TTT CTC TTA ATT AAA TTT ATA TTT ACA GAA GCT CAA GAG TTG CCC ATC CTG CAG CAA TGT TAT TCC CTG AAA AAT TG -3'	
T-104(AS)	5'-CAA TTT TTC AGG GAA TAA CAT TGC TGC AGG ATG GGC AAC TCT TGA GCT TCT GTA AAT ATA AAT TTA ATT AAG AGA AAA TAC AAT GTC ATC AAG ATC TGA ACT TT-3'	
PCR primers		
E_{157}eae/F	5'- CAA TTT TTC AGG GAA TAA CAT TGC-3'	
E_{157}eae/R	5'- AAA GTT CAG ATC TTG ATG ACA TTG-3'	

Probe (P) sequences are designed according to the region of *E. coli* O157:H7 *eaeA* gene and used to detect the sequence of *E. coli* O157:H7. P1, Probe 1 is used to immobilize on the Au surface of QCM device; P2, Probe 2 is used to cap onto Au nanoparticles. /12T and /24, additional 12 mer and 24 mer of dT oligonucleotides to the probes.

Target (T) sequences include complementary target oligonucleotides, T-104(AS) (104-mer; AS, anti-sense strand to the probe sequence, i.e., complementary target oligonucleotides) and T-104(S) (104-mer; S, sense strand to the probe sequence, i.e., non-complementary target oligonucleotides).

The primer pair is used to amplify the 104-bp DNA fragment of the *eaeA* gene from *E. coli* O157:H7 genomic DNA.

Table 7-3. Sequences of the probe, target, and primer oligonucleotides for the dengue virus serotype-2 (DENV2) detection used in this study.

Probe oligonucleotides [a]	
DENV2-P1	5'-GTATCCAATTTGATCCTTGTGTGTCCGCTC$(T)_{12}$-$(CH_2)_6$-SH-3' (42 mer)
DENV2-P2	5'-HS-$(CH_2)_6$-$(T)_{12}$GATTCTTGAAGGTGACCAATGTCTCTTTCT-3' (42 mer)
Synthesized target oligonucleotide [b]	
DENV2-T	5'-GAGCGGACACACAAGGATCAAATTGGATACAGAAAGAGACATTGG TGACTTTCAAAAATC-3' (60 mer)
PCR primer pair [c]	
DENV-UF	5'-TGGTGCACAGACAATGGTT-3' (19 mer)
DENV-UR	5'-ACATCCTGTTTCTTCGCATG-3' (20 mer)
RT primer [d]	
DENV-URT	5'-GCCATTCTCTTCGCTCCCCT-3' (20 mer)

a. Probe (P) oligonucleotides are designed according to the gene region of DENV E protein and used to detect the sequence of DENV2. P1, probe 1 is used to immobilize on the gold surface of QCM chip, and cap onto AuNPs surface to purposely enhance the detection signal of QCM sensor; P2, probe 2 is used to cap onto AuNPs.

b. The sequence of synthesized target (T) oligonucleotide is complementary to the P1 at its 5' terminus and to the P2 at its 3' terminus.

c. Universal primer pair (UF and UR) is used to amplify a 130 bp DNA fragment within the gene encoding DENV E protein.

d. The universal RT (URT) primer is used to reverse-transcript DENV mRNA to cDNA.

Table 10-1. Comparisons of the present study with the related detection technologies for dengue virus

Method	Detected entity	Pretreatment procedure	Virus typing	Label-free	Detection time	Detection limit	Timing of infectious virus can be detected	Reference
Plaque assay	Viable virus	None	No	Yes	Days-weeks	1-10 infectious virus	After disease onset	Kao et al., 2005, Chen et al., 2000
ELISA	Antigen	Protein extraction	Yes	No	1-3 h	15-50 ng/mL	Viremia phase	Young et al 2000, Alcon et al., 2002
Immuno-QCM	Antigen	Protein extraction	Yes	Yes	2 h	7-17 ng/mL	Viremia phase	Wu et al., 2005
Fluorescent real-time PCR	Nucleic acid (i.e., viral RNA)	RNA extraction, reverse transcription, and PCR amplification	Yes	No	Hours	1-50 PFU/mL	Initial stage of infection	Kao et al., 2005; Chen et al., 2000
DNA-QCM	Nucleic acid (i.e., viral RNA)	RNA extraction, reverse transcription, and PCR amplification	Yes	Yes	1.5 h	2 PFU/mL	Initial stage of infection	This study